VYSOKÉ UČENÍ TECHNICKÉ V BRNĚ

BRNO UNIVERSITY OF TECHNOLOGY

FAKULTA STROJNÍHO INŽENÝRSTVÍ

ÚSTAV MECHANIKY TĚLES, MECHATRONIKY A BIOMECHANIKY

FACULTY OF MECHANICAL ENGINEERING

INSTITUTE OF SOLID MECHANICS, MECHATRONICS AND BIOMECHANICS

COMPUTATIONAL MODELLING OF MECHANICAL BEHAVIOUR OF "ELASTOMER-STEEL FIBRE" COMPOSITE

VÝPOČTOVÉ MODELOVÁNÍ MECHANICKÉHO CHOVÁNÍ KOMPOZITU "ELASTOMER - OCELOVÉ VLÁKNO"

DISERTAČNÍ PRÁCE
DOCTORAL THESIS

AUTOR PRÁCE — **Ing. Tomáš Lasota**
AUTHOR

VEDOUCÍ PRÁCE — **prof. Ing. Jiří Burša, PhD.**
SUPERVISOR

BRNO 2013

Abstrakt

Tato práce se zabývá výpočtovými simulacemi zkoušek jednoosým tahem a tříbodovým ohybem kompozitního vzorku složeného z elastomerové matrice a ocelových výztužných vláken orientovaných pod různými úhly, jakož i jejich experimentální verifikací. Simulace byly provedeny pomocí dvou různých modelů - bimateriálového a unimateriálového výpočtového modelu. Při použití bimateriálového modelu, který detailně zohledňuje strukturu kompozitu, tzn. pracuje s matricí a jednotlivými vlákny, je zapotřebí vytvořit model každého vlákna obsaženého v kompozitu, což přináší řadu nevýhod (pracná tvorba výpočtového modelu, řádově větší množství elementů potřebných k diskretizaci v MKP systémech a delší výpočetní časy). Na druhé straně v unimateriálovém modelu se nerozlišují jednotlivá vlákna, pracuje se pouze s kompozitem jako celkem tvořeným homogenním materiálem a výztužný účinek vláken je zahrnut v měrné deformační energii.

Porovnání experimentů se simulacemi ukázalo, že bimateriálový model je v dobré shodě s experimenty, na rozdíl od unimateriálového modelu, který je schopen poskytnou odpovídající výsledky pouze v případě tahového namáhání. Z tohoto důvodu byl hledán způsob, který by umožnil rozšířit unimateriálový model o ohybovou tuhost výztužných vláken. V roce 2007 Spencer a Soldatos publikovali rozšířený unimateriálový model, který je schopen pracovat nejen s tahovou, ale i ohybovou tuhostí vlákna. Představený obecný model je však založen na Cosseratově teorii kontinua a jeho praktické využití je pro jeho složitost nemožné. Proto byl vytvořen zjednodušený model (částečně podle Spencera a Soldatose) s vlastní navrženou formou měrné deformační energie.

Za účelem ověření nového unimateriálového modelu s ohybovou tuhostí vláken byly odvozeny všechny potřebné rovnice a byl napsán vlastní konečno-prvkový řešič. Tento řešič je založen na Cosseratově teorii kontinua a obsahuje zmíněný anizotropní hyperelastický unimateriálový model zahrnující ohybovou tuhost vláken. Vzhledem k tomu, že v případě Cosseratovy teorie jsou při výpočtu potřebné i druhé derivace posuvů, bylo nutné použít tzv. C^1 prvky, které mají spojité jak pole posuvů, tak jejich prvních derivací.

Nakonec byly provedeny nové simulace s využitím vlastního řešiče, které ukazují, že tuhost vláken lze u nového unimateriálového modelu řídit odpovídající materiálovou konstantou. V závěru práce je pak diskutováno, zda je nový unimateriálový model s ohybovou tuhostí

schopen poskytnout stejné výsledky jako model bimateriálový, a to jak při tahovém tak i ohybovém namáhání kompozitního vzorku.

Klíčová slova

hyperelasticita, anizotropie, Cosseratovo kontinuum, C^1 prvky, Hermitovy polynomy, kompozitní materiál, metoda konečných prvků

Abstract

This thesis deals with composite materials made of elastomer matrix and steel reinforcement fibres with various declinations. It presents computational simulations of their mechanical tests in uniaxial tension and three-point bending realized using finite element (FE) method, and their experimental verification. The simulations were carried out using two different models - bimaterial and unimaterial computational models. The bimaterial model reflects structure of the composite in detail, i.e. it works with the matrix and individual fibres. When the bimaterial model is used, then it is necessary to create each fibre of the composite in the model and it makes numbers of disadvantages (creation of the model is laborious, higher number of elements are needed for discretization of an individual fibre in FE softwares and computational time is higher). On the other side, the unimaterial model does not distinguish the individual fibres, but it works with a model of the whole composite as a homogeneous material and the reinforcing effect of the fibres is included in the strain energy density function.

Comparison between experiments and simulations shows that the bimaterial model is in good agreement with the experiments unlike the unimaterial one being able to provide adequate results in the case of tension load only. Hence, a new way was sought of how to extend the unimaterial model by the bending stiffness of fibres. In 2007 Spencer and Soldatos published a new extended unimaterial model that is able to work with both tension and bending stiffnesses of fibres. However, their model is based on Cosserat continuum theory, it is very complicated and is not suitable for practical application. Hence, a new simplified model was created in the thesis (partially according to the Spencer and Soldatos) with own strain energy density function proposed.

In order to verify the new unimaterial model with bending stiffness, all the needed equations were derived and a new own finite element solver was written. This solver is based on Cosserat continuum theory and contains the mentioned anisotropic hyperelastic unimaterial model with bending stiffness. It was necessary to use the so called C^1 elements, since the Cosserat theory works with second derivatives of displacements. The C^1 elements ensure continuity of both displacements field and their first derivatives.

Finally, new simulations were performed using the created FE solver and they show that

the bending stiffness of fibres can be driven by the appropriate material parameter. In conclusion of this work it is discussed whether the new unimaterial model with bending stiffness is able to provide the same results as the bimaterial model, namely for both tension and bending loads of a composite specimen.

Keywords

hyperelasticity, anisotropy, Cosserat continuum, C^1 elements, Hermite polynoms, composite material, finite element method

Prohlašuji, že tuto disertační práci jsem vypracoval samostatně pod vedením prof. Jiřího Burši a všechny použité zdroje jsou řádně uvedeny v odkazech.

I hereby declare that I have written the doctoral thesis by myself under the supervision of prof. Jiří Burša and all used sources are properly mentioned in references.

Ing. Tomáš Lasota

Acknowledgement

I would like to express my gratitude to my supervisor prof. Ing. Jiří Burša, Ph.D. for his guidance, kindness, support, and friendly attitude throughout my study.
I also want to thank to Ing. Pavel Skácel, Ph.D. for his willingness to consult whatever was necessary during whole study and for help in experimental field.
Last but not least, I would like to thank to my family and my girlfriend Věrka for their support during my whole Ph.D. study.

Contents

1 Introduction

Composite materials can be found increasingly in many practical applications of various specializations. These materials have many advantages, especially high strength at low weight. A design or assessment of stress-strain state of such materials is very important for their proper use in practise. For this purpose, computational methods based on finite element method are commonly used. This work is focused on composite materials with elastomer hyperelastic matrix and steel reinforcement fibres. Such composite materials can be found e.g. in construction of tyres, nevertheless, these composite materials do not differ so much from bio-composite materials, e.g. artery wall can be understood as a composite material consisting of hyperelastic matrix and collagen fibres. The difference from the technical composites mentioned above is primarily in the nonlinear behaviour of the fibres. Nowadays, the fibre-reinforced composites can be computationally modeled essentially in two ways. Either the matrix with individual steel fibres is modeled (bimaterial computational model) or we can use a computational model where the geometric shape of the whole composite body is created without distinguishing the fibres (unimaterial computational model). The reinforcement effect of the fibres is then included mathematically in the constitutive equations which include fibre directions.

The main goal of this work is to compare both levels of the mentioned computational models and to found out if the unimaterial model is able to give the same results as the bimaterial one. In order to this, computational simulations were carried out with both models. A detailed description of such models can be found in chapter 4, where results of these simulations are discussed in detail and simulations are compared with performed experiments.

It is obvious from the results of simulations that the unimaterial model is not able to include bending stiffness of fibres, therefore, a new model was sought which could be able to include their bending stiffness. Among many papers an only one was found that deals with the unimaterial model and bending stiffness of the fibres - Spencer and Soldatos in 2007 [32] introduced a new constitutive model with bending stiffness of the reinforcement fibres. However, this model is based on the Cosserat continuum unlike conventional models which are based on Cauchy continuum.

The Cosserat theory of continuum is shortly mentioned in chapter 5 where only basic knowledge is introduced needed for formulation of new constitutive equations is introduced. The constitutive equations introduced by Spencer and Soldatos are described in detail in chapter 6 where their simplified version is also presented. A new form of strain energy density function was proposed both for nearly incompressible and incompressible hyperelastic materials in chapters 7 and 8. The new forms of strain energy density function contain a few material parameters that have to be determined. Hence, chapter 9 deals with a feasible determination of such material parameters. A practical implementation of the simplified constitutive equations based on Cosserat continuum required a new finite element solver, because there is no available solver based on the Cosserat continuum and hyperelasticity. Hence, a new own finite element solver was written in Matlab software. Chapter 10 deals with finite element formulation based on constraint Cosserat theory using a new C^1 element needed to ensure convergence and it presents the results obtained with the new finite element solver.

2 Formulations of problems and goals

Computational simulations performed by bimaterial computational model have several disadventages. Due to a three-dimensional model of fibres diverted by any angle, the regular mesh with low number of elements can not be used. Hence, a very fine mesh has to be used with very high numbers of elements which leads to high computational times. The increase of computational time is on orders of magnitude compared to the unimaterial model. Hence, the bimaterial model should be replaced by the unimaterial one where fibres are included mathematically in the constitutive model and the three-dimensional model of them is not required. Material models based on directions of fibres were implemented into the FEA systems recently and the range of their use has not yet been studied properly. The main goal of this work is to compare both of the mentioned computational models and to find out if the very time consuming bimaterial computational model, can be replaced by a unimaterial model.

Main goals are:

- to perform computational simulations of uniaxial tension and bending tests with the bimaterial computational model
- to perform computational simulations of uniaxial tension and bending tests with the unimaterial computational model
- to compare the simulations
- to perform experiments of uniaxial tension and bending tests of composite material
- to compare simulations and experiments
- to explain differences between simulations and experiments (if any)
- to explain differences between unimaterial and bimaterial models (if any)
- to modify the unimaterial computational model in order to obtain the same results as with the bimaterial model

3 Hyperelasticity

The following chapter provides some basic knowledge used in hyperelastic materials. The most of this chapter can be found in [2].

Hyperelasticity refers to a constitutive response that is derivable from an elastic free energy potential and is typically used for materials which experience large elastic deformation (strains). Applications for elastomers such as vulcanized rubber and synthetic polymers, along with some biological materials, often fall into this category.

The microstructure of polymer solids consists of chain-like molecules. The flexibility of these molecules allows for an irregular molecular arrangement and, as a result, the behaviour is very complex. Polymers are usually isotropic at small deformation and anisotropic at larger deformation as the molecule chains realign to the loading direction. Under an essentially monotonic loading condition, however, many polymer materials can be approximated as isotropic, which has been popular historically in the modeling of polymers.

Some classes of hyperelastic materials cannot be modeled as isotropic. An example is represented by fibre reinforced polymer composites. Typical fibre patterns include their unidirectional and bidirectional arrangement, and the fibres can have a stiffness that is 50-1000 times that of the polymer matrix, resulting in a strongly anisotropic material behaviour. Also some biomaterials, such as muscles and arteries, can represent anoter class of anisotropic materials experiencing large deformation; their anisotropic behaviour occurs also due to their fibrous structure.

The typical volumetric behaviour of hyperelastic materials can be grouped into two classes. The first is represented by polymers materials that show small volumetric changes during deformation - incompressible or nearly-incompressible materials. Examples of the second class of materials are foams, which can experience large volumetric changes during deformation - compressible materials.

The available hyperelastic constitutive models of materials are derived from strain-energy potentials that are functions of the deformation invariants. The hyperelastic material models can be divided into several families:

- Incompressible or nearly-incompressible isotropic models (chapter 3.3)
- Compressible isotropic models (chapter 3.4)
- Invariant-based anisotropic strain-energy potentials (chapter 3.5)

3.1 Finite Strain Elasticity

A material is said to be hyperelastic if there exists an elastic potential function W (or strain-energy density function) which is a scalar function of one of the strain or deformation tensors, whose derivative with respect to a strain component determines the corresponding stress component. This can be expressed by:

$$S_{IJ} = \frac{\partial W}{\partial E_{IJ}} = 2\frac{\partial W}{\partial C_{IJ}}, \tag{1}$$

where S_{IJ} are components of the second Piola-Kirchhoff stress tensor, W is strain-energy function per unit undeformed volume, E_{IJ} are components of the Lagrangian strain tensor and C_{IJ} are components of the right Cauchy-Green deformation tensor. The Lagrangian strain may be expressed as follows:

$$E_{IJ} = \frac{1}{2}(C_{IJ} - \delta_{IJ}), \tag{2}$$

where δ_{IJ} is Kronecker delta. The deformation tensor C_{IJ} is comprised of the products of the deformation gradients F_{iJ}

$$C_{IJ} = F_{kI}F_{kJ}, \tag{3}$$

and deformation gradient

$$F_{iJ} = \frac{\partial x_i}{\partial X_J} = \delta_{iJ} + \frac{\partial u_i}{\partial X_J}, \tag{4}$$

where X_J is coordinate of the undeformed position of a point in direction J, $x_i = X_i + u_i$ is the deformed position of the point in direction i and u_i is displacement of the point in direction i.

The Kirchhoff stress is defined

$$\tau_{ij} = F_{iK}S_{KL}F_{jL} \tag{5}$$

and the Cauchy stress is obtained by:

$$\sigma_{ij} = \frac{1}{J}\tau_{ij} = \frac{1}{J}F_{iK}S_{KL}F_{iL}. \tag{6}$$

The eigenvalues squared (principal stretch ratios) of C_{ij} are $\lambda_1^2, \lambda_2^2, \lambda_3^2$ and exist only if

$$det \mid C_{IJ} - \lambda_p^2 \delta_{IJ} \mid = 0 \tag{7}$$

which can be re-expressed as

$$\lambda_p^6 - I_1\lambda_p^4 + I_2\lambda_p^2 - I_3 = 0, \tag{8}$$

where I_1, I_2, I_3 are invariants of C_{IJ},

$$I_1 = \lambda_1^2 + \lambda_2^2 + \lambda_3^2 \tag{9}$$

$$I_2 = \lambda_1^2\lambda_2^2 + \lambda_2^2\lambda_3^2 + \lambda_3^2\lambda_1^2 \tag{10}$$

$$I_3 = \lambda_1^2\lambda_2^2\lambda_3^2 = J^2. \tag{11}$$

J is invariant of deformation gradient and represents the ratio of the deformed elastic volume over the reference (undeformed) volume of materials ([37], [38]).

3.2 Deviatoric-volumetric multiplicative split

Under the assumption that material response is isotropic, it is convenient to express the strain-energy function in terms of strain invariants or principal stretches [39]:

$$W = W(I_1, I_2, I_3) = W(I_1, I_2, J) \tag{12}$$

or

$$W = W(\lambda_1, \lambda_2, \lambda_3). \tag{13}$$

Define the volume-preserving part of the deformation gradient, $\overline{F}_{iJ}$, as

$$\overline{F}_{iJ} = J^{-1/3}F_{iJ} \tag{14}$$

and thus

$$\overline{J} = det \mid \overline{F}_{iJ} \mid = 1. \tag{15}$$

The modified principal stretch ratios and invariants are then

$$\overline{\lambda}_p = J^{-1/3}\lambda_p \tag{16}$$

$$\overline{I}_p = J^{-2/3}I_p. \tag{17}$$

The strain-energy potencial can then be defined as

$$W = W(\overline{I}_1, \overline{I}_2, J) = W(\overline{\lambda}_1, \overline{\lambda}_2, \overline{\lambda}_3, J), \tag{18}$$

where the modified invariants $\overline{I}_1, \overline{I}_2$ or stretch ratios $\overline{\lambda}_1, \overline{\lambda}_2, \overline{\lambda}_3$ describe the deviatoric (volume preserving) part of deformation, while the volumetric part of deformation can be described independently by means of the J invariant.

The constitutive strain-energy density function W can be devided into volumetric W_V and deviatoric (often called isochoric) W_d part

$$W = W_V(J) + W_d(\overline{I}_1, \overline{I}_2). \tag{19}$$

The volumetric part W_V is absolutely independent of the isochoric part W_d and the volumetric part W_V is asumed to be only function of J as

$$W_V(J) = \frac{1}{d}(J-1)^2, \tag{20}$$

where d is compressibility parameter. The isochoric part W_d is a function of the invariants $\overline{I}_1, \overline{I}_2$ of the isochoric part of the right Cauchy-Green tensor $\overline{\boldsymbol{C}}$.

3.3 Isotropic hyperelasticity - nearly incompressible materials

In the following paragraphs several forms of strain-energy potential (W) provided for the simulation of nearly incompressible hyperelastic materials are summarized on the basis of [2]. In all of them volumetric change contribution is expressed separately by means of compressibility parameter d as was described in the previous chapter (3.2).

3.3.1 Neo-Hookean

The form Neo-Hookean strain-energy potential is

$$W = \frac{\mu}{2}(\overline{I}_1 - 3) + \frac{1}{d}(J-1)^2, \tag{21}$$

where μ is initial shear modulus of material.

3.3.2 Arruda-Boyce Model

The form of the strain-energy potential for Arruda-Boyce model is

$$W = \mu\left[\frac{1}{2}(\overline{I}_1 - 3) + \frac{1}{20\lambda_L^2}(\overline{I}_1^2 - 9) + \frac{11}{1050\lambda_L^4}(\overline{I}_1^3 - 27) + \frac{19}{7000\lambda_L^6}(\overline{I}_1^4 - 81) + \right.$$

$$\left. + \frac{519}{673750\lambda_L^8}(\overline{I}_1^5 - 243)\right] + \frac{1}{d}\left(\frac{J^2-1}{2} - lnJ\right), \tag{22}$$

where μ is initial shear modulus of the material, λ_L is its limiting network stretch. As the parameter λ_L tends to infinity, the model is converted into the Neo-Hookean form.

3.3.3 Gent Model

The form of the strain-energy potential for the Gent model is

$$W = \frac{\mu J_m}{2} ln\left(1 - \frac{\overline{I}_1 - 3}{J_m}\right)^{-1} + \frac{1}{d}\left(\frac{J^2-1}{2} - lnJ\right), \tag{23}$$

where μ is initial shear modulus of material and J_m is limiting value of $\overline{I}_1 - 3$.

3.3.4 Mooney-Rivlin

This option includes two-, three-, five-, and nine-term Mooney-Rivlin models. The form of the strain-energy potential for a **two-parameter** Mooney-Rivlin model is

$$W = c_{10}(\overline{I}_1 - 3) + c_{01}(\overline{I}_2 - 3) + \frac{1}{d}(J-1)^2. \tag{24}$$

The form of the strain-energy potential for a **three-parameter** Mooney-Rivlin model is

$$W = c_{10}(\overline{I}_1 - 3) + c_{01}(\overline{I}_2 - 3) + c_{11}(\overline{I}_1 - 3)(\overline{I}_2 - 3) + \frac{1}{d}(J-1)^2, \tag{25}$$

The form of the strain-energy potential for **five-parameter** Mooney-Rivlin model is

$$W = c_{10}(\overline{I}_1-3)+c_{01}(\overline{I}_2-3)+c_{20}(\overline{I}_1-3)^2+c_{11}(\overline{I}_1-3)(\overline{I}_2-3)+c_{02}(\overline{I}_2-3)^2+\frac{1}{d}(J-1)^2, \quad (26)$$

The form of the strain-energy potential for **nine-parameter** Mooney-Rivlin model is

$$\begin{aligned} W =& c_{10}(\overline{I}_1-3)+c_{01}(\overline{I}_2-3)+c_{20}(\overline{I}_1-3)^2+c_{11}(\overline{I}_1-3)(\overline{I}_2-3)+ \\ &+c_{02}(\overline{I}_2-3)^2+c_{30}(\overline{I}_1-3)^3+c_{21}(\overline{I}_1-3)^2(\overline{I}_2-3)+c_{12}(\overline{I}_1-3)(\overline{I}_2-3)^2+ \\ &+c_{03}(\overline{I}_2-3)^3+\frac{1}{d}(J-1)^2, \end{aligned} \quad (27)$$

where $c_{10}, c_{01}, c_{20}, c_{11}, c_{02}, c_{30}, c_{21}, c_{12}, c_{03}$ are material constants describing the deviatoric part of the strain energy.

The initial shear modulus is given by

$$\mu = 2(c_{10}+c_{01}). \quad (28)$$

3.3.5 Polynomial form

The polynomial form of strain-energy potential is

$$W = \sum_{i+j=1}^{N} c_{ij}(\overline{I}_1-3)^i(\overline{I}_2-3)^j + \sum_{k=1}^{M}\frac{1}{d_k}(J-1)^{2k}, \quad (29)$$

where N, M, c_{ij}, d_k are material constants.

A higher N may provide better fit with the exact solution, however, it may, on the other hand, cause numerical difficulty in fitting the material constants and requires enough data to cover the entire range of interest of deformation. Therefore a very high N value is not usually recommended.

The Neo-Hookean model can be obtained by setting $M = N = 1$ and $c_{01} = 0$. Also for $M = N = 1$, the two parameters Mooney-Rivlin model is obtained, while the five parameters Mooney-Rivlin model is obtained for $N = 2$, and the nine parameters Mooney-Rivlin model is obtained for $N = 3$. Equation (28) for the initial shear modulus is valid here as well.

3.3.6 Yeoh model

The Yeoh model is also called the reduced polynomial form. The strain-energy potential is

$$W = \sum_{i=1}^{N} c_{i0}(\overline{I}_1 - 3)^i + \sum_{k=1}^{M} \frac{1}{d_k}(J-1)^{2k}, \tag{30}$$

where N, M, c_{i0}, d_k are material constants.

The Neo-Hookean model can be obtained by setting M=N = 1. The initial shear modulus is defined

$$\mu = 2c_{10}. \tag{31}$$

3.3.7 Ogden potential

The Ogden form of strain-energy potential is based on the principal stretches of left-Cauchy strain tensor, which has the form

$$W = \sum_{i=1}^{N} \frac{\mu_i}{\alpha_i}(\overline{\lambda}_1^{\alpha_i} + \overline{\lambda}_2^{\alpha_i} + \overline{\lambda}_3^{\alpha_i} - 3) + \sum_{k=1}^{M} \frac{1}{d_k}(J-1)^{2k}, \tag{32}$$

where $N, M, \mu_i, \alpha_i, d_k$ are material constants.

Similar to the Polynomial form, there is no limitation on N or M. A higher N can provide better fit the exact solution, however, it may, on the other hand, cause numerical difficulty in fitting the material constants and also it requests to have enough data to cover the entire range of interest of the deformation. Therefore a value of N $>$ 3 is not usually recommended.

The initial shear modulus, μ, is given as

$$\mu = \frac{1}{2}\sum_{i=1}^{N} \alpha_i \mu_i. \tag{33}$$

For $M = N = 1, \alpha_1 = 2$, the Ogden potential is equivalent to the Neo-Hookean potential.

3.4 Isotropic hyperelasticity - compressible foam-like materials

3.4.1 Ogden compressible foam model

The strain-energy potential of the Ogden compressible foam model is based on the principal stretches of left-Cauchy strain tensor, which has the form

$$W = \sum_{i=1}^{N} \frac{\mu_i}{\alpha_i}(J^{\alpha_i/3}(\overline{\lambda}_1^{\alpha_i} + \overline{\lambda}_2^{\alpha_i} + \overline{\lambda}_3^{\alpha_i}) - 3) + \sum_{i=1}^{N} \frac{\mu_i}{\alpha_i\beta_i}(J^{-\alpha_i\beta_i} - 1), \tag{34}$$

where $N, \mu_i, \alpha_i, \beta_i$ are material constants. The initial shear modulus, μ, is given as

$$\mu = \frac{\sum_{i=1}^{N} \mu_i\alpha_i}{2}. \tag{35}$$

For $N = 1, \alpha_1 = -2, \mu_1 = -\mu, \beta = 0.5$, the Ogden option is equivalent to the Blatz-Ko option.

3.4.2 Blatz-Ko model

The form of strain-energy potential for the Blatz-Ko model is

$$W = \frac{\mu}{2}\left(\frac{I_2}{I_3} + 2\sqrt{I_3} - 5\right), \tag{36}$$

where μ is initial shear modulus of material.

3.5 Anisotropic hyperelasticity

The anisotropic constitutive strain-energy density function W is defined

$$W = W_V(J) + W_d(\overline{\mathbf{C}}, \mathbf{A} \otimes \mathbf{A}, \mathbf{B} \otimes \mathbf{B}), \tag{37}$$

where W_V is volumetric part of the strain energy and W_d is isochoric part of strain energy. The isochoric part W_d is a function of the invariants $\overline{I}_1, \overline{I}_2, \overline{I}_4, \overline{I}_5, \overline{I}_6, \overline{I}_7, \overline{I}_8$ of the isochoric part of the right Cauchy Green tensor $\overline{\mathbf{C}}$ and the two constitutive material directions $\mathbf{A}, \mathbf{B}$ in the undeformed configuration. The material directions yield so-called structural tensors $\mathbf{A} \otimes \mathbf{A}, \mathbf{B} \otimes \mathbf{B}$ of the microstructure of the material, it holds

$$| \mathbf{A} | = 1, | \mathbf{B} | = 1. \tag{38}$$

Thus, the strain-energy density yields

$$W_d(\mathbf{C}, \mathbf{A}\otimes\mathbf{A}, \mathbf{B}\otimes\mathbf{B}) = \sum_{i=1}^{3} a_i(\overline{I}_1 - 3)^i + \sum_{j=1}^{3} b_j(\overline{I}_2 - 3)^j + \sum_{k=2}^{6} c_k(\overline{I}_4 - 1)^k +$$

$$+ \sum_{l=2}^{6} d_l(\overline{I}_5 - 1)^l + \sum_{m=2}^{6} e_m(\overline{I}_6 - 1)^m + \sum_{n=2}^{6} f_n(\overline{I}_7 - 1)^n + \sum_{o=2}^{6} g_o(\overline{I}_8 - \varsigma)^o, \qquad (39)$$

The third invariant $\overline{I}_3$ is ommited here because the volumetric change is described separately by eq. (20). Invariants $\overline{I}_1, \overline{I}_2$ describe the contribution of the matrix, while the other invariants describe the contribution of fibres to the strain energy density function. In eq. (39) the irreducible basis of invariants

$$\overline{I}_1 = tr\overline{\mathbf{C}}, \qquad \overline{I}_2 = \frac{1}{2}[(tr\overline{\mathbf{C}})^2 - tr\overline{\mathbf{C}}^2], \qquad \overline{I}_4 = \mathbf{A}\overline{\mathbf{C}}\mathbf{A}, \qquad \overline{I}_5 = \mathbf{A}\overline{\mathbf{C}}^2\mathbf{A},$$

$$\overline{I}_6 = \mathbf{B}\overline{\mathbf{C}}\mathbf{B}, \qquad \overline{I}_7 = \mathbf{B}\overline{\mathbf{C}}^2\mathbf{B}, \qquad \overline{I}_8 = (\mathbf{A}\mathbf{B})\mathbf{A}\overline{\mathbf{C}}\mathbf{B}. \qquad (40)$$

and the parameter ς is defined as

$$\varsigma = (\mathbf{A}\mathbf{B})^2. \qquad (41)$$

3.6 Assessment of material parameters

The hyperelastic constants in the strain-energy density function of a material model determine mechanical response. Therefore, in order to obtain credible results of a hyperelastic analysis, it is necessary to assess parameters of the material being examined. Material constants are generally obtained for a material using experimental stress-strain data. It is recommended that this test data be taken from several modes of deformation over a wide range of strain components.

For hyperelastic materials, simple deformation tests (consisting of six deformation modes) can be used to characterize the material constants. All the available laboratory test data will be used to determine the hyperelastic material constants. Basic deformation modes are graphically illustrated in fig. 1. Combinations of data from multiple tests will enhance the characterization of the hyperelastic behaviour of the material.

It can be shown that apparently different loading conditions have identical deformations,

and are thus equivalent. Superposition of tensile or compressive hydrostatic stresses on a loaded incompressible body results in different stresses, but does not alter deformation of a material. As depicted in fig. 2, we find that upon the addition of hydrostatic stresses, the following modes of deformation can be identical:

1. Uniaxial Tension and Equibiaxial Compression.
2. Uniaxial Compression and Equibiaxial Tension.
3. Planar Tension and Planar Compression and Pure shear

With several equivalent modes of testing, we are left with only three independent deformation states for which one can obtain experimental data.

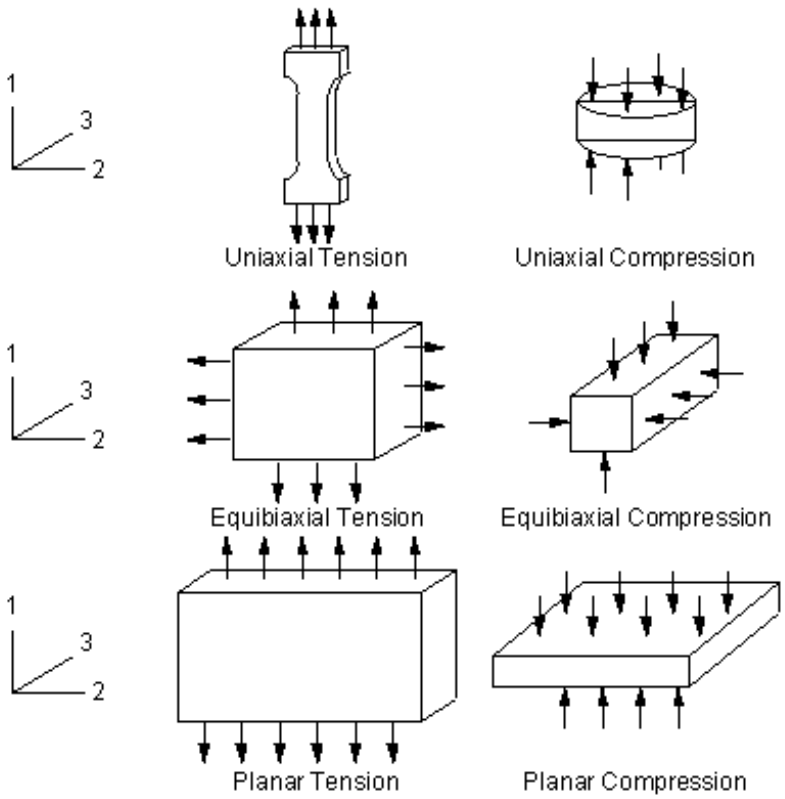

Figure 1: Illustration of Deformation Modes. (reprint from [2])

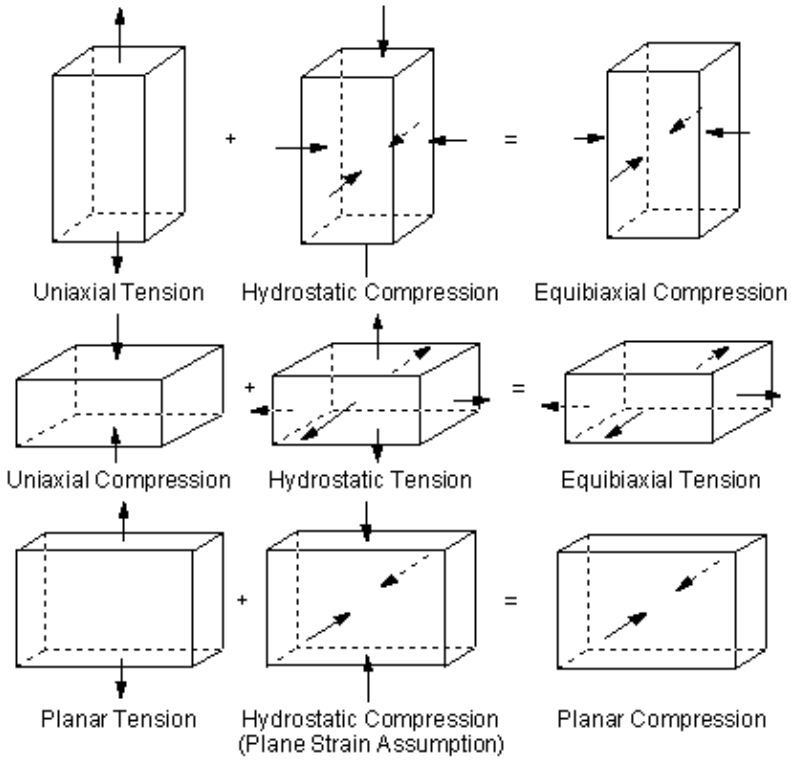

Figure 2: Equivalent Deformation Modes. (reprint from [2])

The following sections outline the development of hyperelastic stress relationships for each independent testing mode. In the analyses, the coordinate system is chosen to coincide with the principal directions of deformation. Thus, the right Cauchy-Green strain tensor can be written in matrix form by

$$C = \begin{bmatrix} \lambda_1^2 & 0 & 0 \\ 0 & \lambda_2^2 & 0 \\ 0 & 0 & \lambda_3^2 \end{bmatrix} \tag{42}$$

where principal stretch ratio in the ith direction λ_i is

$$\lambda_i = 1 + \varepsilon_i \tag{43}$$

and ε_i is principal value of the engineering strain tensor in the ith direction. The principal invariants of C_{ij} are

$$I_1 = \lambda_1^2 + \lambda_2^2 + \lambda_3^2 \tag{44}$$

$$I_2 = \lambda_1^2\lambda_2^2 + \lambda_1^2\lambda_3^2 + \lambda_2^2\lambda_3^2 \tag{45}$$

$$I_3 = \lambda_1^2\lambda_2^2\lambda_3^2 \tag{46}$$

For each mode of deformation, a fully incompressible material behaviour is also assumed so that third principal invariant, I_3, is identically one

$$\lambda_1^2\lambda_2^2\lambda_3^2 = 1. \tag{47}$$

Finally, the hyperelastic Piola-Kirchhoff stress tensor, (1) can be algebraically manipulated to determine components of the Cauchy (true) stress tensor. In terms of the left Cauchy-Green strain tensor, the Cauchy stress components for a volumetrically constrained material can be shown to be

$$\sigma_{ij} = -p\delta_{ij} + dev\left[2\frac{\partial W}{\partial I_1}b_{ij} - 2I_3\frac{\partial W}{\partial I_2}b_{ij}^{-1}\right] \tag{48}$$

where p is pressure and b_{ij} is left Cauchy-Green deformation tensor

$$b_{ij} = F_{ik}F_{jk}. \tag{49}$$

3.6.1 Uniaxial tension (equivalently, equibiaxial compression)

As shown in fig. (1) a hyperelastic specimen is loaded along one of its axis during a uniaxial tension test. For this deformation state, the principal stretch ratios in the directions orthogonal to the 'pulling' axis will be identical. Therefore, during uniaxial tension, the principal stretches, λ_i, are given by

$$\lambda_1 \text{ - stretch in direction being loaded}$$
$$\lambda_2 = \lambda_3 \text{ - stretches in directions not being loaded.}$$

Due to incompressibility (47)

$$\lambda_2\lambda_3 = \lambda_1^{-1} \tag{50}$$

and since $\lambda_2 = \lambda_3$ we have

$$\lambda_2 = \lambda_3 = \lambda_1^{-1/2}. \tag{51}$$

For uniaxial tension, the first and second invariants then become

$$I_1 = \lambda_1^2 + 2\lambda_1^{-1} \tag{52}$$

and

$$I_2 = 2\lambda_1 + \lambda_1^{-2}. \tag{53}$$

Substituting the uniaxial tension principal stretch ratio values into the eq. (48), we obtain the following stresses in the 1 and 2 directions

$$\sigma_{11} = -p + 2\frac{\partial W}{\partial I_1}\lambda_1^2 - 2\frac{\partial W}{\partial I_2}\lambda_1^{-2} \tag{54}$$

and

$$\sigma_{22} = -p + 2\frac{\partial W}{\partial I_1}\lambda_1^{-1} - 2\frac{\partial W}{\partial I_2}\lambda_1 = 0. \tag{55}$$

Subtracting eq. (55) from eq. (54), we obtain the principal true stress for uniaxial tension

$$\sigma_{11} = 2(\lambda_1^2 - \lambda_1^{-1})\left[\frac{\partial W}{\partial I_1} + \lambda_1^{-1}\frac{\partial W}{\partial I_2}\right]. \tag{56}$$

The corresponding engineering stress is

$$T_1 = \sigma_{11}\lambda_1^{-1}. \tag{57}$$

3.6.2 Equibiaxial tension (equivalently, uniaxial compression)

During an equibiaxial tension test, a hyperelastic specimen is equally loaded along two of its axes, as shown in fig. (1). For this case, the principal stretch ratios in the directions being loaded are identical. Hence, for equibiaxial tension, the principal stretches λ_i, are given by

$$\lambda_1 = \lambda_2 \text{ - stretch ratios in directions being loaded}$$
$$\lambda_3 \text{ - stretch ratio in direction not being loaded.}$$

Utilizing incompressibility (47), we find

$$\lambda_3 = \lambda_1^{-2}. \tag{58}$$

For equibiaxial tension, the first and second invariants then become

$$I_1 = 2\lambda_1^2 + \lambda_1^{-4} \tag{59}$$

and

$$I_2 = \lambda_1^4 + 2\lambda_1^{-2}. \tag{60}$$

Substituting the principal stretch ratio values for equibiaxial tension into the Cauchy stress eq. (48), we obtain the stresses in the 1 and 3 directions

$$\sigma_{11} = -p + 2\frac{\partial W}{\partial I_1}\lambda_1^2 - 2\frac{\partial W}{\partial I_2}\lambda_1^{-2} \tag{61}$$

and

$$\sigma_{33} = -p + 2\frac{\partial W}{\partial I_1}\lambda_1^{-4} - 2\frac{\partial W}{\partial I_2}\lambda_1^4 = 0. \tag{62}$$

Subtracting eq. (62) from eq. (61), we obtain the principal true stress for uniaxial tension

$$\sigma_{11} = 2(\lambda_1^2 - \lambda_1^{-4})\left[\frac{\partial W}{\partial I_1} + \lambda_1^2\frac{\partial W}{\partial I_2}\right]. \tag{63}$$

The corresponding engineering stress is

$$T_1 = \sigma_{11}\lambda_1^{-1}. \tag{64}$$

3.6.3 Pure shear

(Uniaxial Tension and Uniaxial Compression in Orthogonal Directions)

Pure shear deformation experiments on hyperelastic materials are generally performed by loading thin, short and wide rectangular specimens, as shown in fig. (3). For pure shear, plane strain is generally assumed so that there is no deformation in the 'wide' direction of the specimen: $\lambda_2 = 1$.

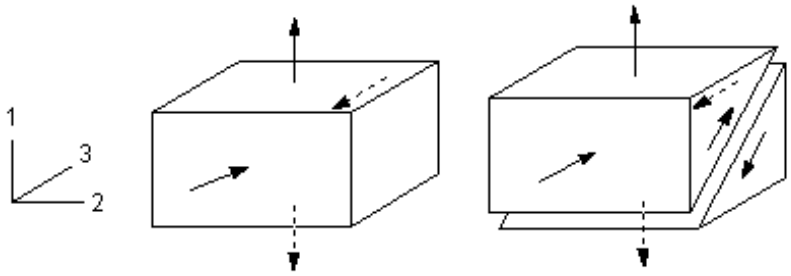

Figure 3: Pure Shear from Direct Components.(reprint from [2]

Due to incompressibility (47), it is found that

$$\lambda_3 = \lambda_1^{-1}. \tag{65}$$

For pure shear, the first and second invariants are

$$I_1 = \lambda_1^2 + \lambda_1^{-2} + 1 \tag{66}$$

and

$$I_2 = \lambda_1^2 + \lambda_1^{-2} + 1. \tag{67}$$

Substituting the principal stretch ratio values for pure shear into the Cauchy stress eq. (48), we obtain the following stresses in the 1 and 3 directions

$$\sigma_{11} = -p + 2\frac{\partial W}{\partial I_1}\lambda_1^2 - 2\frac{\partial W}{\partial I_2}\lambda_1^{-2} \tag{68}$$

$$\sigma_{33} = -p + 2\frac{\partial W}{\partial I_1}\lambda_1^{-2} - 2\frac{\partial W}{\partial I_2}\lambda_1^2 = 0. \tag{69}$$

Subtracting eq. (69) from eq. (68), we obtain the principal pure shear true stress equation

$$\sigma_{11} = 2(\lambda_1^2 - \lambda_1^{-2})\left[\frac{\partial W}{\partial I_1} + \frac{\partial W}{\partial I_2}\right] \tag{70}$$

The corresponding engineering stress is

$$T_1 = \sigma_{11}\lambda_1^{-1}. \tag{71}$$

3.6.4 Volumetric deformation

The volumetric deformation is described as

$$\lambda_1 = \lambda_2 = \lambda_3 = \lambda, \qquad J = \lambda^3. \tag{72}$$

As nearly incompressible is assumed, we have

$$\lambda \approx 1. \tag{73}$$

The pressure, p, is directly related to the volume ratio J through

$$p = \frac{\partial W}{\partial J}. \tag{74}$$

3.7 Deformation measures used in finite elasticity

Suppose that a solid is subjected to a displacement field $u_i(x_k)$. Define:

- **The deformation gradient and its Jacobian**

$$F_{iJ} = \delta_{ij} + \frac{\partial u_i}{\partial X_J} \qquad J = det(\mathbf{F}) \tag{75}$$

- **The right Cauchy-Green deformation tensor**

$$\mathbf{C} = \mathbf{F}^T\mathbf{F} \qquad C_{RS} = F_{iR}F_{iS} \tag{76}$$

- **The Left Cauchy-Green deformation tensor**

$$\mathbf{B} = \mathbf{F}\mathbf{F}^T \qquad B_{ij} = F_{iR}F_{jR} \tag{77}$$

- **Invariants of the left and right Cauchy-Green deformation tensors**

$$I_1 = tr\mathbf{C} = tr\mathbf{B} \tag{78}$$

$$I_2 = \frac{1}{2}[tr(\mathbf{C})^2 - tr\mathbf{C}^2] = \frac{1}{2}[tr(\mathbf{B})^2 - tr\mathbf{B}^2] \tag{79}$$

$$I_3 = det\mathbf{C} = det\mathbf{B} = J^2 \tag{80}$$

- **Stretch tensors**

  At each point $\mathbf{X}$ from reference configuration and each time, we have the following **unique polar decomposition** of the deformation gradient $\mathbf{F}$

$$\mathbf{F} = \mathbf{RU} = \mathbf{vR}. \tag{81}$$

  This is a fundamental theorem in continuum mechanics. In (81) $\mathbf{R}$ is a proper orthogonal tensor called the **rotation tensor**. It measures the local rotation that is a change of local orientation. Next, in (81) $\mathbf{U}$ and $\mathbf{v}$ define unique, positive definite, symmetric tensors, which we call the **right** (or **material**) **stretch tensor** and the left (or **spatial**) **stretch tensor**, respectively. They measure local stretching (or contraction) along their mutually orthogonal eigenvectors, that is a change of local shape.

  The positive definite and symmetric tensors $\mathbf{U}$ and $\mathbf{v}$ are introduced, so that

$$\mathbf{U}^2 = \mathbf{UU} = \mathbf{C} \qquad \mathbf{v}^2 = \mathbf{vv} = \mathbf{B}. \tag{82}$$

- **Eigenvalues and eigenvectors of strain tensors** We introduce the mutually orthogonal and normalized set of eigenvectors $\{\hat{\mathbf{N}}_a\}$ and their corresponding eigenvalues $\lambda_a, a = 1, 2, 3$, of the material tensor $\mathbf{U}$ as

$$\mathbf{U}\hat{\mathbf{N}}_a = \lambda_a\hat{\mathbf{N}}_a, \qquad |\,\hat{\mathbf{N}}_a\,| = 1, \qquad a = 1, 2, 3. \tag{83}$$

  Furthermore, after combining first eq. in (82) with (83) we obtain the eigenvalue problem for $\mathbf{C}$, i.e.

$$\mathbf{C}\hat{\mathbf{N}}_a = \mathbf{U}^2\hat{\mathbf{N}}_a = \lambda_a^2\hat{\mathbf{N}}_a. \tag{84}$$

Clearly $\mathbf{U}$ and $\mathbf{C}$ have the same orthonormal eigenvectors, i.e. the set $\{\hat{\mathbf{N}}_a\}$, called the **principal referential directions** (or **principal referential axes**). However, the corresponding positive and real eigenvalues differ. The eigenvalues of the symmetric tensor $\mathbf{U}$ are λ_a, called the **principal stretches**, while for the symmetric tensor $\mathbf{C}$ we find the squares of the principal stretches denoted by λ_a^2.

- **Spectral decomposition**

$$\mathbf{U}^2 = \mathbf{C} = \sum_{a=1}^{3} \lambda_a^2 \hat{\mathbf{N}}_a \otimes \hat{\mathbf{N}}_a \tag{85}$$

and

$$\mathbf{U} = \mathbf{C}^{1/2} = \sum_{a=1}^{3} \lambda_a \hat{\mathbf{N}}_a \otimes \hat{\mathbf{N}}_a \tag{86}$$

- **Hencky (logarithmic) strain tensor**

In the material form

$$\boldsymbol{\varepsilon}_{log} = ln\mathbf{U}. \tag{87}$$

3.8 Stress Measures used in finite elasticity

Usually stress-strain laws are given as equations relating Cauchy stress ('true' stress) σ_{ij} to left or right Cauchy-Green deformation tensor. For some computations it may be more convenient to use other stress measures. They are defined below, for convenience.

- **Cauchy (true) stress**

The Cauchy stress represents the force $dF_j^{\mathbf{n}}$ per unit deformed area ds in the solid and is defined by

$$n_i \sigma_{ij} = \lim_{ds \to 0} \frac{dF_j^{\mathbf{n}}}{ds} \tag{88}$$

- **Kirchhoff stress**

$$\boldsymbol{\tau} = J\boldsymbol{\sigma} \qquad \tau_{ij} = J\sigma_{ij} \tag{89}$$

- **First Piola-Kirchhoff (nominal) stress**

$$\boldsymbol{\Sigma} = J\mathbf{F}^{-1}\boldsymbol{\sigma} \qquad \Sigma_{Ij} = JF_{Ik}^{-1}\sigma_{kj} \tag{90}$$

- **Second Piola-Kirchhoff (material) stress**

$$\mathbf{S} = J\mathbf{F}^{-1}\boldsymbol{\sigma}\mathbf{F}^{-T} \qquad S_{IJ} = JF^{-1}_{Ik}\sigma_{kl}F^{-1}_{Jl} \tag{91}$$

As the applied theory deals with nearly or perfectly incompressible materials, we do not need to distinguish between Cauchy and Kirchhoff stresses ($J \doteq 1$ in eq. (89)).

4 Tension and bending tests of composite material

The main goal of this chapter is to find out if we are able to obtain the same results with an unimaterial computational model and a bimaterial one. For this purpose, computational simulations of uniaxial tension tests and bending tests were performed by both of the mentioned models. Next, the simulations were compared with experiments performed with real specimens of the composite material. Specimens were made from elastomer matrix and contained steel fibres. Dimensions of specimens were 125x25x2.9 mm, diameter of the fibre was 0.45mm and fibres were diverted from the longitudinal axis of the specimen by various angles: 0°, 15°, 45°, 60° a 90°.

4.1 Experiments

4.1.1 Uniaxial tension tests

The first of the experiments, which were carried out on the mechanical testing device Zwick Z020 were uniaxial tensile tests (fig. 4). Dimensions of specimens and declinations of the fibres were mentioned above. Each test with the same declination of the fibres was repeated three times with three various specimens. Before measuring, each specimen was pre-cycled in order to eliminate so called Mullins effect [25] – each specimen was loaded by a total elongation of the specimen 5 mm, then unloaded and loaded again to the same value of elongation. Each specimen was pre-cycled by four such cycles, since the fifth cycle showed no substantial change compared to the previous one.

The specimen was clamped into the testing jaws and an extensometer was placed in the middle part of the specimen before measurement. Dependency between force and elongation of the specimen was obtained as an output of these tests. The measured data was recalculated into the dependency between engineering stress and engineering strain and can be found in [23] (or in the appendix A.3).

4.1.2 Bending tests

Bending tests followed after the uniaxial tests and the specimens used in the bending tests were exactly the same pre-cycled specimens which had been used in the uniaxial tests. Each specimen was put on two supports and its loading was realized in the middle part of

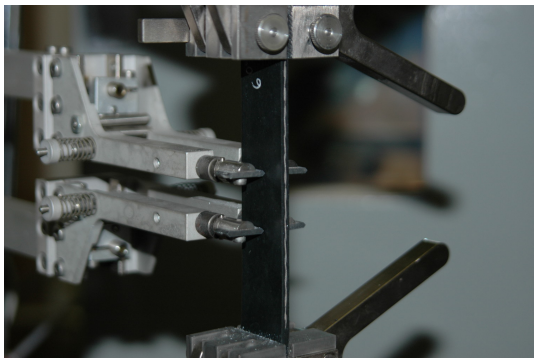

Figure 4: Uniaxial tension test.

the specimen (fig. 5). Supports and load were realized throughout the entire width of the specimen. Dependency between force and deflection of the specimen was obtained as an output of this test. The results can be found in [23] (or in the appendix A.3).

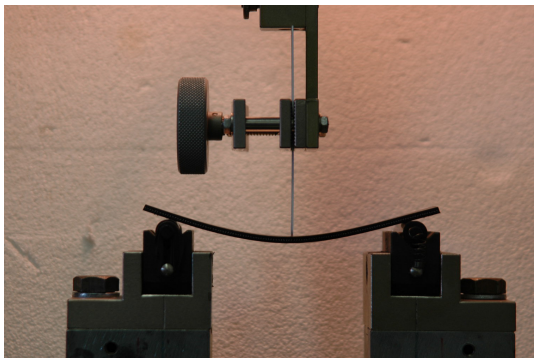

Figure 5: Bending test.

4.2 Simulations

Simulations of the above experiments were realized using two different types of models, i.e. **bimaterial** and **unimaterial** computational models.

4.2.1 Bimaterial FE model

This computational model contains two different materials (therefore bimaterial) – one for fibres and one for the matrix. Hence, geometric model of matrix (block with dimensions

125x25x2.9 mm) was created and then each fibre (cylinder with the diameter of 0.45mm) was created inside the matrix (fig. 6).

In case of simulations of uniaxial tension tests, 2-parametric Mooney-Rivlin incompressible hyperelastic model of material was used for matrix, which is introduced by a strain energy density function W (or sometimes known as Helmholz free energy W=U-T.S, where U is internal energy, T is temperature and S is entropy) in the form

$$W = c_1(I_1 - 3) + c_2(I_2 - 3) \tag{92}$$

where c_1, c_2 are material parameters and I_1, I_2 are invariants of right Cauchy-Green tensor of deformation. In case of simulations of bending tests, the material properties of the matrix were defined by incompressible Yeoh third order model of material with the following form of the strain energy density function

$$W = d_1(I_1 - 3) + d_2(I_1 - 3)^2 + d_3(I_1 - 3)^3. \tag{93}$$

Material parameters c_1, c_2 or d_1, d_2, d_3 were determined by standard procedure, i.e. from experiments with the elastomer matrix without fibres. This includes the following experiments: uniaxial tension test, equibiaxial tension test and planar tension test. Specimens for such experiments of pure elastomer matrix were pre-cycled by 4 cycles and loaded to 100 % strain. A reason of such pre-cycling was change in material properties of elastomer matrix – so called Mullins effect [25]. A stress-strain curve after fifth cycle was almost the same as in the fourth cycle, therefore, only four cycles were used for pre-cycling. After pre-cycling, the mentioned experiments of pure elastomer matrix were performed and the measured data was used for determination of the material parameters. The following material parameters were found by using the least square method: $c_1 = 0.4727MPa, c_2 = 0.6992MPa$ and $d_1 = 4.034MPa, d_2 = -306.48MPa, d_3 = 16478MPa$. Process of determination (curve fitting) of these material parameters is described in detail in chapter 3.6.

The choice of hyperelastic constitutive model was based on its availability in some FEM software and ability of a good approximation of experimental data. As was mentioned above, for simulation of uniaxial tension tests of composites Mooney-Rivlin hyperelastic model was used for matrix while Yeoh's model was used in case of simulations of bending tests. The reason of different hyperelastic models is given by the maximal achieved strain

at each kind of test (tension or bending). The maximal strain differs at different declinations of the fibres, but in general, the max. strain was around 50 % in case of tension tests (the best approximation between experiments and hyperelastic constitutive models in such range of strain was given by 2-parametric Mooney-Rivlin model) and only 4 % in case of bending tests (the best approximation was achieved by Yeoh third order model).

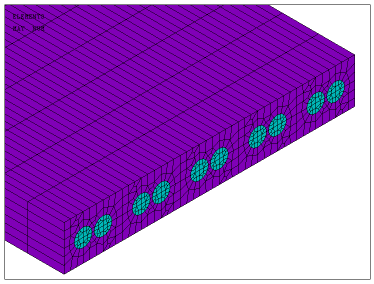

Figure 6: Bimaterial computational model.

The steel fibres were described by linear elastic material constitutive model with well known material parameters (Young's modulus 210 GPa and Poisson's ratio 0.3).

4.2.2 Unimaterial FE model

In the unimaterial computational model material behaviour of the composite material was described by only one model of material (therefore unimaterial model), which describes behaviour both of matrix and fibres. Hence, only a 3D geometric model of the composite specimen was created (a block 125x25x2.9mm) without distinguishing between the matrix and fibres and without any geometric model of the fibres. There are many anisotropic hyperelastic models based on such principle (reinforcement effect of the fibres is included into the strain energy function). Some of these models are for fibres which are linear elastic; others are to able work with a nonlinear behaviour of the fibres (especially constitutive models in the field of biomechanics). However, all these models work with unit vector of undeformed fibre's direction and all these models are based on an assumption of infinitely thin fibre. Some of these models can be found in [19], [20],[4], [16].

The 3D geometric model of the composite specimen was divided into three layers as it is depicted in fig. 7. Two outer layers (in purple color) correspond to pure elastomer matrix

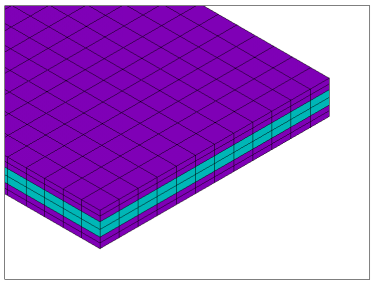

Figure 7: Unimaterial computational model.

and the middle layer (the blue one) corresponds to both fibres and elastomer matrix with volume fraction of the fibres $v_f = 0.3534$. Thickness of the middle layer equals to the diameter of the fibres, i.e. 0.45 mm, and as it was mentioned above, the 3D model of the fibres is not considered in this type of computational model. In case of simulations of uniaxial tension tests the material description of the middle layer (i.e. matrix+fibres) was realized by the following anisotropic hyperelastic model (it is the only one anisotropic hyperelastic model which is implemented in ANSYS software ; more about this can be found in [2] chapter "Hyperelasticity")

$$W = c_1(I_1 - 3) + c_2(I_2 - 3) + k_2(I_4 - 1)^2 \tag{94}$$

and in case of bending tests the following model was used

$$W = d_1(I_1 - 3) + d_2(I_1 - 3)^2 + d_3(I_1 - 3)^3 + k_2(I_4 - 1)^2. \tag{95}$$

The material description of the outer layers (only matrix) was realized by the same anisotropic models, i.e. eq. (94) in case of tension tests and eq. (95) in case of bending tests, but the material parameter k_2 that corresponds to the fibres only (as it will be described below) was set to zero.

Material parameters c_1, c_2 or d_1, d_2, d_3 are exactly the same ones as the parameters mentioned in the previous chapter. By comparing strain energy density function (94) with (92), or (95) with (93), we can see that both of these functions differ only in the term

$$k_2(I_4 - 1)^2. \tag{96}$$

This term relates to the fibres only, while the other terms relate to the matrix only. Invariant I_4 is square of the stretch ratio of the fibres in the fibres direction and is defined

as

$$I_4 = \mathbf{A}.\mathbf{C}\mathbf{A} \tag{97}$$

where $\mathbf{A}$ is unit vector of the fibres direction and $\mathbf{C}$ is right Cauchy-Green tensor of deformation.

Material parameter k_2 was determined under the following assumption – in case of tension in fibres direction a stress contribution of matrix is very small (and can be neglected) in comparison with the stress contribution of steel fibres. In such case, an average stress of composite is basically given by stress in the fibre. Then we can calculate the stress in the fibre for the known stretches of the fibre and determine material parameter k_2, which was in this case $k_2 = 9180$ MPa. Determination of this material parameter is described in chapter 9 in details.

4.3 Discussion of results

Results of computational simulations both for uniaxial tension tests and bending tests for various declinations of fibres are depicted in appendix A.3 in comparison with the corresponding experiments.

Uniaxial tension tests

First, let's compare the results obtained by both computational simulations, i.e. by bimaterial and unimaterial computational models. All results are depicted in appendix A.3, where the bimaterial model is always rendered by a red curve, the unimaterial one by a green curve. As we can see from the figures related to the individual declination of the fibres (fig. 20 to fig. 24), both models give almost the same results. Remind that both computational models have the same models of material related to the matrix (including material constants) and differ only in the material models related to the fibres. However, the material constant k_2 was determined so that the stress in the fibres of the unimaterial model was the same as the stress in the fibres of the bimaterial model. Therefore, both models should give the same results by principle.

In tension test with longitudinal fibres (under 0° - fig. 20), the unimaterial model appears slightly stiffer than the bimaterial one. Here the stiffness of longitudinal fibres constraints

any elongation of the specimen so that most deformation occurs between the jaws and the fibres as shear of the rubber layer. While the thickness of this rubber layer is constant in the unimaterial model, in the bimaterial one the same thickness occurs in the axes of fibres only and the rubber layer is thicker anywhere else, which makes the specimen more compliant.

Both model curves in fig. 24 should be identical in an ideal case. However the unimaterial model appears some 10% more compliant than the bimaterial one. This difference can be explained by the absence of steel in the unimaterial model where the fibres are replaced by an additional member in the strain energy density function. The percentage of steel in the material does not correspond to the percentual decrease of stiffness of the unimaterial model because of two features of the bimaterial model:

- all the cross sections of the specimen contain some amount of rubber so that stiffness of no cross section corresponds to the very high stiffness of steel, and the specimen is more compliant,
- rubber in a vicinity of steel undergoes a nearly uniform triaxial stress state in tension which emphasizes the volumetric component of strain and makes the material less compliant.

It's obvious from figures 20 to 24 that difference between the results of simulations using both computational models is maximally 10% (fibres under 90°, fig. 24). Hence, we can say that both models under **tension** load give nearly the same results, therefore the bimaterial model can be replaced (with advantages) by the unimaterial one. Comparing the results of simulations and experiments we can see that the agreement between the results is good in case of declination of the fibres being 0° (fig. 20) (simulations are at the upper bound of the confidential interval), but in the other cases simulations and experiments disagree (fig. 21 to fig. 24). Determining of material parameters related to the matrix (parameters c_1, c_2, d_1, d_2 and d_3) was carried out on the basis of the material tests of the pure matrix. As it was mentioned in the previous paragraph, each specimen of the pure matrix was pre-cycled by 100% of strain, then unloaded and loaded again to the same strain value. The pre-cycling was repeated four times until the stress-strain curve showed no substantial change. Composite specimens used in the uniaxial tension tests were also pre-cycled, but by

a different strain amplitude. Each composite specimen, regardless of the fibres declination, was loaded by 5 mm displacement. Due to the various declinations of the fibres, various values of the strain were generated in the specimens and basically each specimen (with various declination of the fibre) was pre-cycled by a different strain amplitude. Moreover, the stresses and strains are not homogenous in the specimens, but they vary throughout the specimen. Hence, it is impossible to carry out such composite experiments where the specimen would be loaded by the same strain amplitude along its whole length.

A feasible solution how to improve the agreement between simulations and experiments can be application of a material model which is able to take into account the Mullins effect [25] including the various strain amplitudes, e.g. Ogden-Roxburg model [27]. However, in case of unimaterial computational model the Ogden-Roxburg model has not been implemented yet in any known FEM software, therefore, for practical use of this model it is necessary to implement it first into a FEM software.

Consequently, a new group of experiments were caried out in order to check out if Mullins effect can really cause the above differences between simulations and experiments. For this purpose, another elastomer matrix was chosen showing negligible Mullins effect. It is evident from fig. 8 and from others results presented in [11] that simulations are in good agreement with the tests for all fibre declinations. Hence, the hypothesis was confirmed that Mullins effect is responsible for the differences between simulations and experiments.

Bending tests

The bending test experiments contain the same problem as in case of tension tests, i.e. simulations and experiments can not be compared due to various strain amplitude in the pre-cycling of specimens. As we can see from the results in appendix A.3 related to the bending tests, results of simulations disagree with experiments except the case with zero declination of the fibres. I think that this discrepancy is caused again by different amplitude in the pre-cycling in the all specimens, even in the specimen with zero declination of the fibres. However, the agreement between simulations and experiments is good in such case of declination, because zero declination means that fibres are substantial part of composite material which carries most of the load (in other words contribution of the matrix is insignificant). Therefore Mullins effect does not influence the results. For illustration,

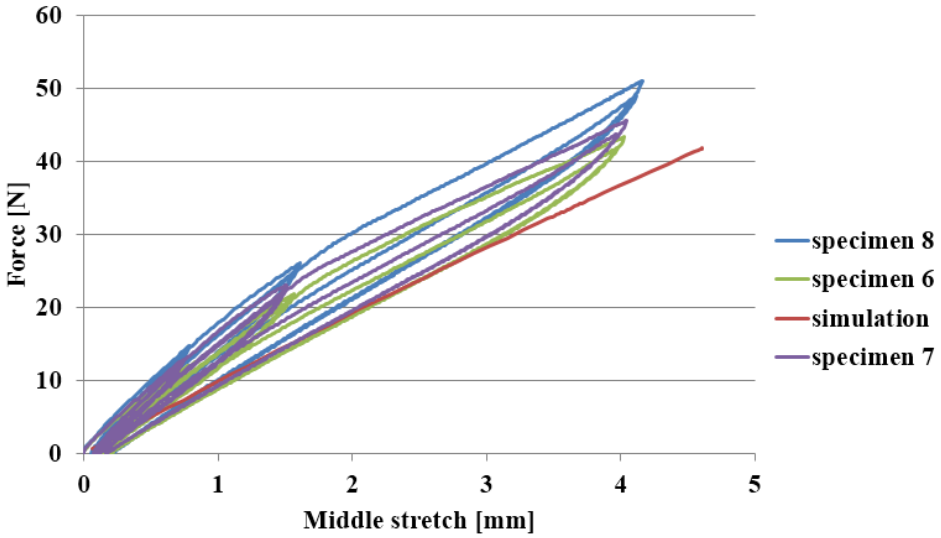

Figure 8: Results of the tension test and its simulation for 45° declination of fibres.

figure 30 represents the influence of cycling, where specimens 1 and 2 were cycled to 5 mm of the total elongation of the specimen, while specimen 3 was cycled up to 10 mm of total elongation. The difference in the results is obvious.

In bending test with longitudinal fibres (under 0° - fig. 25), the unimaterial model appears slightly stiffer than the bimaterial one. It might be explained by different distribution of steel throughout the height of the specimen. The structure of the unimaterial model is sandwich-like, i.e. fictive fibres are assumed to be uniformly distributed in the middle layer with thickness of 0.45 mm, and their tension stiffness does not depend on the distance from the neutral axis of bending. In contrast, the fibres in the bimaterial model are cylindrical (with the same diameter of 0.45 mm) so that the amount of steel is decreasing with distance from the neutral axis, which makes the model more compliant.

When comparing the results of simulations with experiments we can see that both models disagree except for the declination of 90° (fig. 29). At first glance, it might seem that both models give the same results in case of declination 0° and 15° (fig. 25 and fig. 26), but it is not the case. In this case both models give the same results till some magnitude of deflection, but above a certain limit the unimaterial model begins with unstable behaviour, i.e. the force is almost constant for any deflection and the simulation fails.

It was found out upon closer examination of the material model (94) or (95) that this model is based on assumption of infinitely thin fibres, i.e. fibres have zero bending stiffness. When we go back to the results of simulations we can see that in case of declinations 0° and 15° (obr. 25 and obr. 26) after certain limit an instability occurred. We can see very well in case of declinations 45° and 60° (fig. 27 and fig. 28) that the unimaterial model (i.e. model without bending stiffness of the fibres) gives significantly softer results than the bimaterial model (i.e. model with bending stiffness of the fibres). In case of declination of 90° (fig. 29), the agreement between both models is very good, since fibres do not contribute to the composite stiffness significantly (it is basically bending of the elastomer matrix), therefore both models (with the same material models and material parameters) must give the same results. New experiments with negligible stiffness of the textile fibres were carried out in order to check out if the unimaterial model is able to provide results that correspond to experiments. It was verified in [11] that the anisotropic hyperelastic constitutive model (in a polynomial form) is able to simulate results of tension and bending tests of fibre composites showing large strains credibly under the following conditions:

- elastomer matrix shows negligible Mullins effect
- bending stiffness of fibres is negligible.

Next, the sensitivity analysis in [22] and fig. 9 show that bending stiffness provided by the unimaterial model is limited. This model gives the same results as the bimaterial one only when Young's modulus of the fibres is up to 100 MPa. A further increase of Young's modulus results in disagreement between both models, and from a certain limit a further increasing of Young's modulus (10 000MPa) does not make sence. Based on these results it is obvious that the unimaterial model is not able to include bending stiffness of fibres.
In contradiction to tension test, the bending test simulations with declination angle of fibres 15° show a higher stiffness of the bimaterial model in comparison with experiments (see fig. 26). This discrepancy may be caused by a specific behaviour of these specimens: during bending only two corners (situated in the diagonal closer to the direction of fibres) of the specimen remain in contact with the lateral supports and the other two corners go up. The boundary conditions prescribed in the FE model, however, constrain the vertical displacement of both ends of the specimen, i.e. of all its four corners, which makes the

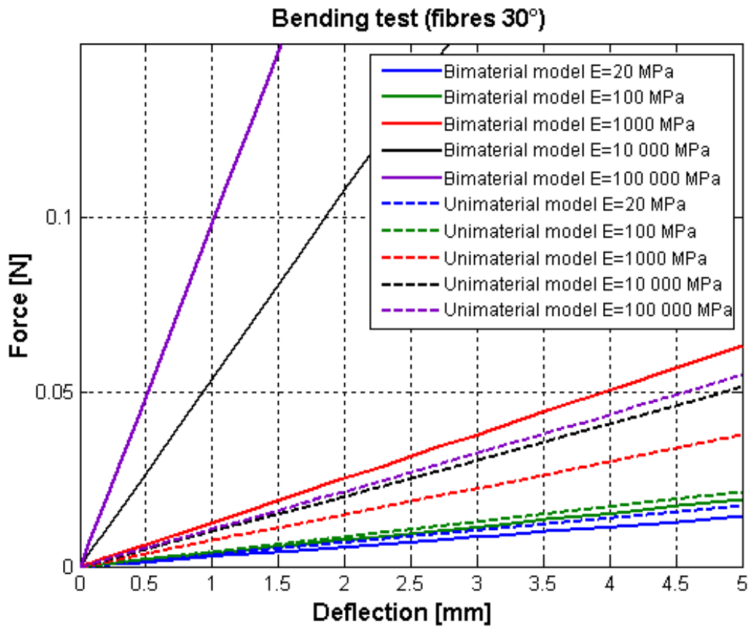

Figure 9: Bending test - impact of Young's modulus.

specimen stiffer

After summarizing the results, we can say that in case of uniaxial tension tests both models give the same results. Next, it was find out that in the case of bending tests the unimaterial model doesn't include the bending stiffness of the fibres, therefore, the model is not able to give correct results. Hence, the unimaterial model can be used in such applications where fibres are loaded in tension (or compression) and/or in such application where fibres don't have significant bending stiffness (e.g. composite material with textile fibres).

It was found out that in case of the specific rubber used in experiments the Mullins effect influences the results significantly, since (due to the various declinations of the fibres) strains in the specimens are locally varied and also stresses and strains are not homogenous throughout the specimen. Then each part of the specimen is loaded by different strain and due to the Mullins effect mentioned above different stress-strain curves are applied.

The only one paper was found, after many searches on this topic, published by Spencer and Soldatos [32] in 2007. They introduced a new unimaterial model which is able to include bending stiffness of the fibres. However, this model is based on Cosserat continuum and is quite complicated for practical application. Hence, next chapter introduces basic knowledge on Cosserat continuum and a part of chapter 6 deals with simplification of this theory.

5 Cosserat theory of continuum

Classical continuum mechanics is based on the fundamental idea that all material bodies possess continuous mass densities, and that the laws of motion and the axioms of constitution are valid for every part of the body no matter how small they may be. A loss of accuracy requiring a more general description may occur in classical continuum mechanics if the response of a body to an external physical effect is sought, in which the length scale is comparable to the average grain or molecular size contained in the body, because the granular or molecular constituents of the body are excited individually. In this case, the intrinsic motions of the constituents (microelements) must be taken into account. This situation prevails in practical applications when the material under consideration is a composite material containing macromolecules, fibres, and grains [10]. The existence and basis of couple stress in elasticity was postulated by Voigt [35] in 1887 in connection with polar molecules. He took an assumption into account that the interaction between two parts of the body through an area element is transmitted not only by a force vector, but also by a moment vector. Such assumption consists in the fact that not only force stresses, but also couple stresses must be taken into account. The complete theory was developed in 1909 by brothers E. and F. Cosserat [5]. In their theory being nonlinear from the very beginning , the deformation of the body is described by a displacement vector and an independent rotation vector, therefore each material element has six degrees of freedom. The Cosserat brothers formulated balance equations for force stress and couple stress, but they didn't formulate constitutive equations.

Next works dealing with Cosserat theory were concentrated on the simplified Cosserat theory (known as indeterminate couple stress theory or Cosserat pseudo continuum). In this theory, the rotation vector is not an independent vector, although force and couple stresses are still taken into account. The most important works are those by Truesdell and Toupin [34], Mindlin and Tiersten [24], Toupin [33] and Eringen [6]. Next in 1964 Eringen and Suhubi [7] introduced a general theory of a nonlinear microelastic continuum in which the balance laws of continuum mechanics are supplemented with additional ones, and intrinsic motion of microelements contained in a macrovolume were taken into account. This theory was renamed later to the micropolar theory. Basics of thermo-elasticity in terms of

Cosserat continuum were formulated by Nowacki in 1968 [26].

This chapter was taken mainly from [10] and [26].

5.1 Deformation and microdeformation

I will distinguish between *material* and *space* description in the following text. *Material* (or reference) description works with particles X determined by position (X_1, X_2, X_3) and attention is payed to the particle - we are observing what will happen with the particle during the motion. Independent variables are particle and time. Material coordinates are usually used in so called Lagrangian description.

The current configuration is taken as the reference configuration in the *space* description or Eulerian description. Independent variables are position (x_1, x_2, x_3) and time and we are observing what will happen in a fixed part of the space.

A material point P of a body B having volume V and surface S in its undeformed and unstressed state may be defined by its rectangular coordinates X_1, X_2 and X_3. If the body is allowed to move and deform under some external loads, it will occupy a region having volume v and surface s. Referred to the same rectangular frame of reference, the new position of the point P will be x_1, x_2 and x_3 (fig. 10). The deformation of the body at time t may be prescribed by a one-to-one mapping

$$x_k = x_k(X_1, X_2, X_3, t), \quad k = 1, 2, 3 \tag{98}$$

or its inverse form

$$X_K = X_K(x_1, x_2, x_3, t), \quad K = 1, 2, 3. \tag{99}$$

We now consider a volume element ΔV enclosed within its surface ΔS in the undeformed body. Let the center of mass of ΔV have the position vector $\mathbf{X}$. All materials possess certain granular or fibrous structures with different sizes and shapes. If the physical phenomenon under study has a certain characteristic length (such as wavelength), comparable with the size of grains in the body, then the microstructure of the material must be taken into consideration. In such situations, classical continuum mechanics should be modified by considering the effect of the granular or fibrous character of the medium.

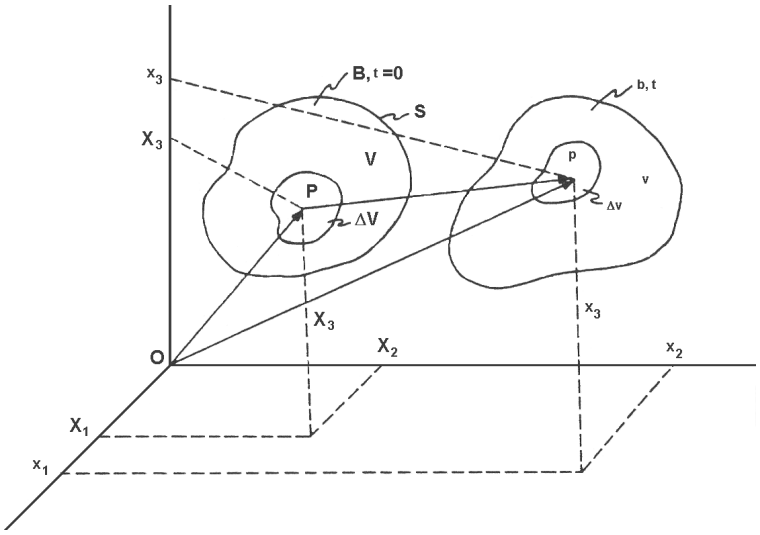

Figure 10: Material and spatial coordinates. (reprint from [10])

Suppose that the element $\Delta V + \Delta S$ contains N discrete micromaterial elements $\Delta V^{(\alpha)} + \Delta S^{(\alpha)} (\alpha = 1, 2, ..., N)$. The position vector of a material point in the αth microelement may be expressed as

$$\mathbf{X}^{(\alpha)} = \mathbf{X} + \boldsymbol{\Xi}^{(\alpha)} \tag{100}$$

where $\boldsymbol{\Xi}^{(\alpha)}$ is the position of a point in the microelement relative to the center of mass of $\Delta V + \Delta S$ (fig. 11). Upon the deformation of the body, the position of the αth particle will be

$$\mathbf{x}^{(\alpha)} = \mathbf{x} + \boldsymbol{\xi}^{(\alpha)} \tag{101}$$

where $\boldsymbol{\xi}^{(\alpha)}$ is the new relative position vector of the point originally located at $\mathbf{X}^{(\alpha)}$. The relative position vector depends not only on $\mathbf{X}, t$, but also on $\boldsymbol{\Xi}^{(\alpha)}$, i.e.

$$\boldsymbol{\xi}^{(\alpha)} = \boldsymbol{\xi}^{(\alpha)}(\mathbf{X}, \boldsymbol{\Xi}^{(\alpha)}, t) \tag{102}$$

Eringen and Suhubi [7], [8] and Eringen [9] have constructed a general theory in which (102) is linear in $\boldsymbol{\Xi}^{(\alpha)}$. The basic assumption underlying this theory is the:
The material points in $\Delta V + \Delta S$ undergo a homogeneous deformation about their center of mass.

On the basis of the motion and deformation of the microelement we can distinguish:
Micromorphic materials - microelement may be deformed, moved and rotated.

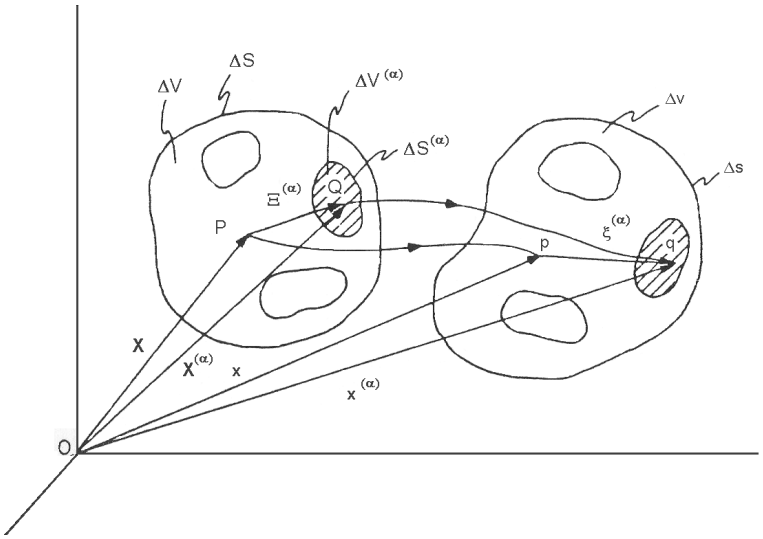

Figure 11: Deformation of microvolume. (reprint from [10])

Micropolar theory of elasticity (or Cosserat theory of elasticity) - this theory admits only rigid microrotations of the microvolume elements about the center of mass of the volume element.

Constrained Cosserat theory (or Indeterminate couple stress theory)- microrotations and macrorotations are the same, only rigid motion of microelements is possible.

5.2 Strain and microstrain tensors

On the basis of the motion and inverse motion of a material point in a microelement may be written [10]

$$x_k^{(\alpha)} = x_k(\mathbf{X}, t) + \xi_k^{(\alpha)} \tag{103}$$

$$X_K^{(\alpha)} = X_K(\mathbf{x}, t) + \Xi_K^{(\alpha)}, \tag{104}$$

where vectors $\xi_k^{(\alpha)}$ and $\Xi_K^{(\alpha)}$ from fig. 11 are given

$$\xi_k^{(\alpha)} = \chi_{kK}(\mathbf{X}, t)\Xi_K^{(\alpha)}, \tag{105}$$

$$\Xi_K^{(\alpha)} = \mathfrak{X}_{Kk}(\mathbf{x}, t)\xi_k^{(\alpha)}, \tag{106}$$

and where $\chi_{kK}(\mathbf{X},t)$ and $\mathfrak{X}_{Kk}(\mathbf{X},t)$ are nine scalar functions in general in micromorphic materials (for details see [10]).

The square of the arc length is calculated by forming

$$(ds^{(\alpha)})^2 = d\mathbf{x}^{(\alpha)}.d\mathbf{x}^{(\alpha)} = (C_{KL} + 2\Gamma_{KML}\Xi_M + \frac{\partial\chi_{kM}}{\partial X_K}\frac{\partial\chi_{kN}}{\partial X_L}\Xi_M\Xi_N)dX_k dX_L +$$

$$+2(\Psi_{KL} + \chi_{kL}\frac{\partial\chi_{kM}}{\partial X_K}\Xi_M)dX_K d\Xi_L + \chi_{kK}\chi_{kL}d\Xi_K d\Xi_L \tag{107}$$

where

$$C_{KL}(\mathbf{X},t) = \frac{\partial x_k}{\partial X_K}\frac{\partial x_k}{\partial X_L} \tag{108}$$

$$\Psi_{KL}(\mathbf{X},t) = \frac{\partial x_k}{\partial X_K}\frac{\partial \chi_k}{\partial X_L} \tag{109}$$

$$\Gamma_{KLM}(\mathbf{X},t) = \frac{\partial x_k}{\partial X_K}\frac{\partial \chi_{kL}}{\partial X_M}. \tag{110}$$

C_{KL} is the commonly known Cauchy-Green tensor of deformation, tensors Ψ_{KL} and Γ_{KLM} are new tensors of microdeformation.

Let's introduce the displacement vector $\mathbf{u}^{(\alpha)}$ (fig. 12)

$$\mathbf{u}^{(\alpha)} = \mathbf{x} - \mathbf{X} + \boldsymbol{\xi} - \boldsymbol{\Xi} = \mathbf{u} + \boldsymbol{\xi} - \boldsymbol{\Xi} \tag{111}$$

where

$$\mathbf{u} = \mathbf{x} - \mathbf{X} \tag{112}$$

and

$$U_L = \mathbf{u}.\mathbf{I}_L = x_k\delta_{kL} - X_L, \tag{113}$$

$$u_l = \mathbf{u}.\mathbf{i}_l = x_l - X_K\delta_{Kl}. \tag{114}$$

By partial differentiation of the last two equations, we obtain

$$\frac{\partial x_k}{\partial X_K} = \left(\delta_{LK} + \frac{\partial U_L}{\partial X_K}\right)\delta_{kL} \tag{115}$$

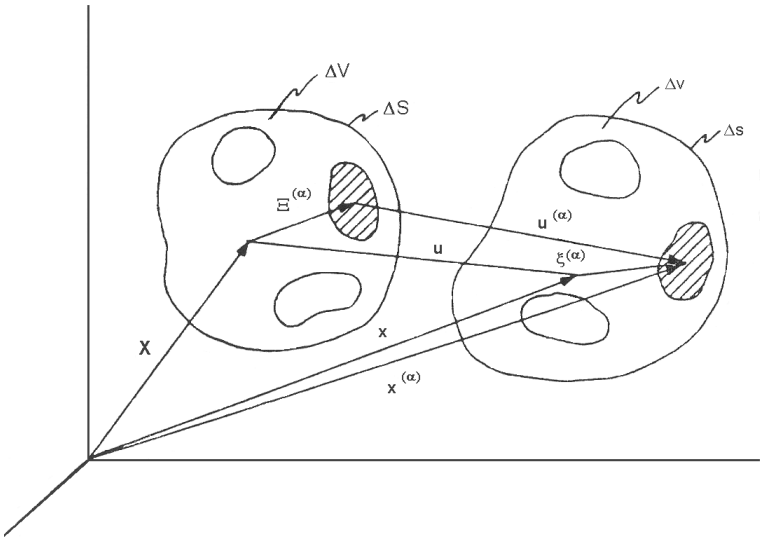

Figure 12: Displacement vectors. (reprint from [10])

$$\frac{\partial X_K}{\partial x_k} = \left(\delta_{lk} - \frac{\partial u_l}{\partial x_k}\right)\delta_{Kl} \tag{116}$$

Similary, we introduce the microdisplacement tensors $\Phi(\mathbf{X}, t)$ (material representation) and $\phi(\mathbf{x}, t)$ (spatial representation)

$$\chi_{kK} = (\delta_{LK} + \Phi_{LK})\delta_{kL} \tag{117}$$

$$\mathfrak{X}_{Kk} = (\delta_{lk} + \phi_{lk})\delta_{Kl}. \tag{118}$$

Substituting (115) and (117) into tensors (108), (109) and (110), we can write

$$C_{KL} = \delta_{KL} + \frac{\partial U_K}{\partial X_L} + \frac{\partial U_L}{\partial X_K} + \frac{\partial U_M}{\partial X_K}\frac{\partial U_M}{\partial X_L} \tag{119}$$

$$\Psi_{KL} = \delta_{KL} + \Phi_{KL} + \frac{\partial U_L}{\partial X_K} + \frac{\partial U_M}{\partial X_K}\Phi_{ML} \tag{120}$$

$$\Gamma_{KLM} = \frac{\partial \Phi_{KL}}{\partial X_M} + \frac{\partial U_N}{\partial X_K}\frac{\partial \Phi_{NL}}{\partial X_M}. \tag{121}$$

These relations are valid in general for micromorphic materials and for nonlinear theory.

5.3 Micropolar and constrained Cosserat theory

We now consider a special class of materials in which the state of microdeformation can be described by a local rigid motion of the microelements. Materials consisting of rigid fibres or elongated grains fall into this category. Mathematically, this specialization in the linear theory is obtained by setting

$$\Phi_{KL} = -\Phi_{LK} \qquad \text{(material notation)} \tag{122}$$

$$\phi_{kl} = -\phi_{lk} \qquad \text{(spatial notation)} \tag{123}$$

where Φ_{KL}, ϕ_{kl} are material and spatial microdisplacement tensors, respectively. It doesn't make sence to distinguish between material and spatial coordinates in the linear theory since it holds

$$\Phi_{KL} = (\delta_{KM} + \Phi_{KM})\phi_{ml}\delta_{Mm}\delta_{lL} \tag{124}$$

and when we omit members in product

$$\Phi_{KL} \approx \phi_{ml}\delta_{Km}\delta_{lL}. \tag{125}$$

Next, according chapter IV. from [10], it is apparent that vector $\boldsymbol{\Phi}$

$$\Phi_K = \frac{1}{2}\epsilon_{KLM}\Phi_{ML}, \qquad \Phi_{KL} = -\epsilon_{KLM}\Phi_M, \tag{126}$$

represents an angular rotation of a microelement about the center of mass of the deformed macrovolume element, i.e. vectors $\boldsymbol{\Phi} \simeq \boldsymbol{\phi}$ represent ***microrotation***.

Constraint Cosserat theory means that microrotations ϕ_k are the same as macrorotations φ_k, i.e.

$$\phi_k = \varphi_k = \frac{1}{2}\epsilon_{klm}\frac{\partial u_m}{\partial x_l}. \tag{127}$$

Velocity of the macroelement

The velocity field in material description is given by the following equation

$$\mathbf{V}(\mathbf{X}, t) = \dot{\mathbf{x}}(\mathbf{X}, t) = \frac{\partial \mathbf{x}(\mathbf{X}, t)}{\partial t}, \tag{128}$$

where $\mathbf{X}$ is constant. If we substitute herein equation (99) for $\mathbf{X}$, we can write

$$\mathbf{V}(\mathbf{X}, t) = \mathbf{V}[\mathbf{X}(\mathbf{x}, t), t] = \mathbf{v}(\mathbf{x}, t), \tag{129}$$

where $\mathbf{v}(\mathbf{x},t)$ is a velocity field in the spatial description. Note that velocity relations metioned above describe the movement of center of mass P or p of macroelement $\Delta V+\Delta S$ or $\Delta v+\Delta s$, respectively.

Relative velocity of the microelement

Let's establish the relative velocity of the point $\mathbf{x}+\boldsymbol{\xi}$ to the center of mass p (fig. 12). Because of equation (105), we can write for velocity of a microparticle

$$\dot{\xi}_l = \dot{\chi}_{lK}(\mathbf{X},t)\Xi_K \tag{130}$$

and on replacing Ξ_K by (106) we obtain

$$\dot{\boldsymbol{\xi}} = \boldsymbol{\nu}_k(\mathbf{x},t)\xi_k \tag{131}$$

or

$$\dot{\xi}_l = \nu_{lk}\xi_k, \tag{132}$$

where

$$\boldsymbol{\nu}_k(\mathbf{x},t) = \dot{\boldsymbol{\chi}}_{\boldsymbol{K}}(\mathbf{X},t)\mathfrak{X}_{Kk}(\mathbf{x},t) \tag{133}$$

and

$$\nu_{lk} = \dot{\chi}_{lK}\mathfrak{X}_{Kk}. \tag{134}$$

The three vectors $\boldsymbol{\nu}_k$ defined by equation (133) are called gyration vectors, and their components ν_{lk} form the gyration tensor.

Gyration tensor ν_{lk} is related to the moment of inertia. In case of moment of inertia the position of particles is multiplied by weighting factor - weight of particles, while gyration tensor depends only on the particles position (weight of particles is not considered).

By substituting to eg. (134) from equations (117) and (118) we get

$$\nu_{kl} = -\epsilon_{klM}\dot{\Phi}_M - \epsilon_{kKM}\epsilon_{Klm}\dot{\Phi}_M\phi_m. \tag{135}$$

In case of the linear theory we can write

$$\nu_{kl} \approx -\epsilon_{klM}\dot{\Phi}_M \simeq -\epsilon_{klm}\dot{\phi}_m. \tag{136}$$

On introducing an axial vector ν_k, called the microgyration vector, by the formula

$$\nu_k = \frac{1}{2}\epsilon_{klm}\nu_{ml} \qquad\qquad \nu_{kl} = -\epsilon_{klm}\nu_m, \tag{137}$$

then by comparing two last equations and with regard to the constraint Cosserat theory, we get

$$\nu_m = \dot{\phi}_m = \dot{\varphi}_m = \frac{1}{2}\epsilon_{mlk}\frac{\partial \dot{u}_k}{\partial x_l}. \tag{138}$$

Then we repeat the mentioned process of determination of relative velocity and determine this relative velocity again, but now we determine the velocity of material point $\mathbf{X} + \boldsymbol{\Xi}$ relatively to the center of mass P (obr. 12). With help of eq. (106), we can write

$$\dot{\Xi}_L = \dot{\mathfrak{X}}_{Lk}(\mathbf{x}, t)\xi_k \tag{139}$$

and when substituting for ξ_k from equation (105) we get

$$\dot{\Xi}_L = \dot{\mathfrak{X}}_{Lk}(\mathbf{x}, t)\chi_{kK}(\mathbf{X}, t)\Xi_K \tag{140}$$

By introducing the gyration tensor in the material description

$$\mathfrak{N}_{KL} = \chi_{kK}(\mathbf{X}, t)\dot{\mathfrak{X}}_{Lk}(\mathbf{x}, t), \tag{141}$$

we can rewrite the last equation into the form

$$\dot{\Xi}_L = \mathfrak{N}_{KL}\Xi_K. \tag{142}$$

Substituting to the (141) from equations (117) and (118) we get

$$\mathfrak{N}_{KL} = -\epsilon_{KLm}\dot{\phi}_m - \epsilon_{Lkm}\epsilon_{kKM}\Phi_M\dot{\phi}_m. \tag{143}$$

In case of linear theory we can consider that

$$\mathfrak{N}_{KL} \approx -\epsilon_{KLm}\dot{\phi}_m \simeq -\epsilon_{KLM}\dot{\Phi}_M. \tag{144}$$

Since microgyration tensor in material description can be written

$$\mathfrak{N}_{KL} = -\epsilon_{KLM}\mathfrak{N}_M, \tag{145}$$

then we can see by comparing of two last equations that

$$\mathfrak{N}_M = \dot{\Phi}_M. \tag{146}$$

And for linear constraint Cosserat theory we'll find then

$$\dot{\boldsymbol{\phi}} = \dot{\boldsymbol{\varphi}} = \dot{\boldsymbol{\Phi}} = \boldsymbol{\nu} = \boldsymbol{\mathfrak{N}}. \tag{147}$$

Total velocity

Total velocity of material point $\mathbf{X}+\boldsymbol{\Xi}$ is then given as

$$\mathbf{V}^{(\alpha)} = \mathbf{V} + \dot{\boldsymbol{\Xi}}^{(\alpha)} = \mathbf{V} + \mathfrak{N}_{KL}\Xi_K^{(\alpha)} = \mathbf{V} + \dot{\boldsymbol{\varphi}}^{(\alpha)}. \tag{148}$$

Similarly, the total velocity of the point $\mathbf{x}+\boldsymbol{\xi}$ is given

$$\mathbf{v}^{(\alpha)} = \mathbf{v} + \dot{\boldsymbol{\xi}}^{(\alpha)} = \mathbf{v} + \nu_{lk}\xi_k^{(\alpha)} = \mathbf{v} + \dot{\boldsymbol{\varphi}}^{(\alpha)}. \tag{149}$$

5.4 Force stress and couple stress

This chapter introduces force and moment (couple) stresses according to [26].

Let us imagine a volume element ΔV separated from the body and bounded by surface ΔS; the interactions between the particles inside and outside the separated volume are transmitted across the surface ΔS. The transmission of the interactions across the arbitrary element dS located on the surface ΔS is expressed by the force $\mathbf{t}$dS and the moment $\mathbf{l}$dS. Consider the point $\mathbf{x}$ of an elastic body. To determine the stresses acting at this point, let us imagine three coordinate planes passing through this point and perpendicular to the axes of a rectangular Cartesian coordinate system. Let $\mathbf{t}^{(1)}$ denote a **force**-stress vector acting on the surface element $dA_1 = dx_2dx_3$ and $\mathbf{l}^{(1)}$ a similar **couple**-stress vector. Vectors $\mathbf{t}^{(1)}$ and $\mathbf{l}^{(1)}$, both called traction in this theory, and their components, i.e. force stresses σ_{1j} and couple stresses m_{1j} are shown in fig. 13.

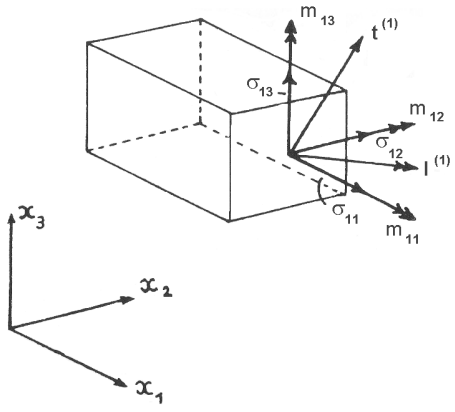

Figure 13: Force and couple stresses. (reprint from [26])

It is obvious from the fig. 13 that

$$\mathbf{t}^{(1)} = (\sigma_{11}, \sigma_{12}, \sigma_{13}), \quad \mathbf{l}^{(1)} = (m_{11}, m_{12}, m_{13}) \tag{150}$$

and similarly vectors in other coordinate planes

$$\mathbf{t}^{(2)} = (\sigma_{21}, \sigma_{22}, \sigma_{23}), \quad \mathbf{l}^{(2)} = (m_{21}, m_{22}, m_{23})$$

$$\mathbf{t}^{(3)} = (\sigma_{31}, \sigma_{32}, \sigma_{33}), \quad \mathbf{l}^{(3)} = (m_{31}, m_{32}, m_{33}). \tag{151}$$

When we consider an infinitesimal tetrahedron according to fig. 14, then

$$\mathbf{t}dS = \mathbf{t}^{(1)}dS_1 + \mathbf{t}^{(2)}dS_2 + \mathbf{t}^{(3)}dS_3 \tag{152}$$

$$\mathbf{l}dS = \mathbf{l}^{(1)}dS_1 + \mathbf{l}^{(2)}dS_2 + \mathbf{l}^{(3)}dS_3. \tag{153}$$

By introducing

$$dS_i = dSn_i, \quad n_i = cos(n, x_i), \tag{154}$$

equations (152) and (153) can be then rewritten into the form

$$\mathbf{t} = \mathbf{t}^{(1)}n_1 + \mathbf{t}^{(2)}n_2 + \mathbf{t}^{(3)}n_3 \tag{155}$$

$$\mathbf{l} = \mathbf{l}^{(1)}n_1 + \mathbf{l}^{(2)}n_2 + \mathbf{l}^{(3)}n_3. \tag{156}$$

and these vector equations can be written in the stress components, i.e.

$$t_i = \sigma_{ji}n_j \tag{157}$$

and

$$l_i = m_{ji}n_j. \tag{158}$$

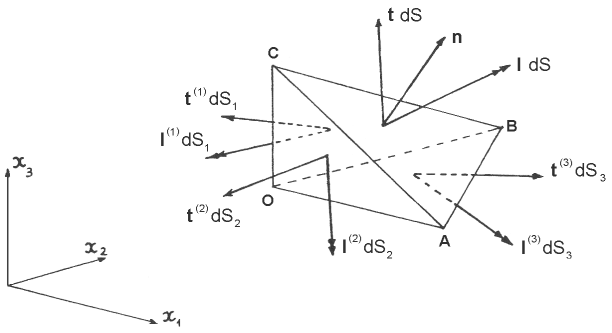

Figure 14: Tetrahedron OABC. (reprint from [26])

5.5 Momentum and moment of momentum

Equations of momentum and moment of momentum are introduced in this chapter for Cosserat continuum. This balance principles will be used in determination of constitutive equations and are introduced both in material and spatial description. The equations in the spatial description were taken from [10] while equations in material description were derived.

5.5.1 Spatial description

It is obvious from fig. (12) that $\mathbf{X}$ is the position vector of the center of mass of a macroelement and $\boldsymbol{\Xi}$ is the relative position vector of a microparticle to the center of mass of macroelement. Accordingly,

$$\sum_{\alpha} \rho_0^{(\alpha)} \boldsymbol{\Xi}^{(\alpha)} \Delta V^{(\alpha)} = \mathbf{0}. \tag{159}$$

With help of relation (106) the last equation can be rewritten into the form

$$\mathfrak{X}_{Kk} \sum_{\alpha} \rho_0^{(\alpha)} \Delta V^{(\alpha)} \xi_k^{(\alpha)} = 0 \tag{160}$$

and since

$$\rho_0^{(\alpha)} \Delta V^{(\alpha)} = \rho^{(\alpha)} \Delta v^{(\alpha)}, \tag{161}$$

we get

$$\mathfrak{X}_{Kk} \sum_{\alpha} \rho^{(\alpha)} \Delta v^{(\alpha)} \xi_k^{(\alpha)} = 0. \tag{162}$$

Since, $\mathfrak{X}_{Kk} \neq 0$ the equation (162) is fulfilled if

$$\sum_{\alpha} \rho^{(\alpha)} \xi_k^{(\alpha)} \Delta v^{(\alpha)} = 0. \tag{163}$$

This shows that the position vector $\mathbf{x}$ is the center of mass of the deformed macrovolume. Consequently, the motion carries the center of mass of the undeformed macrovolume to the center of mass of the deformed macrovolume.

Total momentum

The mechanical momentum of a microelement $\Delta v^{(\alpha)}$ is the product of its mass with its velocity, namely, $\rho^{(\alpha)}\mathbf{v}^{(\alpha)}\Delta v^{(\alpha)}$. The total momentum of a macroelement is the vector sum of the micromomenta of its microelements. For a micropolar body with help of relation of total velocity of particle (149), we have

$$\Delta \mathbf{p} = \sum_{\alpha} \rho^{(\alpha)} \mathbf{v}^{(\alpha)} \Delta v^{(\alpha)} = \sum_{\alpha} \rho^{(\alpha)} (\mathbf{v} + \dot{\boldsymbol{\xi}}^{(\alpha)}) \Delta v^{(\alpha)} = \tag{164}$$

$$= \mathbf{v} \sum_{\alpha} \rho^{(\alpha)} \Delta v^{(\alpha)} + \boldsymbol{\nu} \times \sum_{\alpha} \rho^{(\alpha)} \boldsymbol{\xi}^{(\alpha)} \Delta v^{(\alpha)}.$$

The last term vanishes (due to the relation (163)), and in the limit we write

$$d\mathbf{p} = \rho \mathbf{v} dv. \tag{165}$$

The total momentum of the body is therefore given by

$$\mathbf{p} = \int_v \rho \mathbf{v} dv. \tag{166}$$

Principle of balance of momentum

The principle of balance of momentum has the general form

$$\frac{D}{Dt} \int_v \rho \mathbf{v} dv = \mathbf{F}(t) \tag{167}$$

where $\mathbf{F}(t)$ is the resultant force acting onto the body. If we don't consider any volume forces then the principle of balance of momentum can be expressed by (with help of relation (157))

$$\frac{d}{d_t} \int_v \rho v_i dv = \int_{\partial s} \sigma_{ji} n_j ds. \tag{168}$$

Total moment of momentum

The mechanical moment of momentum of a microelement is defined as the moment of its momentum, namely,

$$\mathbf{x}^{(\alpha)} \times \rho^{(\alpha)}\mathbf{v}^{(\alpha)}\Delta v^{(\alpha)}.$$

The total moment of momentum of a macroelement is calculated by

$$\Delta\mathbf{m} = \sum_{\alpha} \mathbf{x}^{(\alpha)} \times \rho^{(\alpha)}\mathbf{v}^{(\alpha)}\Delta v^{(\alpha)} = \sum_{\alpha}(\mathbf{x} + \boldsymbol{\xi}^{(\alpha)}) \times \rho^{(\alpha)}(\mathbf{v} + \dot{\boldsymbol{\xi}}^{(\alpha)})\Delta v^{(\alpha)}. \tag{169}$$

On carrying out the multiplication, we get

$$\Delta\mathbf{m} = \mathbf{x}\times\mathbf{v}\sum_{\alpha}\rho^{(\alpha)}\Delta v^{(\alpha)} + \sum_{\alpha}\boldsymbol{\xi}^{(\alpha)}\times\rho^{(\alpha)}\dot{\boldsymbol{\xi}}^{(\alpha)}\Delta v^{(\alpha)} + \mathbf{x}\times\sum_{\alpha}\rho^{(\alpha)}\dot{\boldsymbol{\xi}}^{(\alpha)}\Delta v^{(\alpha)} - \mathbf{v}\times\sum_{\alpha}\rho^{(\alpha)}\boldsymbol{\xi}^{(\alpha)}\Delta v^{(\alpha)}. \tag{170}$$

The last two summations vanish, since ξ is measured from the center of mass of the deformed macroelement and the total moment of momentum is then given by

$$\Delta\mathbf{m} = \mathbf{x} \times \mathbf{v}\sum_{\alpha}\rho^{(\alpha)}\Delta v^{(\alpha)} + \sum_{\alpha}\boldsymbol{\xi}^{(\alpha)} \times \rho^{(\alpha)}\dot{\boldsymbol{\xi}}^{(\alpha)}\Delta v^{(\alpha)}. \tag{171}$$

Due to the relations (15.8) and (15.10) in [10])

$$\sum_{\alpha}\rho^{(\alpha)}\xi_j^{(\alpha)}\xi_l^{(\alpha)}\Delta v^{(\alpha)} = \rho i_{jl}\Delta v \tag{172}$$

and

$$j_{mi} = i_{jj}\delta_{im} - i_{mi}, \tag{173}$$

where i is the spatial microinertia tensor, the last term in the equation (171) can be derived (with considering of (138)) as follows

$$\sum_{\alpha}\boldsymbol{\xi}^{(\alpha)} \times \rho^{(\alpha)}\dot{\boldsymbol{\xi}}^{(\alpha)}\Delta v^{(\alpha)} = \rho\boldsymbol{\theta}\Delta v, \tag{174}$$

where $\theta_i = j_{mi}\dot{\varphi}_m$. Then the total moment of momentum of the macroelement is given by

$$\Delta\mathbf{m} = \mathbf{x} \times \mathbf{v}\sum_{\alpha}\rho^{(\alpha)}\Delta v^{(\alpha)} + \rho\boldsymbol{\theta}\Delta v \tag{175}$$

a the total moment of momentum of the body is

$$\mathbf{m} = \int_v (\mathbf{x} \times \rho\mathbf{v} + \rho\boldsymbol{\theta})dv. \tag{176}$$

Principle of balance of moment of momentum

The principle of balance of moment of momentum has the general form

$$\frac{D}{Dt}\int_v (\mathbf{x}\times\rho\mathbf{v}+\rho\boldsymbol{\theta})dv=\mathbf{M}(t), \tag{177}$$

where $\mathbf{M}(t)$ is the resultant moment act on the body. Considering that no volume forces and volume couples acting on the body, the principle of moment of momentum (with help of relations (157), (158)) is given by

$$\frac{d}{d_t}\int_v (\epsilon_{ijk}x_j\rho v_k+\rho\theta_i)dv=\int_{\partial s}(\epsilon_{ijk}x_j\sigma_{lk}n_l+m_{ji}n_j)ds. \tag{178}$$

5.5.2 Material description

The equations of momentum and moment of momentum in material description will be formulated in the following part.

Total momentum

Due to the relation (eq. (15.5) in [10])

$$\rho_0 dV=\rho dv \tag{179}$$

the total momentum in spatial description (166) can be rewrite into the form

$$\mathbf{p}=\int_v \rho\mathbf{v}dv=\int_V \rho_0\mathbf{v}dV. \tag{180}$$

Principle of balance of momentum

We can write for every surface element (eq. (3.1) in [18])

$$\mathbf{t}ds=\mathbf{T}dS \tag{181}$$

where Cauchy traction vector $\mathbf{t}$ is given by equation (157) and $\mathbf{T}$ represents first Piola-Kirchoff traction vector, which can be written with help of first Piola-Kirchoff stress and outward normal of the element

$$T_i=P_{Ji}N_J. \tag{182}$$

With help of the two last equations and eq. (179) , we are able to derive from the principle of balance of momentum in the spatial description (168) its equivalent in the material description

$$\frac{d}{d_t}\int\limits_V \rho_0 v_i dV = \int\limits_{\partial S} P_{Ji} N_J dS. \tag{183}$$

Total moment of momentum

With help of relation (179), the total moment of momentum in spatial description (176) can be rewritten into the equivalent form in material description, therefore

$$\mathbf{m} = \int\limits_v (\mathbf{x} \times \rho \mathbf{v} + \rho \boldsymbol{\theta}) dv = \int\limits_V (\mathbf{x} \times \rho_0 \mathbf{v} + \rho_0 \boldsymbol{\theta}) dV. \tag{184}$$

Principle of balance of moment of momentum

If the following equation is valid

$$m_{ji} n_j ds = M_{Ji} N_J dS \tag{185}$$

where m_{ji} is the couple stress of Cauchy type and M_{Ji} is couple stress of Piola type, then the principle of balance of moment of momentum in spatial description (178) can be rewritten to the equivalent form in material description, therefore

$$\frac{d}{d_t}\int\limits_V (\epsilon_{ijk} x_j \rho_0 v_k + \rho_0 \theta_i) dV = \int\limits_{\partial S} (\epsilon_{ijk} x_j P_{Lk} N_L + M_{Ji} N_J) dS. \tag{186}$$

It should be noted that

$$\theta_i = j_{mi} \nu_m \qquad \text{(spatial description)} \tag{187}$$

$$\Theta_I = J_{MI} \mathfrak{N}_M \qquad \text{(material description)} \tag{188}$$

where $\mathfrak{N} = \boldsymbol{\nu}$ (equation (147)). Due to the following equality

$$\int\limits_v \rho j_{mi} \nu_m dv = \int\limits_V \rho_0 J_{MI} \mathfrak{N}_M dV, \tag{189}$$

and with respect (147), it is obvious that

$$J_{MI} = j_{mi} \delta_{Mm} \delta_{Ii}. \tag{190}$$

This result is a consequence of considered linear theory of microrotation. However, the following equation is valid in general (more about this can be found in [10])

$$J_{MI} = j_{mi}\mathfrak{X}_{Mm}\mathfrak{X}_{Ii}. \tag{191}$$

5.6 Balance of mechanical energy

The balance equations of mechanical energy are introduced in this chapter both for material and spatial description. Derivation of these equations in case of spatial description can be found e.g. in [10]. The equations in material description were derived.

According [18], the balance equation of mechanical energy can be written in the form

$$\frac{d}{dt}K(t) + P_{int}(t) = P_{ext}(t) \tag{192}$$

where $K(t)$ is the kinetic energy, $P_{int}(t)$ is the stress power and $P_{ext}(t)$ is the external mechanical power.

5.6.1 Spatial description

In order to derive the balance equation of mechanical energy, the kinetic energy, stress power and external mechanical power have to be determined. Let's start from the principle of balance of momentum (168) and of moment of momentum (178), i.e. from the equations

$$\frac{d}{d_t}\int_v \rho v_i dv = \int_{\partial s} \sigma_{ji} n_j ds \tag{193}$$

$$\frac{d}{d_t}\int_v (\epsilon_{ijk} x_j \rho v_k + \rho\theta_i) dv = \int_{\partial s} (\epsilon_{ijk} x_j \sigma_{lk} n_l + m_{ji} n_j) ds. \tag{194}$$

Using Gauss-Ostrogradsky theorem and after some manipulations, the local balance equations will be obtained in the form

$$\frac{\partial \sigma_{ji}}{\partial x_j} - \rho\dot{v}_i = 0 \tag{195}$$

$$\frac{\partial m_{ji}}{\partial x_j} + \epsilon_{ijk}\sigma_{jk} - \rho\dot{\theta}_i = 0. \tag{196}$$

After introducing a spin vector as

$$\omega_i = \frac{1}{2}\epsilon_{ijk}\frac{\partial v_k}{\partial x_j} = -\frac{1}{2}\epsilon_{ijk}\omega_{jk}, \qquad \omega_{jk} = -\epsilon_{ijk}\omega_i, \qquad \omega_{jk} = \frac{1}{2}\left(\frac{\partial v_j}{\partial x_k} - \frac{\partial v_k}{\partial x_j}\right), \tag{197}$$

then after comparison with eq. (138) and also with eq.(147), it's obvious that

$$\boldsymbol{\omega} = \dot{\boldsymbol{\varphi}} = \boldsymbol{\nu}. \tag{198}$$

Multiplying the local balance equations (195) by velocity vector v_i, and local balance equations (196) by spin vector ω_i, (since it's identical with vector $\boldsymbol{\nu}$) both equations will be integrated over the whole deformed volume of the body to obtain

$$\int_v \rho \dot{v}_i v_i dv = \int_v \frac{\partial \sigma_{ji}}{\partial x_j} v_i dv \tag{199}$$

$$\int_v \rho \dot{\theta}_i \omega_i dv = \int_v \left(\frac{\partial m_{ji}}{\partial x_j}\omega_i - \omega_{jk}\sigma_{jk}\right) dv. \tag{200}$$

Next,

$$\frac{\partial(\sigma_{ji}v_i)}{\partial x_j} = \frac{\partial \sigma_{ji}}{\partial x_j}v_i + \sigma_{ji}\frac{\partial v_i}{\partial x_j}, \qquad \frac{\partial(m_{ji}\omega_i)}{\partial x_j} = \frac{\partial m_{ji}}{\partial x_j}\omega_i + m_{ji}\frac{\partial \omega_i}{\partial x_j}. \tag{201}$$

Substituting from eq. (201) to the eq. (199) and (200) and using Gauss-Ostrogradsky theorem we get

$$\frac{d}{dt}\int_v \frac{1}{2}\rho v_i v_i dv + \int_v \sigma_{ji}\frac{\partial v_i}{\partial x_j} dv = \int_{\partial s} \sigma_{ji} v_i n_j ds \tag{202}$$

$$\frac{d}{dt}\int_v \frac{1}{2}\rho \theta_i \omega_i dv + \int_v \left(m_{ji}\frac{\partial \omega_i}{\partial x_j} + \omega_{jk}\sigma_{jk}\right) dv = \int_{\partial s} m_{ji}\omega_i n_j ds. \tag{203}$$

Using eq. (192) the kinetic energy is

$$K(t) = \frac{1}{2}\int_v \rho(v_i v_i + \theta_i \omega_i) dv = \frac{1}{2}\int_v \rho(v_i v_i + j_{mi}\omega_m \omega_i) dv, \tag{204}$$

stress power is

$$P_{int}(t) = \int_v \left(\sigma_{ji}\frac{\partial v_i}{\partial x_j} + m_{ji}\frac{\partial \omega_i}{\partial x_j} + \omega_{jk}\sigma_{jk}\right) dv \tag{205}$$

and external mechanical power is

$$P_{ext}(t) = \int_{\partial s} (\sigma_{ji} v_i n_j + m_{ji}\omega_i n_j) ds. \tag{206}$$

Next, the stress power can be expressed

$$P_{int}(t) = \int_V \dot{W} dV \tag{207}$$

where W is a strain energy density function. Using so-called Nanson's formula

$$dv = JdV, \tag{208}$$

we can write

$$P_{int}(t) = \int_V \dot{W} dV = \int_v \frac{1}{J} \dot{W} dv = \int_v \left(\sigma_{ji} \frac{\partial v_i}{\partial x_j} + m_{ji} \frac{\partial \omega_i}{\partial x_j} + \omega_{jk} \sigma_{jk} \right) dv, \tag{209}$$

where J is determinant of the deformation gradient. Then the time derivative of strain energy density function in the spatial description has the form

$$\dot{W} = J \left(\sigma_{ji} \frac{\partial v_i}{\partial x_j} + m_{ji} \frac{\partial \omega_i}{\partial x_j} + \omega_{ji} \sigma_{ji} \right). \tag{210}$$

5.6.2 Material description

The kinetic energy, stress power and external mechanical power is derived in material description in this chapter, similary to the spatial description. Let's start again from balance equations of momentum (183) and moment of momentum (186), but now in material description, i.e. from equations

$$\frac{d}{d_t} \int_V \rho_0 v_i dV = \int_{\partial S} P_{Ji} N_J dS \tag{211}$$

$$\frac{d}{d_t} \int_V (\epsilon_{ijk} x_j \rho_0 v_k + \rho_0 \theta_i) dV = \int_{\partial S} (\epsilon_{ijk} x_j P_{Lk} N_L + M_{Ji} N_J) dS. \tag{212}$$

Using Gauss-Ostrogradsky theorem and after some manipulation the local balance equation in material description will be obtained in the form

$$\frac{\partial P_{Ji}}{\partial X_J} - \rho_0 \dot{v}_i = 0 \tag{213}$$

$$\frac{\partial M_{Ji}}{\partial X_J} + \epsilon_{ijk} F_{jL} P_{Lk} - \rho_0 \dot{\theta}_i = 0. \tag{214}$$

Multiplying the local balance equations (213) by velocity vector v_i, the local balance equations (214) by spin vector ω_i and both equations will be integrated over the undeformed volume of the body, we get

$$\int_V \rho_0 \dot{v}_i v_i dV = \int_V \frac{\partial P_{Ji}}{\partial X_J} v_i dV \tag{215}$$

$$\int_V \rho_0 \theta_i \omega_i dV = \int_V \left(\frac{\partial M_{Ji}}{\partial X_J} \omega_i + \epsilon_{ijk} \omega_i P_{Lk} F_{jL} \right) dV. \tag{216}$$

Next,

$$\frac{\partial (P_{Ji} v_i)}{\partial X_J} = \frac{\partial P_{Ji}}{\partial X_J} v_i + P_{Ji} \frac{\partial v_i}{\partial X_J}, \quad \frac{\partial (M_{Ji} \omega_i)}{\partial X_J} = \frac{\partial M_{Ji}}{\partial X_J} \omega_i + M_{Ji} \frac{\partial \omega_i}{\partial X_J}. \tag{217}$$

Substituting from eq. (217) to the eq. (215) and (216) and using Gauss-Ostrogradsky theorem, we obtain

$$\frac{d}{dt} \int_V \frac{1}{2} \rho_0 v_i v_i dV + \int_V P_{Ji} \frac{\partial v_i}{\partial X_J} dV = \int_{\partial S} P_{Ji} v_i N_J dS \tag{218}$$

$$\frac{d}{dt} \int_V \frac{1}{2} \rho_0 \dot{\theta}_i \omega_i dV + \int_V \left(M_{Ji} \frac{\partial \omega_i}{\partial X_J} + \omega_{jk} P_{Lk} F_{jL} \right) dV = \int_{\partial S} M_{Ji} \omega_i N_J dS. \tag{219}$$

With respect to the eq. (192) the kinetic energy is

$$K(t) = \frac{1}{2} \int_V \rho_0 (v_i v_i + \theta_i \omega_i) dV = \frac{1}{2} \int_V \rho_0 (v_i v_i + j_{mi} \omega_m \omega_i) dV, \tag{220}$$

the stress power is

$$P_{int}(t) = \int_V \left(P_{Ji} \frac{\partial v_i}{\partial X_J} + M_{Ji} \frac{\partial \omega_i}{\partial X_J} + \omega_{jk} P_{Lk} F_{jL} \right) dV \tag{221}$$

and external mechanical power equals to the

$$P_{ext}(t) = \int_{\partial S} (P_{Ji} v_i N_J + M_{Ji} \omega_i N_J) dS. \tag{222}$$

Due to the eq. (207), the time derivative of strain energy density function in material description can be written in the form

$$\dot{W} = P_{Ji} \frac{\partial v_i}{\partial X_J} + M_{Ji} \frac{\partial \omega_i}{\partial X_J} + \omega_{jk} P_{Lk} F_{jL}. \tag{223}$$

6 Hyperelastic constitutive model with bending stiffness of fibres

The theory of finite deformations of elastic materials reinforced by fibres was founded by Adkins and Rivlin [1]. Their theory described an isotropic elastic material with no extensibility in the direction of fibres and they assumed that the reinforcing fibres lay in discrete surfaces. Green and Adkins described the development of this theory in [15].
A different approach was established by Spencer [30]. In his theory the fibre direction is characterized by a unit vector in the reference configuration. The fibre vector formulation has been applied to many kinds of material behaviour. Particular applications of the theory of finite elastic deformations are in Spencer [30], [31] and Rivlin [28]. Presently, this theory based on [30] is used in various kinds of applications of composite materials, either in industry or in composite biomaterials. Concerning examples of industrial use, readers are referred e.g. to [17], where authors simulated response of an air-spring (rubber matrix and textile cords) used for inhibition of vibrations of driver's seat. On the other side, arterial walls represent characteristic examples of composite biomaterials. The arterial wall is composed mainly of isotropic matrix material (elastin) and two families of fibres (collagen). A multi-layer model for arterial wall was proposed by Holzapfel [20].

All of the above mentioned theories are based on assumption of infinitesimaly thin fibres. This fibre is then perfectly flexible, i.e. fibre shows zero bending stiffness.
In order to incorporate bending stiffness into the previous theory (in [30], [31]), Spencer considered in [32] that the strain energy density function depends not only on the deformation gradient F_{iJ} and on the unit vector of undeformed fibre A_J, but also on the space derivatives of the deformed fibre vector G_{iJ}, i.e.

$$W = W(F_{iJ}, G_{iJ}, A_J) \tag{224}$$

where

$$F_{iJ} = \frac{\partial x_i}{\partial X_J}, \qquad G_{iJ} = \frac{\partial b_i}{\partial X_J} = \frac{\partial}{\partial X_J}(F_{iR}A_R), \qquad b_i = F_{iR}A_R. \tag{225}$$

However, this new theory requires including of both force and couple stresses, i.e. ***Cosserat theory of continuum has to be used.***

6.1 General constitutive model

Spencer and Soldatos in [32] introduce the constitutive assumption that W depends, in addition to the displacement gradients F_{iR} and $\mathbf{A}$, on the gradients of the deformed fibre vectors. However, rather than including dependence on the gradients $\partial a_i/\partial X_R$, it is more convenient to introduce a vector $\mathbf{b}$, with Cartesian components b_i, such that

$$\mathbf{b} = \lambda \mathbf{a}, \quad b_i = \lambda a_i = A_R \frac{\partial x_i}{\partial X_R} = F_{iR} A_R, \tag{226}$$

and to assume that W depends instead on the gradients $\partial b_i/\partial X_R$. Since stretch ratio $\lambda^2 = A_R A_S F_{iR} F_{iS}$, the dependence on $\mathbf{F}, \mathbf{a}$ and $\mathbf{A}$ is equivalent to dependence of $\mathbf{F}, \mathbf{b}$ and $\mathbf{A}$. The advantage of using $\mathbf{b}$ rather than $\mathbf{a}$ is that

$$\dot{b}_i = A_R \frac{\partial v_i}{\partial X_R} = A_R \frac{\partial v_i}{\partial x_j} \frac{\partial x_j}{\partial X_R} = b_j \frac{\partial v_i}{\partial x_j}, \tag{227}$$

which is a simpler form than a material derivative $\dot{\mathbf{a}}$ of the fibre vector $\mathbf{a}$ (for more details about material derivative $\dot{\mathbf{a}}$ refer to [30])

$$\dot{a}_i = (\delta_{ij} - a_i a_j) a_k \frac{\partial v_j}{\partial x_k}. \tag{228}$$

Therefore we postulate that

$$W = W(F_{iR}, G_{iR}, A_R) \tag{229}$$

where

$$F_{iR} = \frac{\partial x_i}{\partial X_R}, \quad G_{iR} = \frac{\partial b_i}{\partial X_R}. \tag{230}$$

Therefore

$$\dot{W} = \frac{\partial W}{\partial F_{iR}} \dot{F}_{iR} + \frac{\partial W}{\partial G_{iR}} \dot{G}_{iR} = \frac{\partial W}{\partial F_{iR}} \frac{\partial v_i}{\partial X_R} + \frac{\partial W}{\partial G_{iR}} \frac{\partial \dot{b}_i}{\partial X_R}. \tag{231}$$

Hence

$$\dot{W} = \frac{\partial W}{\partial F_{iR}} \frac{\partial x_j}{\partial X_R} \frac{\partial v_i}{\partial x_j} + \frac{\partial W}{\partial G_{iR}} \frac{\partial x_j}{\partial X_R} \frac{\partial \dot{b}_i}{\partial x_j} = F_{jR} \left(\frac{\partial W}{\partial F_{iR}} \frac{\partial v_i}{\partial x_j} + \frac{\partial W}{\partial G_{iR}} \frac{\partial \dot{b}_i}{\partial x_j} \right), \tag{232}$$

and from (227)

$$F_{jR} \frac{\partial \dot{b}_i}{\partial x_j} = \frac{\partial x_j}{\partial X_R} \frac{\partial b_k}{\partial x_j} \frac{\partial v_i}{\partial x_k} + F_{jR} b_k \frac{\partial^2 v_i}{\partial x_j \partial x_k} = G_{kR} \frac{\partial v_i}{\partial x_k} + F_{jR} b_k \frac{\partial^2 v_i}{\partial x_j \partial x_k}. \tag{233}$$

Next, let's introduce the rate of deformation

$$d_{ij} = \frac{1}{2} \left(\frac{\partial v_i}{\partial x_j} + \frac{\partial v_j}{\partial x_i} \right), \tag{234}$$

then we can write

$$\frac{\partial v_i}{\partial x_j} = d_{ij} + \omega_{ij}, \tag{235}$$

where ω_{ij} is the spin tensor defined by eq. (197). From (231) and (232) with help of (233) and (235) we get

$$\dot{W} = \left(F_{jR}\frac{\partial W}{\partial F_{iR}} + G_{jR}\frac{\partial W}{\partial G_{iR}} \right)(d_{ij} + \omega_{ij}) + F_{jR}\frac{\partial W}{\partial G_{iR}} b_k \frac{\partial^2 v_i}{\partial x_j \partial x_k}. \tag{236}$$

We now denote the components of the symmetric $\sigma_{(ij)}$ and antisymetric $\sigma_{[ij]}$ parts of the force stress σ_{ij}, so that

$$\sigma_{ij} = \sigma_{(ij)} + \sigma_{[ij]}, \quad \sigma_{(ij)} = \frac{1}{2}(\sigma_{ij} + \sigma_{ji}), \quad \sigma_{[ij]} = \frac{1}{2}(\sigma_{ij} - \sigma_{ji}) \tag{237}$$

and note that

$$\sigma_{(ij)}\omega_{ij} = 0 \qquad \sigma_{[ij]}d_{ij} = 0. \tag{238}$$

Now, we can rewrite strain energy density function in eq. (210) using symetric and anti-symetric stress from eq. (237) and with help of (235) and (238) into the form

$$\dot{W} = J\left(\sigma_{(ij)}d_{ij} + m_{ji}\frac{\partial \omega_i}{\partial x_j} \right). \tag{239}$$

Hence, by comparing (236) and (239), we obtain

$$\left[\sigma_{(ij)} - \frac{\rho}{\rho_0}\left(F_{jR}\frac{\partial W}{\partial F_{iR}} + G_{jR}\frac{\partial W}{\partial G_{iR}} \right) \right] d_{ij} - \frac{\rho}{\rho_0}\left(F_{jR}\frac{\partial W}{\partial F_{iR}} + G_{jR}\frac{\partial W}{\partial G_{iR}} \right)\omega_{ij} + \tag{240}$$

$$+ m_{ji}\frac{\partial \omega_i}{\partial x_j} - \frac{\rho}{\rho_0}F_{jR}\frac{\partial W}{\partial G_{iR}} b_k \frac{\partial^2 v_i}{\partial x_j \partial x_k} = 0.$$

Since d_{ij} and ω_{ij} are arbitrary, it follows that

$$\sigma_{(ij)} = \frac{\rho}{\rho_0}\left(F_{jR}\frac{\partial W}{\partial F_{iR}} + G_{jR}\frac{\partial W}{\partial G_{iR}} \right), \tag{241}$$

and that the coefficient of ω_{ij} in (240) is symmetric with respect to interchanges of i and j, thus

$$F_{jR}\frac{\partial W}{\partial F_{iR}} + G_{jR}\frac{\partial W}{\partial G_{iR}} = F_{iR}\frac{\partial W}{\partial F_{jR}} + G_{iR}\frac{\partial W}{\partial G_{jR}}. \tag{242}$$

Equation (241) is the constitutive equation for the symmetric part of the stress $\boldsymbol{\sigma}$; (242) is a restriction on the admissible forms of W, the validity of which is confirmed below. There now remains from (240)

$$m_{ji}\frac{\partial \omega_i}{\partial x_j} - \frac{\rho}{\rho_0}F_{jR}\frac{\partial W}{\partial G_{iR}} b_k \frac{\partial^2 v_i}{\partial x_j \partial x_k} = 0, \tag{243}$$

or equivalently, using (197),

$$\left(-\frac{1}{2}\epsilon_{pik}m_{jp} - \frac{\rho}{\rho_0}F_{jR}\frac{\partial W}{\partial G_{iR}}b_k\right)\frac{\partial^2 v_i}{\partial x_j \partial x_k} = 0. \tag{244}$$

It follows that the symmetric part (with respect to the indicies j and k) of the bracket term in (244) must be zero, and therefore

$$-\frac{1}{2}(\epsilon_{pik}m_{jp} + \epsilon_{pij}m_{kp}) = \frac{\rho}{\rho_0}\frac{\partial W}{\partial G_{iR}}(F_{jR}b_k + F_{kR}b_j). \tag{245}$$

By multiplying each side of (245) by ϵ_{rik} and using the $\epsilon - \delta$ identities, there follows

$$2\delta_{pr}m_{jp} + (\delta_{pr}\delta_{kj} - \delta_{rj}\delta_{kp})m_{kp} = -2\epsilon_{erik}\frac{\rho}{\rho_0}\frac{\partial W}{\partial G_{iR}}(F_{jR}b_k + F_{kR}b_j), \tag{246}$$

and hence

$$3m_{jr} - m_{kk}\delta_{rj} = -2\epsilon_{rik}\frac{\rho}{\rho_0}\frac{\partial W}{\partial G_{iR}}(F_{jR}b_k + F_{kR}b_j) \tag{247}$$

which is a constitutive equation for the couple stress m_{ij}. If we set $r = j$ in (247), then each side reduces to zero, and so the spherical part m_{kk} of m_{ij} is indeterminate. This is consistent with the observation that if m_{ij} is decomposed into its spherical and deviatoric parts

$$m_{jr} = \overline{m}_{jr} + \frac{1}{3}m_{kk}\delta_{rj}, \tag{248}$$

then, beacuse $\partial\omega_i/\partial x_i = 0, m_{kk}$ makes no contribution to the energy balance equation (239). This indeterminacy in the couple stress is not specific to fibre-reinforced materials, but is a general result in couple stress theory. Using (248) we can write (247) as

$$\overline{m}_{jr} = -\frac{2}{3}\epsilon_{rik}\frac{\rho}{\rho_0}\frac{\partial W}{\partial G_{iR}}(F_{jR}b_k + F_{kR}b_j), \quad \overline{m}_{kk} = 0. \tag{249}$$

Clearly, if $r \neq j$, then $\overline{m}_{jr} = m_{jr}$. Invariance under the superposed rigid rotation $\mathbf{x} \to \mathbf{Q}\mathbf{x}$ requires that

$$W(\mathbf{F}, \mathbf{G}, \mathbf{A}) = W(Q\mathbf{F}, Q\mathbf{G}, \mathbf{A}), \tag{250}$$

for any ortogonal tensor $\mathbf{Q}$. It follows that W depends on the scalar products of the vectors with components (for each fixed R)F_{iR} and G_{iR}, and therefore W can be expressed as a function of the tensors

$$\mathbf{C} = \mathbf{F}^T\mathbf{F}, \quad \mathbf{\Gamma} = \mathbf{G}^T\mathbf{G}, \quad \mathbf{\Lambda} = \mathbf{F}^T\mathbf{G}, \quad \mathbf{\Lambda}^T = \mathbf{G}^T\mathbf{F} \tag{251}$$

and the vector $\mathbf{A}$, where $\mathbf{C}, \mathbf{\Gamma}, \mathbf{\Lambda}, \mathbf{A}$ have components, respectively,

$$C_{RS} = \frac{\partial x_i}{\partial X_R}\frac{\partial x_i}{\partial X_S} = F_{iR}F_{iS},$$

$$\Gamma_{RS} = \frac{\partial b_i}{\partial X_R}\frac{\partial b_i}{\partial X_S} = G_{iR}G_{iS},$$

$$\Lambda_{RS} = \frac{\partial x_i}{\partial X_R}\frac{\partial b_i}{\partial X_S} = F_{iR}G_{iS},$$

and

$$A_R. \tag{252}$$

However, from (251)

$$\mathbf{\Gamma} = \mathbf{\Lambda}^T\mathbf{C}^{-1}\mathbf{\Lambda}, \quad \mathbf{C} = \mathbf{\Lambda}\mathbf{\Gamma}^{-1}\mathbf{\Lambda}^T, \tag{253}$$

and, by the Cayley-Hamilton Theorem for $\mathbf{C}$

$$I_3\mathbf{C}^{-1} = \mathbf{C}^2 - I_1\mathbf{C} + I_2\mathbf{I}. \tag{254}$$

Hence $\mathbf{\Gamma}$ can be expressed in terms of $\mathbf{C}, \mathbf{\Lambda}$ and invariants of $\mathbf{C}$, and therefore W can be expressed as a function of these quantities. Invariance under rigid rotations of the undeformed body then requires that

$$W(\mathbf{C}, \mathbf{\Lambda}, \mathbf{A}) = W(\mathbf{Q}\mathbf{C}\mathbf{Q}^T, \mathbf{Q}\mathbf{\Lambda}\mathbf{Q}^T, \mathbf{Q}\mathbf{A}), \tag{255}$$

so that W can be expressed as an isotropic invariant of $\mathbf{C}, \mathbf{\Lambda}, \mathbf{A}$. If the sense of the fibres is not significant, then W must also be even in the components of $\mathbf{A}$ and even in the components of $\mathbf{\Lambda}$. In this case dependence on the vector $\mathbf{A}$ can be replaced by dependence on the tensor $\mathbf{A} \otimes \mathbf{A}$, but we do not impose this restriction at this stage.

Since W depends on $\mathbf{F}$ and $\mathbf{G}$ only through the tensors $\mathbf{C}$ and $\mathbf{\Lambda}$, we have

$$\frac{\partial W}{\partial F_{iR}} = \frac{\partial W}{\partial C_{PQ}}\frac{\partial C_{PQ}}{\partial F_{iR}} + \frac{\partial W}{\partial \Lambda_{PQ}}\frac{\partial \Lambda_{PQ}}{\partial F_{iR}},$$

$$\frac{\partial W}{\partial G_{iR}} = \frac{\partial W}{\partial C_{PQ}}\frac{\partial C_{PQ}}{\partial G_{iR}} + \frac{\partial W}{\partial \Lambda_{PQ}}\frac{\partial \Lambda_{PQ}}{\partial G_{iR}}, \tag{256}$$

and, since $C_{PQ} = F_{kP}F_{kQ}$ and $\Lambda_{PQ} = F_{kP}G_{kQ}$

$$\frac{\partial C_{PQ}}{\partial F_{iR}} = \delta_{ik}\delta_{PR}F_{kQ} + \delta_{ik}\delta_{QR}F_{kP} = F_{iQ}\delta_{PR} + F_{iP}\delta_{QR},$$

$$\frac{\partial C_{PQ}}{\partial G_{iR}} = 0,$$

$$\frac{\partial \Lambda_{PQ}}{\partial F_{iR}} = \delta_{ik}\delta_{RP}G_{kQ} = G_{iQ}\delta_{RP},$$

$$\frac{\partial \Lambda_{PQ}}{\partial G_{iR}} = \delta_{ik}\delta_{RQ}F_{kP} = F_{iP}\delta_{RQ}. \tag{257}$$

Hence from (256), using (257)

$$F_{jR}\frac{\partial W}{\partial F_{iR}} = F_{jR}\left(\frac{\partial W}{\partial C_{PQ}}\frac{\partial C_{PQ}}{\partial F_{iR}} + \frac{\partial W}{\partial \Lambda_{PQ}}\frac{\partial \Lambda_{PQ}}{\partial F_{iR}}\right) =$$

$$= F_{jR}\left[(F_{iQ}\delta_{PR} + F_{iP}\delta_{QR})\frac{\partial W}{\partial C_{PQ}} + G_{iQ}\delta_{RP}\frac{\partial W}{\partial \Lambda_{PQ}}\right] =$$

$$= F_{jR}F_{iP}\left(\frac{\partial W}{\partial C_{PR}} + \frac{\partial W}{\partial C_{RP}}\right) + F_{jR}G_{iP}\frac{\partial W}{\partial \Lambda_{RP}},$$

$$G_{jR}\frac{\partial W}{\partial G_{iR}} = G_{jR}\frac{\partial W}{\partial \Lambda_{PQ}}\frac{\partial \Lambda_{PQ}}{\partial G_{iR}} = G_{jR}F_{iP}\frac{\partial W}{\partial \Lambda_{PR}},$$

$$F_{jR}\frac{\partial W}{\partial G_{iR}} = F_{jR}\frac{\partial W}{\partial \Lambda_{PQ}}\frac{\partial \Lambda_{PQ}}{\partial G_{iR}} = F_{jR}F_{iP}\frac{\partial W}{\partial \Lambda_{PR}}. \tag{258}$$

Hence from (258)

$$F_{jR}\frac{\partial W}{\partial F_{iR}} + G_{jR}\frac{\partial W}{\partial G_{iR}} = F_{jR}F_{iP}\left(\frac{\partial W}{\partial C_{PR}} + \frac{\partial W}{\partial C_{RP}}\right) + (F_{jR}G_{iP} + F_{iR}G_{jP})\frac{\partial W}{\partial \Lambda_{RP}}, \tag{259}$$

from which (242) follows immediately. Hence (241) and (249) can now be expressed (with some renaming of indicies) as

$$\sigma_{(ij)} = \frac{\rho}{\rho_0}\left[F_{iR}F_{jS}\left(\frac{\partial W}{\partial C_{RS}} + \frac{\partial W}{\partial C_{SR}}\right) + (G_{iR}F_{jS} + G_{jR}F_{iS})\frac{\partial W}{\partial \Lambda_{SR}}\right], \tag{260}$$

$$\overline{m}_{ji} = \frac{2}{3}\epsilon_{ikm}\frac{\rho}{\rho_0}\frac{\partial W}{\partial \Lambda_{PR}}F_{mP}(F_{jR}b_k + F_{kR}b_j). \tag{261}$$

The strain energy W is an isotropic invariant of tensors $\mathbf{C}, \mathbf{\Lambda}$ and vector $\mathbf{A}$. Canonical forms for these invariants are known and can be read from tables (for example,[36] Table1). A

list of the invariants is given in the Appendix (A.1). This list contains 33 independent invariants which, in a general case, leads to excessively complicated constitutive equations. In order to progress, therefore, it is necessary to make further simplifying assumptions. There are several plausible ways in which this may be done; for example by considering only restricted classes of deformations, as in plane strain theory discussed in [32] in Section 7, or by adopting the linearized theory which is described in [32] Section 9. In appropriate cases, a certain simplification can be achieved by introducing the kinematic constrains of incompressibility and/or fibre inextensibility. Another simplified theory is described in the next section.

6.2 Dependence on fibre curvature

The following section was introduced by Spencer and Soldatos in 2007 and can be found in [32] Section 6.

In this section it is assumed that, rather than general dependence on the gradients of $\mathbf{b}$, the strain-energy depends on the gradients of $\mathbf{b}$ only through the directional derivative of the fibre vector in the fibre direction; that is, essentially, on the curvature of the fibres. In doing this, we exclude effects due to fibre "splay" and fibre "twist", both of which feature in liquid crystal theory, but it is plausible that in fibre composite solids the major factor is fibre curvature.

Accordingly we make the initial assumption that the strain-energy depends on the deformation gradients $\partial x_i/\partial X_R$, on the directional derivatives $A_R \partial b_i/\partial X_R$, and on the initial fibre direction vector $\mathbf{A}$. Invariance under a superposed rigid rotation $\mathbf{x} \to \mathbf{Q}\mathbf{x}$ of the deformed body requires that W can be expressed as a function of the scalar products, formed by contracting on the index i, of the vectors $\partial x_i/\partial X_R = F_{iR}$, and $A_R \partial b_i/\partial X_R = G_{iR}A_R = \kappa_i$. These scalar products are

$$C_{RS} = F_{iR}F_{iS}, \qquad K_R = \kappa_i F_{iR} = A_S \frac{\partial x_i}{\partial X_R}\frac{\partial b_i}{\partial X_S} = \Lambda_{RS}A_S,$$

$$\kappa^2 = \kappa_i\kappa_i = A_R A_S \frac{\partial b_i}{\partial X_R}\frac{\partial b_i}{\partial X_S} = A_R A_S \Gamma_{RS}. \tag{262}$$

Then invariance under rotations of the undeformed body requires that W is an isotropic invariant of tensor $\mathbf{C}$ (components C_{RS}), vectors $\mathbf{K}$ (components K_R) and $\mathbf{A}$, and scalar κ^2. It follows from tables of invariants that W can be expressed as a function of 11 invariants. The list of such invariants can be found in the appendix (A.2).

7 Incompressible anisotropic hyperelastic Cosserat continuum

A new form of the strain energy density function of a incompressible hyperelastic matrix is proposed in this chapter. The new form of the strain energy density function is then used to determine the force (260) and couple (261) stress constitutive equations defined in the previous section. Next, derivatives of the force and couple stresses with respect to the deformation gradient $\mathbf{F}$ and tensor $\mathbf{G}$ are introduced. Then these derivatives can be used in a finite element implementation.

7.1 Strain energy density function

The simplified theory introduced in chapter 6.2 contains 11 independent invariants where the first three invariants (I_1, I_2, I_3 in A.2) correspond to the hyperelastic matrix and the rest ($I_4, I_5, I_6, I_7, I_8, I_9, I_{10}, I_{11}$) to fibres. Invariants I_4, I_5 are able to describe only an extension or compression of the fibre and the rest of the fibre invariants ($I_6, I_7, I_8, I_9, I_{10}, I_{11}$) expand the description of the fibre behaviour by e.g. curvature of the fibre. Since linear elastic steel fibres are considered in this work, all invariants with square or higher power of deformation tensors, or invariants with mutual product of deformation tensors were neglected and only I_4 and I_9 were considered as fibre invariants describing extension or compression and bending of the fibre. Hence, the proposed form of the invariant based strain energy density function is

$$W = k_1(I_1 - 3) + k_2(I_4 - 1)^2 + k_6 I_9^2 + p(J - 1), \tag{263}$$

where p is Lagrange multiplier related to incompressibility, k_1, k_2, k_6 are material parameters and the invariants are defined as follows

$$I_1 = C_{AA}, \tag{264}$$

$$I_4 = A_B C_{CB} A_C, \tag{265}$$

$$I_9 = A_B \Lambda_{CB} A_C. \tag{266}$$

The invariants which correspond to the hyperelastic matrix (I_1, I_2 and $I_3 = 1$ due to incompressibility) can be used arbitrarily in order to define any hyperelastic constitutive model. The Neo-Hookean constitutive model was used in the introduced strain energy form (263) for simplicity, but this one can be replaced by any other model (e.g. Mooney-Rivlin, Polynomial, Yeoh).

7.2 Force stress

The relation between symmetric Kirchoff stress $\tau_{(ij)}$ and symmetric Cauchy stress $\sigma_{(ij)}$ can be written as

$$\tau_{(ij)} = J\sigma_{(ij)} \tag{267}$$

and due to incompressibility we can write

$$\tau_{(ij)} = \sigma_{(ij)} = F_{iR}F_{jS}\left(\frac{\partial W}{\partial C_{RS}} + \frac{\partial W}{\partial C_{SR}}\right) + (G_{iR}F_{jS} + G_{jR}F_{iS})\frac{\partial W}{\partial \Lambda_{SR}}. \tag{268}$$

In order to determine the Kirchoff's stress, derivatives of W with respect to right Cauchy-Green deformation tensor and lambda tensor are needed. Let's start with the derivatives of W with respect to the right Cauchy-Green deformation tensor

$$\frac{\partial W}{\partial C_{RS}} = \sum_n \frac{\partial W}{\partial I_n}\frac{\partial I_n}{\partial C_{RS}} + \frac{\partial W}{\partial J}\frac{\partial J}{\partial C_{RS}} \tag{269}$$

and similary we can continue with derivatives with respect to tensor lambda

$$\frac{\partial W}{\partial \Lambda_{SR}} = \sum_n \frac{\partial W}{\partial I_n}\frac{\partial I_n}{\partial \Lambda_{SR}} + \frac{\partial W}{\partial J}\frac{\partial J}{\partial \Lambda_{SR}}, \tag{270}$$

where $n = 1, 4, 9$. The derivatives of the strain energy density function with respect to the appropriate invariant in eq. (269), (270) are defined

$$\frac{\partial W}{\partial I_1} = k_1, \quad \frac{\partial W}{\partial I_4} = 2k_2(I_4 - 1), \quad \frac{\partial W}{\partial I_9} = 2k_6 I_9, \quad \frac{\partial W}{\partial J} = p \tag{271}$$

Derivatives of appropriate invariant and J with respect to the right Cauchy-Green deformation tensor are

$$\frac{\partial I_1}{\partial C_{RS}} = \frac{\partial I_1}{\partial C_{SR}} = \delta_{RS}, \quad \frac{\partial I_4}{\partial C_{RS}} = \frac{\partial I_4}{\partial C_{SR}} = A_R A_S, \tag{272}$$

$$\frac{\partial I_9}{\partial C_{RS}} = \frac{\partial I_9}{\partial C_{SR}} = 0, \quad \frac{\partial J}{\partial C_{RS}} = \frac{\partial J}{\partial C_{SR}} = \frac{J}{2}C^{-1}_{RS}. \tag{273}$$

Derivatives of appropriate invariant and J with respect to lambda tensor are

$$\frac{\partial I_1}{\partial \Lambda_{SR}} = 0, \quad \frac{\partial I_4}{\partial \Lambda_{SR}} = 0, \quad \frac{\partial I_9}{\partial \Lambda_{SR}} = A_R A_S, \quad \frac{\partial J}{\partial \Lambda_{SR}} = 0. \tag{274}$$

After substituting to equation (268) from equations (271), (272), (273) and (274), we obtain a final formula of the symetric force stress

$$\tau_{(ij)} = 2F_{iR}F_{jS}(k_1\delta_{RS} + 2k_2(I_4 - 1)A_R A_S + pJ/2C^{-1}_{RS}) + 2k_6 I_9(G_{iR}F_{jS} + G_{jR}F_{iS})A_R A_S. \tag{275}$$

7.3 Couple stress

Let's introduce a deviatoric part of Kirchoff $\overline{\mu}_{ji}$ and Cauchy $\overline{m}_{ji}$ couple stresses. Due to incompressibiliy, we can write

$$\overline{\mu}_{ji} = J\overline{m}_{ji} = \overline{m}_{ji}, \tag{276}$$

so the formula for the deviatoric part of couple stress is

$$\overline{\mu}_{ji} = \frac{2}{3}\epsilon_{ikm}\frac{\partial W}{\partial \Lambda_{PR}}F_{mP}(F_{jR}b_k + F_{kR}b_j) \tag{277}$$

After substituting from equation (274) the final formula of deviatoric part of couple stress will be obtained in the form

$$\overline{\mu}_{ji} = \frac{4}{3}\epsilon_{ikm}k_6 I_9 A_P A_R F_{mP}(F_{jR}b_k + F_{kR}b_j). \tag{278}$$

7.4 Derivatives of the force stress with respect to deformation gradient

Derivatives of the force stress (268) with respect to deformation gradient can be written

$$\begin{aligned}\frac{\partial \tau_{(ij)}}{\partial F_{kL}} =& 2(\delta_{ik}F_{jS}M_{LS} + F_{iR}\delta_{jk}M_{RL}) + 2F_{iR}F_{jS}\frac{\partial M_{RS}}{\partial F_{kL}} + \\ &+ \frac{\partial N_{RS}}{\partial F_{kL}}(G_{iR}F_{jS} + G_{jR}F_{iS}) + N_{RL}(G_{iR}\delta_{jk} + G_{jR}\delta_{ik}),\end{aligned} \tag{279}$$

where

$$M_{RS} = k_1\delta_{RS} + 2k_2(I_4 - 1)A_R A_S + p\frac{J}{2}C^{-1}_{RS}, \tag{280}$$

$$\frac{\partial M_{RS}}{\partial F_{kL}} = 2k_2 A_R A_S \frac{\partial I_4}{\partial F_{kL}} + p\frac{J}{2}\left(F^{-1}_{Lk}C^{-1}_{RS} + \frac{\partial C^{-1}_{RS}}{\partial F_{kL}}\right) \tag{281}$$

$$N_{RS} = 2k_6 I_9 A_R A_S \tag{282}$$

$$\frac{\partial N_{RS}}{\partial F_{kL}} = 2k_6 A_B G_{kB} A_L A_R A_S \tag{283}$$

and

$$\frac{\partial I_4}{\partial F_{kL}} = 2A_B F_{kB} A_L. \tag{284}$$

Derivatives $\partial C_{RS}^{-1}/\partial F_{kL}$ are calculated as follows:

Inverse matrix of right Cauchy-Green deformation tensor can be written

$$C_{RS}^{-1} = F_{Rj}^{-1} F_{Sj}^{-1}. \tag{285}$$

Then derivation with respect to deformation gradient is

$$\frac{\partial C_{RS}^{-1}}{\partial F_{kL}} = \frac{\partial F_{Rj}^{-1}}{\partial F_{kL}} F_{Sj}^{-1} + F_{Rj}^{-1} \frac{\partial F_{Sj}^{-1}}{\partial F_{kL}}. \tag{286}$$

Now the question is how to calculate derivation of inverse deformation gradient with respect to deformation gradient $\partial F_{Rj}^{-1}/\partial F_{kL}$. Hence, we can write

$$F_{Ri}^{-1} F_{iS} = \delta_{RS} \tag{287}$$

and derivation of the previous equation with respect to deformation gradient is

$$\frac{\partial F_{Ri}^{-1}}{\partial F_{kL}} F_{iS} + F_{Ri}^{-1} \frac{\partial F_{iS}}{\partial F_{kL}} = 0. \tag{288}$$

By multiplying each side of the last equation by F_{Sj}^{-1} there follows

$$\frac{\partial F_{Rj}^{-1}}{\partial F_{kL}} = -F_{Rk}^{-1} F_{Lj}^{-1}. \tag{289}$$

By substituting to (286) from (289) we obtain the final formula for derivation of inverse Cauchy-Green deformation tensor with respect to deformation gradient in the form

$$\frac{\partial C_{RS}^{-1}}{\partial F_{kL}} = -(F_{Rk}^{-1} C_{LS}^{-1} + F_{Sk}^{-1} C_{RL}^{-1}). \tag{290}$$

7.5 Derivative of the force stress with respect to tensor G

Derivative of the force stress (268) with respect to tensor **G** can be written as follows

$$\frac{\partial \tau_{(ij)}}{\partial G_{kL}} = \frac{\partial N_{RS}}{\partial G_{kL}}(G_{iR}F_{jS} + G_{jR}F_{iS}) + N_{LS}(\delta_{ik}F_{jS} + \delta_{jk}F_{iS}), \tag{291}$$

where

$$\frac{\partial N_{RS}}{\partial G_{kL}} = 2k_6 A_L F_{kC} A_C A_R A_S. \tag{292}$$

7.6 Derivative of the couple stress with respect to deformation gradient

Derivative of the equation (278) can be written in the following form

$$\frac{\partial \overline{\mu}_{ji}}{\partial F_{kL}} = \frac{2}{3}\epsilon_{iom}k_6 A_P A_R \Big\{ \delta_{mk}\delta_{LP}(F_{jR}b_o + F_{oR}b_j) + F_{mP}\Big[\delta_{jk}\delta_{LR}b_o + \tag{293}$$

$$+F_{jR}\frac{\partial b_o}{\partial F_{kL}} + \delta_{ok}\delta_{RL}b_j + F_{oR}\frac{\partial b_j}{\partial F_{kL}} + 2A_B G_{kB} A_L(F_{jR}b_o + F_{oR}b_j)\Big]\Big\} \tag{294}$$

where

$$\frac{\partial b_o}{\partial F_{kL}} = A_R\delta_{ok}\delta_{LR} = A_L\delta_{ok}. \tag{295}$$

7.7 Derivative of the couple stress with respect to tensor G

The derivative of the couple stress (278) according tensor **G** yeilds

$$\frac{\partial \overline{\mu}_{ji}}{\partial G_{kL}} = \frac{4}{3}\epsilon_{ikm}k_6 A_L F_{kC} A_C A_P A_R F_{mP}(F_{jR}b_k + F_{kR}b_j). \tag{296}$$

8 Compressible anisotropic hyperelastic Cosserat continuum

8.1 Strain energy density function

The strain energy density function (263) introduced in the previous chapter "is adjusted" now to the compressible form

$$W = k_1(\overline{I}_1 - 3) + k_2(\overline{I}_4 - 1)^2 + k_6\overline{I}_9^2 + \frac{1}{d}(J-1)^2 \tag{297}$$

where $\overline{I}_1, \overline{I}_4, \overline{I}_9$ are modified invariants defined in the following section, k_1, k_2, k_6 are material parameters, d is parameter of compressibility and J is defined as

$$J = det(\mathbf{F}). \tag{298}$$

8.2 Modified invariants

Multiplicative decomposition of the deformation gradient $\mathbf{F}$ into volume-changing (dilational) and volume-preserving (distortional) parts is defined

$$\mathbf{F} = J^{1/3}\overline{\mathbf{F}}, \qquad \mathbf{C} = J^{2/3}\overline{\mathbf{C}}. \tag{299}$$

The terms $J^{1/3}\mathbf{I}$ and $J^{2/3}\mathbf{I}$ are associated with volume-changing deformations, while $\overline{\mathbf{F}}$ and $\overline{\mathbf{C}} = \overline{\mathbf{F}}^T\overline{\mathbf{F}}$ are associated with volume-preserving deformations of the material. Tensors $\overline{\mathbf{F}}$ and $\overline{\mathbf{C}}$ are called modified deformation gradient and modified right Cauchy-Green tensor of deformation, respectively.

Let's introduce modified tensor $\overline{\mathbf{G}}$. Tensor $\mathbf{G}$ is defined by equation (230), and with help of equation (299) we can write for the modified tensor

$$\overline{G}_{iJ} = \frac{\partial \overline{b}_i}{\partial X_J} = \frac{\partial(\overline{F}_{iR}A_R)}{\partial X_J} = A_R\frac{\partial(J^{-1/3}F_{iR})}{\partial X_J}. \tag{300}$$

After some manipulations

$$\overline{G}_{iJ} = G_{iJ}J^{-1/3} - \frac{1}{3}A_R J^{-1/3}F_{iR}\frac{\partial^2 u_k}{\partial X_J \partial X_L}\frac{\partial X_L}{\partial x_k}. \tag{301}$$

It should be noted that in case of incompressibility, where $J = 1$ and it holds

$$\frac{\partial^2 u_k}{\partial X_J \partial X_L}\frac{\partial X_L}{\partial x_k} = 0 \tag{302}$$

(proof is given in the appendix (A.4)), the equation (301) reduces to

$$\overline{G}_{iJ} = G_{iJ}. \tag{303}$$

Let's introduce modified tensor $\overline{\mathbf{\Lambda}}$ by the following formula

$$\overline{\Lambda}_{RS} = \overline{F}_{iR}\overline{G}_{iS}. \tag{304}$$

Substituting from equations (299), (301) and after some manipulations we get the modified tensor in the form

$$\overline{\Lambda}_{RS} = \Lambda_{RS}J^{-2/3} - \frac{1}{3}A_L J^{-2/3}F_{iR}F_{iL}\frac{\partial^2 u_k}{\partial X_S \partial X_O}\frac{\partial X_O}{\partial x_k}. \tag{305}$$

Again, with consideration of incompressibility the last equation is reduced to form

$$\overline{\Lambda}_{RS} = \Lambda_{RS}. \tag{306}$$

Now, based on the previous modified tensors, modified invariants can be introduced

$$\overline{I}_1 = \overline{C}_{AA} = J^{-2/3}C_{AA} \tag{307}$$

$$\overline{I}_4 = A_B\overline{C}_{CB}A_C = J^{-2/3}A_B C_{CB}A_C \tag{308}$$

$$\overline{I}_9 = A_B\overline{\Lambda}_{CB}A_C = J^{-2/3}(A_B\Lambda_{CB}A_C - \frac{1}{3}I_4 G_{kO}F^{-1}_{Ok}), \tag{309}$$

where invariant I_4 is defined in eq. (265).

8.3 Force stress

Constitutive equation of Kirchoff stress $\tau_{(ij)}$ is given by (268) and derivatives $\frac{\partial W}{\partial C_{RS}}$ can be calculated in the same way as in equation (269), i.e.

$$\frac{\partial W}{\partial C_{RS}} = \sum_n \frac{\partial W}{\partial \overline{I}_n}\frac{\partial \overline{I}_n}{\partial C_{RS}} + \frac{\partial W}{\partial J}\frac{\partial J}{\partial C_{RS}} \tag{310}$$

where $n = 1, 4, 9$ and

$$\frac{\partial W}{\partial \overline{I}_1} = k_1, \quad \frac{\partial W}{\partial \overline{I}_4} = 2k_2(\overline{I}_4 - 1), \quad \frac{\partial W}{\partial \overline{I}_9} = 2k_6\overline{I}_9, \quad \frac{\partial W}{\partial J} = \frac{2}{d}(J-1), \tag{311}$$

$$\frac{\partial \overline{I}_1}{\partial C_{RS}} = \frac{\partial \overline{I}_1}{\partial C_{SR}} = J^{-2/3}\left(\delta_{RS} - \frac{1}{3}C^{-1}_{RS}C_{AA}\right), \tag{312}$$

$$\frac{\partial \overline{I}_4}{\partial C_{RS}} = \frac{\partial \overline{I}_4}{\partial C_{SR}} = J^{-2/3}\left(A_R A_S - \frac{1}{3}C^{-1}_{RS}A_B C_{CB} A_C\right), \tag{313}$$

$$\frac{\partial \overline{I}_9}{\partial C_{RS}} = \frac{\partial \overline{I}_9}{\partial C_{SR}} = \frac{1}{3}J^{-2/3}\left[-C^{-1}_{RS}A_B\Lambda_{CB}A_C + G_{kO}F^{-1}_{Ok}\left(\frac{1}{3}C^{-1}_{RS}I_4 - A_R A_S\right)\right], \tag{314}$$

$$\frac{\partial J}{\partial C_{RS}} = \frac{J}{2}C^{-1}_{RS}, \tag{315}$$

Derivatives $\frac{\partial W}{\partial \Lambda_{SR}}$ can be calculated

$$\frac{\partial W}{\partial \Lambda_{SR}} = \sum_n \frac{\partial W}{\partial \overline{I}_n}\frac{\partial \overline{I}_n}{\partial \Lambda_{SR}} + \frac{\partial W}{\partial J}\frac{\partial J}{\partial \Lambda_{SR}}, \tag{316}$$

where $n = 1, 4, 9$ and

$$\frac{\partial \overline{I}_1}{\partial \Lambda_{SR}} = 0, \quad \frac{\partial \overline{I}_4}{\partial \Lambda_{SR}} = 0, \quad \frac{\partial \overline{I}_9}{\partial \Lambda_{SR}} = J^{-2/3}A_R A_S, \quad \frac{\partial J}{\partial \Lambda_{SR}} = 0. \tag{317}$$

By substituting equations (310) and (317) into eq. (268) we obtain the final form of the Kirchoff stress

$$\begin{aligned}\tau_{(ij)} =& 2F_{iR}F_{jS}J^{-2/3}\left\{k_1\left(\delta_{SR} - \frac{1}{3}C^{-1}_{RS}C_{AA}\right) + 2k_2(\overline{I}_4 - 1)(A_R A_S - \right.\\ &- \frac{1}{3}C^{-1}_{RS}A_B C_{CB}A_C) + \frac{2}{3}k_6\overline{I}_9\left[-C^{-1}_{RS}A_B\Lambda_{CB}A_C + G_{pO}F^{-1}_{Op}\left(\frac{1}{3}C^{-1}_{RS}I_4 - \right.\right.\\ &\left.\left.\left. - A_R A_S\right)\right] + \frac{1}{d}(J-1)C^{-1}_{RS}J^{-5/3}\right\} + (G_{iR}F_{jS} + G_{jR}F_{iS})2k_6\overline{I}_9 J^{-2/3}A_R A_S.\end{aligned} \tag{318}$$

8.4 Couple stress

The deviatoric part of Kirchoff couple stress $\overline{\mu}_{ji}$ is given by equation (277), where derivatives $\frac{\partial W}{\partial \Lambda_{PR}}$ can be found from eq. (316). Then the final form of the Kirchoff couple stress $\overline{\mu}_{ji}$ can be written as

$$\overline{\mu}_{ji} = \frac{4}{3}\epsilon_{ikm}k_6 J^{-2/3}\overline{I}_9 A_P A_R F_{mP}(F_{jR}b_k + F_{kR}b_j). \tag{319}$$

8.5 Derivative of the force stress with respect to deformation gradient

Derivatives of the force stress (318) according to the deformation gradient can be written

$$\begin{aligned}\frac{\partial \tau_{(ij)}}{\partial F_{kL}} =& 2(\delta_{ik}F_{jS}M_{LS} + F_{iR}\delta_{jk}M_{RL}) + 2F_{iR}F_{jS}\frac{\partial M_{RS}}{\partial F_{kL}} + \\ &+ \frac{\partial N_{RS}}{\partial F_{kL}}(G_{iR}F_{jS} + G_{jR}F_{iS}) + N_{RL}(G_{iR}\delta_{jk} + G_{jR}\delta_{ik}),\end{aligned} \tag{320}$$

where

$$\begin{aligned}M_{RS} =& k_1\left(J^{-2/3}\delta_{SR} - \frac{1}{3}C_{RS}^{-1}\overline{I}_1\right) + 2k_2(\overline{I}_4 - 1)\left(J^{-2/3}A_RA_S - \frac{1}{3}C_{RS}^{-1}\overline{I}_4\right) - \\ &+ \frac{2}{3}k_6\overline{I}_9\left[-C_{RS}^{-1}\overline{I}_9 + G_{pO}F_{Op}^{-1}\left(\frac{1}{3}C_{RS}^{-1}\overline{I}_4 - J^{-2/3}A_RA_S\right)\right] + \frac{J}{d}(J-1)C_{RS}^{-1},\end{aligned} \tag{321}$$

$$N_{RS} = 2k_6\overline{I}_9J^{-2/3}A_RA_S, \tag{322}$$

$$\begin{aligned}\frac{\partial M_{RS}}{\partial F_{kL}} =& \frac{1}{3}\frac{\partial C_{RS}^{-1}}{\partial F_{kL}}\left[-k_1\overline{I}_1 - 2k_2(\overline{I}_4 - 1)\overline{I}_4 + 2k_6\overline{I}_9\left(\frac{1}{3}G_{pO}F_{Op}^{-1}\overline{I}_4 - \overline{I}_9\right) + \right. \\ &\left. + \frac{3}{d}J(J-1)\right] - \frac{1}{3}k_1\left(2J^{-2/3}F_{Lk}^{-1}\delta_{SR} + C_{RS}^{-1}\frac{\overline{I}_1}{\partial F_{kL}}\right) + \\ &+ \frac{2}{3}k_2\left[J^{-2/3}A_RA_S\left(3\frac{\partial \overline{I}_4}{\partial F_{kL}} - 2\overline{I}_4F_{Lk}^{-1} + 2F_{Lk}^{-1}\right) + \right. \\ &\left. + C_{RS}^{-1}\frac{\partial \overline{I}_4}{\partial F_{kL}}(1 - 2\overline{I}_4)\right] - C_{RS}^{-1}\left[\frac{4}{3}k_6\overline{I}_9\frac{\partial \overline{I}_9}{\partial F_{kL}} - \frac{1}{d}JF_{Lk}^{-1}(2J-1)\right] + \\ &+ \frac{2}{9}k_6G_{pO}\left[\frac{\partial \overline{I}_9}{\partial F_{kL}}F_{Op}^{-1}C_{RS}^{-1}\overline{I}_4 + \overline{I}_9\frac{\partial F_{Op}^{-1}}{\partial F_{kL}}C_{RS}^{-1}\overline{I}_4 + \overline{I}_9F_{Op}^{-1}C_{RS}^{-1}\frac{\partial \overline{I}_4}{\partial F_{kL}} - \right. \\ &\left. - J^{-2/3}A_RA_S\left(3\frac{\partial \overline{I}_9}{\partial F_{kL}}F_{Op}^{-1} + 3\overline{I}_9\frac{\partial F_{Op}^{-1}}{\partial F_{kL}} - 2\overline{I}_9F_{Op}^{-1}\right)\right]\end{aligned} \tag{323}$$

and

$$\frac{\partial N_{RS}}{\partial F_{kL}} = 2k_6J^{-2/3}A_RA_S\left(\frac{\partial \overline{I}_9}{\partial F_{kL}} - \frac{2}{3}\overline{I}_9F_{Lk}^{-1}\right). \tag{324}$$

Derivatives of the inverse Cauchy-Green tensorwith respect to the deformation gradient are given by eq. (290) and derivatives of the modified invariants are

$$\frac{\partial \overline{I}_1}{\partial F_{kL}} = 2J^{-2/3}\left(-\frac{1}{3}F_{Lk}^{-1}C_{AA} + F_{kL}\right) \tag{325}$$

$$\frac{\partial \overline{I}_4}{\partial F_{kL}} = 2J^{-2/3}A_BA_C\left(-\frac{2}{3}F_{Lk}^{-1}C_{CB} + \delta_{CL}F_{kB} + F_{kC}\delta_{LB}\right) \tag{326}$$

$$\frac{\partial \overline{I}_9}{\partial F_{kL}} = J^{-2/3}\left[-\frac{2}{3}F^{-1}_{Lk}\left(A_B\Lambda_{CB}A_C - \frac{1}{3}I_4 G_{pO}F^{-1}_{Op}\right) + A_B G_{kB}A_L - \right. \tag{327}$$

$$\left. -\frac{1}{3}(F_{kB}\delta_{LC} + F_{kC}\delta_{LB})G_{pO}F^{-1}_{Op} + \frac{1}{3}I_4 G_{pO}F^{-1}_{Ok}F^{-1}_{Lp}\right],$$

where

$$\frac{\partial I_4}{\partial F_{kL}} = A_B(\delta_{LC}F_{kB} + \delta_{LB}F_{kC})A_C \tag{328}$$

and

$$\frac{\partial F^{-1}_{Op}}{\partial F_{kL}} = -F^{-1}_{Ok}F^{-1}_{Lp} \tag{329}$$

were used.

8.6 Derivative of the force stress with respect to tensor G

Derivative of the force stress (318) with respect to the tensor **G** can be written

$$\begin{aligned}\frac{\partial \tau_{(ij)}}{\partial G_{kL}} =& 2k_6 J^{-2/3}\left\{A_S\left[A_R\frac{\partial \overline{I}_9}{\partial G_{kL}}(G_{iR}F_{jS} + G_{jR}F_{iS}) + \overline{I}_9 A_L(\delta_{ik}F_{jS} + \delta_{jk}F_{iS})\right] - \right.\\ &+ \frac{2}{3}F_{iR}F_{jS}\left[-C^{-1}_{RS}A_B A_C\left(\frac{\partial \overline{I}_9}{\partial G_{kL}}\Lambda_{CB} + \overline{I}_9 F_{kC}\delta_{LB}\right) + \right.\\ &\left.\left.+ \left(\frac{1}{3}C^{-1}_{RS}I_4 - A_R A_S\right)\left(\frac{\partial \overline{I}_9}{\partial G_{kL}}G_{pO}F^{-1}_{Op} + \overline{I}_9 F^{-1}_{Lk}\right)\right\},\end{aligned} \tag{330}$$

where

$$\frac{\partial \overline{I}_9}{\partial G_{oL}} = J^{-2/3}\left(A_L F_{oC}A_C - \frac{1}{3}I_4 F^{-1}_{Lo}\right) \tag{331}$$

and invariant I_4 is defined in eq. (265).

8.7 Derivative of the couple stress with respect to deformation gradient

Derivatives of the couple stress (319) with respect to the def. gradient can be written in the following form

$$\begin{aligned}\frac{\partial \overline{\mu}_{ji}}{\partial F_{kL}} =& \frac{2}{3}\epsilon_{iom}\left\{F_{mP}\left[\frac{\partial N_{PR}}{\partial F_{kL}}(F_{jR}b_o + F_{oR}b_j) + N_{PR}(\delta_{jk}\delta_{LR}b_o + F_{jR}\delta_{ok}A_L + \right.\right.\\ &\left.\left.+ \delta_{ok}\delta_{LR}b_j + F_{oR}\delta_{jk}A_L)\right] + N_{LR}\delta_{km}(F_{jR}b_o + F_{oR}b_j)\right\},\end{aligned} \tag{332}$$

where N_{PR} or N_{LR} are given by eq. (322) and derivative $\frac{\partial N_{PR}}{\partial F_{kL}}$ is defined in eq. (324).

8.8 Derivatives of the couple stress with respect to tensor G

Derivatives of the couple stress (319) with respect to the tensor **G** can be written in the following form

$$\frac{\partial \overline{\mu}_{ji}}{\partial G_{oL}} = \frac{4}{3}\epsilon_{ikm}k_6 J^{-2/3}\frac{\partial \overline{I}_9}{\partial G_{oL}}A_P A_R F_{mP}(F_{jR}b_k + F_{kR}b_j), \tag{333}$$

where derivatives $\frac{\partial \overline{I}_9}{\partial G_{oL}}$ are defined in (331).

9 Determination of material parameters

There are several material parameters in strain energy density functions (263) or (297) - k_1, k_2 and k_6. that have to be determined. Material parameter k_1 corresponds to the hyperelastic matrix and its determination is described in chapter (3.6). A feasible determination of the other two parameters - k_2, k_6 that correspond to fibres will be described in this chapter.

The following chapter - "9.1 Simplified approach" describes a simplified possible way how the parameters can be determined. Note that the simplified approach is valid only for composite materials with linear elastic fibres and with insignificant Young's modulus of the matrix compared to the fibres. Next, determination of the material parameter k_2 is described in chapter "9.1.1 Tension of fibres " and parameter k_6 is determined in chapter "9.1.2 Bending of fibres". Verification of material parameter k_6 was not performed, therefore, the chapter "9.1.2 Bending of fibres" should be taken as a proposal that needs to be verified.

Finally, homogenization techniques are discussed shortly in the last subchapter. These techniques are able to determine material parameters generally for any composite materials made of either linear or nonlinear components.

9.1 Simplified approach

9.1.1 Tension of fibres

The material parametr k_2 in the strain energy density functions (94) or (95) established in chapter 4.2.2 will be determined in this section. This determination procedure can be also used for the same material parametr k_2 occuring in eq. (263) and (297).

It is reminded that material parametr k_2 corresponds to the fibres only (not to the matrix) and is related to the invariant I_4. Hence, tension or compression of the fibre can be affected by this material parameter only.

Consider uniaxial tension loading of the incompressible composite specimen that was described in chapter 4.2.2, with fibres in the loading direction, so that their unit vector is

$$\mathbf{A}^T = (1, 0, 0). \tag{334}$$

We can write from Hooke's law for the stress σ in the composite (in the loading direction)

$$\sigma = E_c(\lambda - 1), \tag{335}$$

where λ is the stretch ratio in the loading direction and can be defined by engineering strain ε as

$$\lambda - 1 = \varepsilon \tag{336}$$

and E_c is Young's modulus of the composite defined by the well-known mixture rule

$$E_c = E_m v_m + E_f v_f. \tag{337}$$

Young modulus of the elastomer matrix E_m can be neglected in comparison with the Young modulus of the steel fibres E_f (usually $E_m = 20$ MPa and $E_f = 210000$ MPa), and the volume fraction of the fibres was introduced in chapter 4.2.2 as $v_f = 0.3534$. Next, the stress in the incompressible (matrix) composite specimen can be also expressed as (from eq. (275) and considering only terms that correspond to k_2)

$$\sigma_{ij} = 4F_{iR}F_{jS}k_2(I_4 - 1)A_R A_S \tag{338}$$

and in the loading direction

$$\sigma_{11} = 4F_{11}^2 k_2(I_4 - 1). \tag{339}$$

Remind that

$$F_{11} = \frac{\partial x_1}{\partial X_1} = \lambda_{11} = \lambda \tag{340}$$

and

$$I_4 = \mathbf{ACA} = C_{11} = F_{11}^2 + F_{21}^2 + F_{31}^2. \tag{341}$$

Since uniaxial tension loading is considered then

$$I_4 = F_{11}^2 = \lambda^2 \tag{342}$$

and the stress (339) can be rewritten into

$$\sigma_{11} = 4\lambda^2 k_2(\lambda^2 - 1). \tag{343}$$

Now, it is obvious that eq. (335) equals to the eq. (339) , so we have

$$E_c(\lambda - 1) = 4\lambda^2 k_2(\lambda^2 - 1) \tag{344}$$

and from this eq. the material parameter k_2 follows in the form

$$k_2 = \frac{E_c(\lambda - 1)}{4\lambda^2(\lambda^2 - 1)}. \tag{345}$$

Considering that the stretch ratio of the fibres is growing gradually, e.g. $\lambda = [1, 1.001, 1.002, 1.003, ...]$ and using the least square method, we find that $k_2 = 9180$ MPa.

There is another way of how to determine material parameter k_2. This approach is based on the elastic strain energy accumulated in a solid due to its elastic deformation. Consider steel fibres under tensional load with a displacement field as follows (see appendix A.6 for further details):

$$u_1 = \frac{\sigma}{E_c} X_1, \;\; u_2 = -\frac{\mu\sigma}{E_c} X_2, \;\; u_3 = -\frac{\mu\sigma}{E_c} X_3. \tag{346}$$

Using the displacements field (346), the deformation gradient can be expressed as

$$\mathbf{F} = \begin{bmatrix} 1 + \frac{\sigma}{E_c} & 0 & 0 \\ 0 & 1 - \frac{\mu\sigma}{E_c} & 0 \\ 0 & 0 & 1 - \frac{\mu\sigma}{E_c} \end{bmatrix}$$

and with respect to eq. (334)

$$I_4 = \left(1 + \frac{\sigma}{E_c}\right)^2. \tag{347}$$

Next, the part of strain energy density function that corresponds to tension/compression of the fibres is (96)

$$W_{fibres,tens./comp.} = k_2(I_4 - 1)^2 \tag{348}$$

and we can write with respect to eq. (347)

$$W_{fibres,tens./comp.} = k_2\left[\left(1 + \frac{\sigma}{E_c}\right)^2 - 1\right]^2. \tag{349}$$

An integration of equation (349) over the circular cross-section with diameter d gives us the elastic strain energy per unit length of the steel fibre

$$\iint_S W_{fibres,tens./comp.} dX_2 dX_3 = k_2 \frac{\pi d^2}{4}\left[\left(1 + \frac{\sigma}{E_c}\right)^2 - 1\right]^2. \tag{350}$$

In the linear theory of elasticity, it holds for the elastic strain energy per unit length

$$W = 2\frac{F_a^2}{\pi E_c d^2}, \tag{351}$$

where F_a is the loading force. Now, the energy obtained by equation (350) should equal to the energy in (351), so we have

$$\frac{2F^2}{\pi E_c d^2} = k_2 \frac{\pi d^2}{4}\left[\left(1+\frac{\sigma}{E_c}\right)^2 - 1\right]^2. \tag{352}$$

The material parameter k_2 then can be expressed from (352) using least-squares method for different values of the loading force F_a. Using the same condition as in the previous paragraph ($E_c = 74214$ MPa, $d = 0.45$ mm) and loading force $F_a = [1, 2, 3, 4, 5, 6, 7, 8, 9, 10]$ N, the material parameter yields $k_2 = 9200$ MPa. It's obvious by comparing with the value obtained in the previous paragraph $k_2 = 9180$ that the difference is insignificant (only 20MPa).

9.1.2 Bending of fibres

A feasible approach to determination of material parametr k_6 occurring in the strain energy density functions (263) and (297) will be introduced in this section. Let's remind that material parametr k_6 corresponds to the fibres only (not to the matrix), relates to the bending of the fibre and corresponds to the term

$$k_6 I_9^2. \tag{353}$$

Consider a deformation of the steel fibre due to a pair of couples of magnitude M applied at the ends of the fibre. The displacement field (see appendix A.7 for further information) can be described as follows

$$u_1 = \frac{M}{E_f J_f} X_1 X_2, \quad u_2 = \frac{\mu M}{2E_f J_f}(X_3^2 - X_2^2) - \frac{M}{2E_f J_f} X_1^2, \quad u_3 = -\frac{\mu M}{E_f J_f} X_2 X_3, \tag{354}$$

where E_f is Young's modulus of the fibres and J_f is the quadratic cross-sectional moment of the fibres. Then components of deformation gradient can be written as

$$\mathbf{F} = \begin{bmatrix} 1 + \frac{MX_2}{E_f J_f} & \frac{MX_1}{E_f J_f} & 0 \\ -\frac{MX_1}{E_f J_f} & 1 - \frac{\mu M X_2}{E_f J_f} & \frac{\mu M X_3}{E_f J_f} \\ 0 & -\frac{\mu M X_3}{E_f J_f} & 1 - \frac{\mu M X_2}{E_f J_f} \end{bmatrix}$$

and components of tensor G are

$$\mathbf{G} = \begin{bmatrix} 0 & \frac{M}{E_f J_f} & 0 \\ -\frac{M}{E_f J_f} & 0 & 0 \\ 0 & 0 & 0 \end{bmatrix}$$

With respect to the (334), invariant I_9 equals to

$$I_9 = \mathbf{A\Lambda A} = \frac{M^4 X_1^2}{E_f^4 J_f^4} \tag{355}$$

and the part of the strain energy density function that corresponds to bending of the fibres is (263)

$$W_{fibres,bending} = k_6 I_9^2 = k_6 \frac{M^4 X_1^2}{E_f^4 J_f^4}. \tag{356}$$

An integration of equation (356) over a circular cross-section with diameter d gives us the elastic strain energy per unit length of the steel fibre

$$\iint_S W_{fibres,bending} = k_6 \frac{1}{12} \frac{M^4 \pi d^2}{E_f^4 J_f^4}. \tag{357}$$

The elastic strain energy per unit length in the linear theory of elasticity is

$$W = \frac{M^2}{2E_f J_f}. \tag{358}$$

The energy in equation (356) should equal to the energy in (358), so we have

$$\frac{M^2}{2E_f J_f} = k_6 \frac{1}{12} \frac{M^4 \pi d^2}{E_f^4 J_f^4} \tag{359}$$

and for a certain moment M the material parameter k_6 can be determined.

9.2 Homogenization techniques

The unknown material parameters can be determined by methods, where heterogenous material (e.g. fibre composite) is replaced by an equivalent homogenous one with the same macroscopic properties. Material parameters of such equivalent homogenous material, so called effective material properties, are determined from components of the original heterogenous material (i.e. from properties of the matrix and fibres).

Consider two basic approaches for obtaining the overall response of a heterogeneous medium

- the *average field theory* (or the mean-field theory) and the *homogenization theory*. Roughly speaking, these are physics and mathematics based theories, respectively. Here, the basic features of these two theories are interpreted as follows [21]:

Average field theory. This theory works with the reprezentative volume element (RVE) and is based on the fact that the effective mechanical properties measured in experiments are relations between the volume average of the strain and stress of microscopically heterogeneous samples. Hence, macrofields are defined as the volume averages of the corresponding microfelds, and the effective properties are determined as relations between the averaged microfields.

Homogenization theory. This theory works with periodic structure and establishes mathematical relations between the microfields and the macrofields, using a multi-scale perturbation method. Then the effective properties emerge naturally as consequences of these relations, without dependence on specific physical measurements.

A detailed description of both theories can be found in [21]. Homogenization methods based on Cosserat continuum can be found in Forest's works [12], [13] and [14], who deals with both Cosserat continum and micromorphic materials.

The rest of this chapter shows the average field theory process taken from Sluis [29]. The following sections try to adapt the average field procedure presented in [29] to our constitutive equations. Note that presented procedure is not completed and some things have to be solved before its use in practise. However, the presented procedure can be a good starting point for a detailed study and work with the average fields theory based on Cosserat continuum.

Let X be the position of a material point of the macroscopic continuum, and let Y be the position of a material point in the RVE associated with the material point X. In the sequel, the symbols with an overstrike character represent macroscopic quantities, and the symbols without these overstrike characters are microscopic quantities. Now let us split up the microscopic displacement field into a rigid body motion and a part representing the actual deformation

$$\mathbf{u}(\mathbf{X},\mathbf{Y}) = \overline{\mathbf{u}}_0 + \overline{\boldsymbol{\varphi}} \times \mathbf{v}(\mathbf{X},\mathbf{Y}), \qquad \mathbf{v}(\mathbf{X},\mathbf{0}) = \mathbf{0}, \tag{360}$$

or

$$u_i(\mathbf{X},\mathbf{Y}) = \overline{u}_{0i} + \epsilon_{ijK}\overline{\varphi}_j Y_K + v_i(\mathbf{X},\mathbf{Y}), \qquad v_i(\mathbf{X},\mathbf{0}) = \mathbf{0}, \tag{361}$$

where the first two terms represent the rigid macroscopic motion (rigid translation and rigid rotation) and the last term symbolises the (true) deformation which ultimatively causes stresses and strains in the material.

The form of microscopic displacement field u_i can be written out

$$u_1 = \overline{u}_{01} + \overline{\varphi}_2 Y_3 - \overline{\varphi}_3 Y_2 + v_1 \tag{362}$$

$$u_2 = \overline{u}_{02} + \overline{\varphi}_3 Y_1 - \overline{\varphi}_1 Y_3 + v_2 \tag{363}$$

$$u_3 = \overline{u}_{03} + \overline{\varphi}_1 Y_2 - \overline{\varphi}_2 Y_1 + v_3. \tag{364}$$

Relations between micro and macro quantities

Since the first step of the homogenization process is definition of the relations between the macroscopic and microscopic quantities, we define the macroscopic gradient of the displacemnt field as an average of the gradient of the microscopic displacement field,

$$\frac{\partial \overline{u}_i}{\partial X_J} = \left\langle \frac{\partial u_i}{\partial Y_J} \right\rangle = \frac{1}{V}\int\limits_V \frac{\partial u_i}{\partial Y_J} dV \tag{365}$$

where

$$\frac{\partial u_i}{\partial Y_J} = \epsilon_{ikJ}\overline{\varphi}_k + \frac{\partial v_i}{\partial Y_J}. \tag{366}$$

Next, the deformation gradient then can be written out as

$$\overline{F}_{iJ} = \delta_{iJ} + \frac{\partial \overline{u}_i}{\partial X_J} = \delta_{iJ} + \epsilon_{ikJ}\overline{\varphi}_k + \left\langle \frac{\partial u_i}{\partial Y_J} \right\rangle \tag{367}$$

and tensor $\mathbf{G}$

$$\overline{G}_{iJ} = \frac{\partial \overline{b}_i}{\partial X_J} = \frac{\partial(\overline{F}_{iR}\overline{A}_R)}{\partial X_J} = \frac{\partial \overline{F}_{iR}}{\partial X_J}\overline{A}_R = \frac{\partial^2 \overline{u}_i}{\partial X_J \partial X_R}\overline{A}_R = \left\langle \frac{\partial^2 v_i}{\partial Y_J \partial Y_R} \right\rangle \overline{A}_R. \tag{368}$$

True displacement field

To obtain an expression for $\mathbf{v}$, we expand $\mathbf{v}$ into a Taylor series around the origin of the RVE, $\mathbf{Y}$=$\mathbf{0}$, disregarding terms of order $O(\|\mathbf{Y}\|^3)$ and higher, and keeping $\mathbf{X}$ constant,

$$v_i(\mathbf{X},\mathbf{Y}) = v_{0i}(\mathbf{X}) + \left.\frac{\partial v_i(\mathbf{X},\mathbf{Y})}{\partial Y_J}\right|_{Y=0} Y_J + \frac{1}{2}\left.\frac{\partial^2 v_i(\mathbf{X},\mathbf{Y})}{\partial Y_J \partial Y_K}\right|_{Y=0} Y_J Y_K =$$

$$= \alpha_{iJ} Y_J + \frac{1}{2}\beta_{iJK} Y_J Y_K, \tag{369}$$

where, according to (361), we have $v_{0i}(\mathbf{X}) = 0$. Taking the first and second order gradients of this expression and averaging these expressions over the RVE volume V yields

$$\left\langle \frac{\partial v_i}{\partial Y_J} \right\rangle = \alpha_{iJ} + \beta_{ijk} M_k, \tag{370}$$

$$\left\langle \frac{\partial^2 v_i}{\partial Y_J \partial Y_K} \right\rangle = \beta_{iJK}, \tag{371}$$

where

$$M_k = \frac{1}{V} \int_V Y_K dV \tag{372}$$

is a geometry parameter. For example consider a cubic RVE, i.e. $Y_1, Y_2, Y_3 \epsilon [-a, a], then$

$$M_k = \frac{1}{V} \int_V Y_1 dY_1 dY_2 dY_3 = \frac{1}{8a^3} \int_{-a}^{a} \int_{-a}^{a} \int_{-a}^{a} Y_1 dY_1 dY_2 dY_3 = 0 \tag{373}$$

and we have

$$\left\langle \frac{\partial v_i}{\partial Y_J} \right\rangle = \alpha_{iJ} \tag{374}$$

$$\left\langle \frac{\partial^2 v_i}{\partial Y_J \partial Y_K} \right\rangle = \beta_{iJK}. \tag{375}$$

Considering a cubic RVE, eq. (374) and deformation gradient (367) we can write

$$\alpha_{iJ} = \left\langle \frac{\partial v_i}{\partial Y_J} \right\rangle = \overline{F}_{iJ} - \delta_{iJ} + \epsilon_{iJk} \overline{\varphi}_k. \tag{376}$$

Next, we can write from (368) and using (375)

$$\overline{G}_{iJ} = \frac{\partial \overline{F}_{iR}}{\partial X_J} \overline{A}_R = \left\langle \frac{\partial^2 v_i}{\partial Y_J \partial Y_R} \right\rangle \overline{A}_R = \beta_{iJR} \overline{A}_R, \tag{377}$$

therefore, from the last eq. (377) we have

$$\frac{\partial \overline{F}_{iK}}{\partial X_J} = \beta_{iJK}. \tag{378}$$

Then using eq. (376) and (378), the true displacement field (369) can be written out as

$$v_i = (\overline{F}_{iK} - \delta_{iK} - \epsilon_{ijK} \overline{\varphi}_j) Y_K + \frac{1}{2} \frac{\partial \overline{F}_{iK}}{\partial X_J} Y_J Y_K. \tag{379}$$

Finally, we have obtained the formulation of the displacement field in terms of macroscopic deformation quantities

$$u_i = \overline{u}_{0i} + (\overline{F}_{iK} - \delta_{iK})Y_K + \frac{1}{2}\frac{\partial \overline{F}_{iK}}{\partial X_J} Y_J Y_K. \tag{380}$$

The macroscopic potencial energy $\overline{W} = \overline{W}(\overline{F}_{iJ}, \overline{G}_{iJ})$ can be defined as a volume average of its microscopic equivalent $W = W(F_{iJ})$,

$$\overline{W}(\overline{F}_{iJ}, \overline{G}_{iJ}) = \frac{1}{V}\int_V W(F_{iJ})dY. \tag{381}$$

The macroscopic quantities $\overline{F}_{iJ}, \overline{G}_{iJ}$ can be determined using (380) and based on suitable simulations (tension, bending of the composite material) as well as the right side of the eq. (381). Then eq. (381) should contain only the unknown material parameters.

10 Finite element implementation of Cosserat continuum

The new constitutive equations introduced in the chapter 6 contain, inter alia, tensor G_{iJ} that was introduced in (225) as

$$G_{iJ} = \frac{\partial b_i}{\partial X_J} = \frac{\partial F_{iR} A_R}{\partial X_J} = A_R \frac{\partial^2 u_i}{\partial X_J \partial X_R}. \tag{382}$$

Next, the principle of virtual work (401) that will be introduced in the following chapter contains the following term that, due to the constrained Cosserat theory, equals to

$$\frac{\partial \delta\omega_i}{\partial x_j} = \frac{1}{2}\epsilon_{ilk} \frac{\partial^2 \delta u_k}{\partial x_j \partial x_l}. \tag{383}$$

It's obvious from both equations (382) and (383) that Cosserat continuum contains second derivatives of the displacement field. This higher-order theory requires the so called C^1 continuity in order to ensure convergence of the finite element procedure. The C^1 continuity means that both displacements and their first derivatives are continuous over the elements and their boundaries.

There is another possibility how to ensure convergence of the mentioned Cosserat continuum. We can consider two unknown independent fields - displacements u_i and derivatives

$$\phi_{iJ} = \frac{\partial u_i}{\partial X_J}, \tag{384}$$

so equations (382) and (383) can be rewritten into

$$G_{iJ} = A_R \frac{\partial \phi_{iR}}{\partial X_J} \tag{385}$$

$$\frac{\partial \delta\omega_i}{\partial x_j} = \frac{1}{2}\epsilon_{ilk} \frac{\partial \delta\phi_{kM}}{\partial x_j} F^{-1}_{Ml}. \tag{386}$$

Now, the equations (385) and (386) contain only first derivatives of the uknown field ϕ_{iJ}, therefore, the standard C^0 continuity of the both uknown fields is sufficient for ensuring the convergence. However, the uknown fields are not independent (they are constrained by eq. (384)), therefore, an additional constraint (384) has to be incorporated to the finite element equations - this was done with help of Lagrange multipliers.

This chapter formulates the principle of virtual work of the Cosserat continuum and introduces the finite element formulation of constrained Cosserat continuum, based on two different approaches - Lagrange multipliers and C^1 elements. The later approach (C^1 elements) was programmed in Matlab software and comparison between results obtained on the basis of Cauchy and Cosserat continuums can be found at the end of this chapter.

10.1 Principle of virtual work

The principle of virtual work is the starting point for finite element analysis, therefore, let's show the derivation of this principle first.

In quasistatic mechanic the equilibrium equations for the force stress (195) are reduced into the form

$$\frac{\partial \sigma_{ji}}{\partial x_j} = 0 \tag{387}$$

and the equilibrium equations for the couple stress (196) are reduced into

$$\frac{\partial m_{ji}}{\partial x_j} + \epsilon_{ijk}\sigma_{jk} = 0. \tag{388}$$

In order to obtain principle of virtual work, let's multiply equation (387) by virtual velocity field δu_i and equation (388) by virtual spin field $\delta\omega_i$ and integrate their sum over volume v

$$\int_v \frac{\partial \sigma_{(ji)}}{\partial x_j}\delta v_i dv + \int_v \left(\frac{\partial m_{ji}}{\partial x_j}\delta\omega_i + \epsilon_{ijk}\sigma_{jk}\delta\omega_i\right)dv = 0. \tag{389}$$

Because of

$$\frac{\partial}{\partial x_j}(\sigma_{ji}\delta v_i) = \frac{\partial \sigma_{ji}}{\partial x_j}\delta v_i + \sigma_{ji}\frac{\partial \delta v_i}{\partial x_j} \tag{390}$$

$$\frac{\partial}{\partial x_j}(m_{ji}\delta\omega_i) = \frac{\partial m_{ji}}{\partial x_j}\delta\omega_i + m_{ji}\frac{\partial \delta\omega_i}{\partial x_j}$$

and with help of Gauss-Ostrogradsky's theorem, we can rewrite equation (389) into

$$\int_v \left(\sigma_{ji}\frac{\partial \delta v_i}{\partial x_j} + m_{ji}\frac{\partial \delta\omega_i}{\partial x_j} - \varepsilon_{ijk}\sigma_{jk}\delta\omega_i\right)dv = \int_s (t_i\delta v_i + l_i\delta\omega_i)ds \tag{391}$$

where $t_i = \sigma_{ji}n_j$ and $l_i = m_{ji}n_j$ are traction vectors that were introduced by eq. (157) and (158).

Parcial derivatives $\frac{\partial \delta v_i}{\partial x_j}$ can be devided into symetric δd_{ij} and antisymetric $\delta \omega_{ij}$ parts

$$\frac{\partial \delta v_i}{\partial x_j} = \delta d_{ij} + \delta \omega_{ij} \tag{392}$$

where

$$\delta d_{ij} = \frac{1}{2}\left(\frac{\partial \delta v_i}{\partial x_j} + \frac{\partial \delta v_j}{\partial x_i}\right) \tag{393}$$

$$\delta \omega_{ij} = \frac{1}{2}\left(\frac{\partial \delta v_i}{\partial x_j} - \frac{\partial \delta v_j}{\partial x_i}\right).$$

Similarly the force stress can be devided into its symmetric $\sigma_{(ij)}$ and antisymetric $\sigma_{[ji]}$ parts

$$\sigma_{ji} = \sigma_{(ij)} + \sigma_{[ji]} \tag{394}$$

and the couple stress into its volumetric and deviatoric $\overline{m}_{ji}$ parts

$$m_{ji} = \frac{1}{3} m_{ii}\delta_{ij} + \overline{m}_{ji}. \tag{395}$$

Since the following relations are valid

$$\sigma_{(ij)}\delta\omega_{ij} = 0, \qquad -\epsilon_{ijk}\delta\omega_i = \delta\omega_{jk}, \qquad \delta\omega_{ji} = -\delta\omega_{ij}, \tag{396}$$

$$\sigma_{[ji]}\delta d_{ij} = 0, \qquad \frac{\partial \omega_i}{\partial x_i} = 0, \qquad \sigma_{(ij)}\delta d_{ij} = \sigma_{(ij)}\frac{\partial \delta v_i}{\partial x_j},$$

then substituting (392), (394), (395) into (391) leads to the principle of virtual work in the form

$$\int_v \left(\sigma_{(ij)}\frac{\partial \delta v_i}{\partial x_j} + \overline{m}_{ji}\frac{\partial \delta \omega_i}{\partial x_j}\right) dv = \int_s (t_i \delta v_i + l_i \delta \omega_i) ds. \tag{397}$$

Obviously, the principle of virtual work depends on the symmetric part of Cauchy force stress and on deviatoric part of Cauchy couple stress only.

Let's introduce symmetric Kirchhoff force stress $\tau_{(ij)}$ and deviatoric Kirchhoff couple stress $\overline{\mu}_{ji}$

$$\tau_{(ij)} = J\sigma_{(ij)} \qquad \overline{\mu}_{ji} = J\overline{m}_{ji}, \tag{398}$$

where

$$J = \frac{dv}{dV}. \tag{399}$$

Next, we will consider that the right side of equation (397) is integrated only over the boundary where displacements or rotations are prescribed. In other words, traction vector will not be prescribed on the body surface (no external forces or couples). Hence, and because of $\delta v_i = \delta\omega_i = 0$ on $s_{u+\omega}$, it holds

$$\int_{s_{u+\omega}} (t_i \delta v_i + l_i \delta\omega_i) ds = 0. \tag{400}$$

Now, with help of (398), (399), (400), the principle of virtual work (397) can be rewritten into the final form

$$\int_V \left(\tau_{(ij)} \frac{\partial \delta v_i}{\partial x_j} + \overline{\mu}_{ji} \frac{\partial \delta\omega_i}{\partial x_j} \right) dV = 0. \tag{401}$$

10.2 Lagrange multipliers

10.2.1 Total potential energy functional

A total potential energy functional Π is the sum of the elastic energy U accumulated in the deformed body and potential energy V of the applied forces. But as it was mentioned in the previous section, we will consider only deformation load realized through the prescribed displacements and their derivatives, therefore the potencial energy V is omitted. The total energy functional whose directional derivatives yield the principle of virtual work is

$$\Pi = \int_V W dV \tag{402}$$

10.2.2 Total potential energy functional with constraint

In previous section (6.1) the tensor G was introduced as

$$G_{iJ} = A_R \frac{\partial^2 u_i}{\partial X_J \partial X_R}. \tag{403}$$

Let's now introduce a new uknown variable ϕ_{iR} and rewrite tensor G_{iJ} into the form

$$G_{iJ} = A_R \frac{\partial \phi_{iR}}{\partial X_J}. \tag{404}$$

Next, we will consider two different uknowns - displacements u_i and their derivatives ϕ_{iJ}. It's obvious that both kinematic fields u_i, ϕ_{iJ} are mutually dependent

$$\phi_{iJ} = \frac{\partial u_i}{\partial X_J}. \tag{405}$$

However, we will consider in our procedure that both fields are independent. Then the total energy functional (402) has to be extended by the condition (405) and a new functional Π_c with constraint is then

$$\Pi_c = \Pi + \int_V \lambda_{iJ}\left(\frac{\partial u_i}{\partial X_J} - \phi_{iJ}\right)dV \tag{406}$$

where λ_{iJ} are Lagrange multipliers. Directional derivatives of (406) yield the principle of virtual work which is a basis for finite element method. The directional derivatives in directions $\delta v_i, \delta\varphi_{iJ}$ and $\delta\lambda_{iJ}$ will be considered separately

$$D\Pi_c[\delta\mathbf{v}] = D\Pi[\delta\mathbf{v}] + \int_V \lambda_{iJ}\frac{\partial\delta v_i}{\partial X_J}dV \tag{407}$$

$$D\Pi_c[\delta\boldsymbol{\varphi}] = D\Pi[\delta\boldsymbol{\varphi}] - \int_V \lambda_{iJ}\delta\varphi_{iJ}dV \tag{408}$$

$$D\Pi_c[\delta\boldsymbol{\lambda}] = \int_V \delta\lambda_{iJ}\left(\frac{\partial u_i}{\partial X_J} - \phi_{iJ}\right)dV \tag{409}$$

where $D\Pi[\delta\mathbf{v}]$ is the first term in (401), i.e.

$$D\Pi[\delta\mathbf{v}] = \int_V \tau_{(ij)}\frac{\partial\delta v_i}{\partial x_j}dV \tag{410}$$

and $D\Pi[\delta\boldsymbol{\varphi}]$ can be derived from the second term of equation (401), i.e.

$$D\Pi[\delta\boldsymbol{\varphi}] = \int_V \overline{\mu}_{ji}\frac{\partial\delta\omega_i}{\partial x_j}dV = \int_V \frac{1}{2}\epsilon_{ikl}\overline{\mu}_{ji}\frac{\partial}{\partial x_j}(\delta\varphi_{lM}F^{-1}_{Mk})dV, \tag{411}$$

because

$$\delta\omega_i = \frac{1}{2}\epsilon_{ikl}\frac{\partial\delta v_l}{\partial X_M}F^{-1}_{Mk} = \frac{1}{2}\epsilon_{ikl}\delta\varphi_{lM}F^{-1}_{Mk}. \tag{412}$$

So the principle of virtual work can now be written in the final form

$$\begin{aligned}\int_V \Bigg[\tau_{(ij)}\frac{\partial\delta v_i}{\partial x_j} + \frac{1}{2}\overline{\mu}_{ji}\epsilon_{ikl}\frac{\partial}{\partial x_j}(\delta\varphi_{lM}F^{-1}_{Mk}) + \lambda_{iJ}\frac{\partial\delta v_i}{\partial X_J} - \\ - \lambda_{iJ}\delta\varphi_{iJ} + \delta\lambda_{iJ}\left(\frac{\partial u_i}{\partial X_J} - \phi_{iJ}\right)\Bigg]dV = 0\end{aligned} \tag{413}$$

10.2.3 Finite element discretization

The principle of virtual work (413) can be rewritten into the following form

$$\int_V \left[\tau_{(ij)} \frac{\partial \delta v_i}{\partial X_M} F^{-1}_{Mj} + \frac{1}{2} \epsilon_{ikl} \overline{\mu}_{ji} \left(\frac{\partial \delta \varphi_{lM}}{\partial X_N} F^{-1}_{Mk} + \delta \varphi_{lM} \frac{\partial F^{-1}_{Mk}}{\partial X_N} \right) F^{-1}_{Nj} + \right.$$

$$\left. + \lambda_{iJ} \frac{\partial v_i}{\partial X_J} - \lambda_{iJ} \delta \varphi_{iJ} + \delta \lambda_{iJ} \left(\frac{\partial u_i}{\partial X_J} - \phi_{iJ} \right) \right] dV = 0, \tag{414}$$

where

$$\frac{\partial F^{-1}_{Mk}}{\partial X_N} = -F^{-1}_{Pk} \frac{\partial F_{oP}}{\partial X_N} F^{-1}_{Mo} = -F^{-1}_{Pk} \frac{\partial \phi_{oP}}{\partial X_N} F^{-1}_{Mo}. \tag{415}$$

The last equation (415) was obtained on the basis of the following consideration:

$$F_{iJ} F^{-1}_{Jk} = \delta_{ik} \tag{416}$$

and the derivatives of (416) are as follows

$$\frac{\partial F_{iJ}}{\partial X_N} F^{-1}_{Jk} + F_{iJ} \frac{\partial F^{-1}_{Jk}}{\partial X_N} = 0, \tag{417}$$

which leads to equation (415).

The volume integral in the virtual work equation (414) is taken over the reference configuration advantageously, since we can take the given initial shape of the solid as reference, whereas the deformed configuration is unknown.

The displacements field u_i and virtual velocity field δv_i, as well as derivatives field ϕ_{iJ} and virtual gradient of velocity field $\delta \varphi_{iJ}$ are specified in an arbitrary point within the solid by interpolating between nodal values in some convenient way,

$$u_i(\mathbf{X}) = N^a(\mathbf{X}) u^a_i, \qquad \delta v_i(\mathbf{X}) = N^a(\mathbf{X}) \delta v^a_i \tag{418}$$

$$\phi_{iJ}(\mathbf{X}) = M^a(\mathbf{X}) \phi^a_{iJ}, \qquad \delta \varphi_{iJ}(\mathbf{X}) = M^a(\mathbf{X}) \delta \varphi^a_{iJ}. \tag{419}$$

Here, $\mathbf{X}$ denotes coordinates of an arbitrary point in the reference configuration and u^a_i, ϕ^a_{iJ} are unknown displacements and derivatives respectively in each node. N^a and M^a are standard C^0 shape functions and Lagrange multipliers can be interpolated linearly over the element with 4 multiplier's nodes

$$\lambda_{iJ} = O^a \lambda^a_{iJ}, \qquad \delta \lambda_{iJ} = O^a \delta \lambda^a_{iJ}. \tag{420}$$

Now, we can discretize the principle of virtual work (414) by substituting (418), (419) and (420)

$$\int_V \left(\tau_{(ij)}\frac{\partial N^a}{\partial X_M}F^{-1}_{Mj} + \lambda^b_{iJ}O^b\frac{\partial N^a}{\partial X_J}\right)dV.\delta u^a_i + \int_V O^a\left(\frac{\partial N^b}{\partial X_J}u^b_i - \phi^b_{iJ}M^b\right)dV.\delta\lambda^a_{iJ} +$$

$$+\int_V \left[\frac{1}{2}\epsilon_{ikl}\overline{\mu}_{ji}\left(\frac{\partial M^a}{\partial X_N}F^{-1}_{Mk} - M^aF^{-1}_{Pk}\frac{\partial \phi_{oP}}{\partial X_N}F^{-1}_{Mo}\right)F^{-1}_{Nj} - \lambda^b_{lM}O^bM^a\right]dV.\delta\phi^a_{lM} = 0 \tag{421}$$

10.2.4 Newton-Raphson iterative procedure

Since equation (421) must hold for all independent virtual fields $\delta u^a_i, \delta\phi^a_{lM}$ and λ^a_{iJ}, we have

$$\int_V \left(\tau_{(ij)}\frac{\partial N^a}{\partial X_M}F^{-1}_{Mj} + \lambda^b_{iJ}O^b\frac{\partial N^a}{\partial X_J}\right)dV = 0, \tag{422}$$

$$\int_V \left[\frac{1}{2}\epsilon_{ikl}\overline{\mu}_{ji}\left(\frac{\partial M^a}{\partial X_N}F^{-1}_{Mk} - M^aF^{-1}_{Pk}\frac{\partial \phi_{oP}}{\partial X_N}F^{-1}_{Mo}\right)F^{-1}_{Nj} - \lambda^b_{lM}O^bM^a\right]dV = 0, \tag{423}$$

and

$$\int_V O^a\left(\frac{\partial N^b}{\partial X_J}u^b_i - \phi^b_{iJ}M^b\right)dV = 0. \tag{424}$$

Nonlinear equations (422), (423) and (424) can be solved using Newton-Raphson iterative process whereby given a solution estimate $\mathbf{x}_k$ at iteration k. A new value is obtained in terms of an increment by establishing the linear approximation [3]

$$\mathbf{R}(\mathbf{x}_{k+1}) \approx \mathbf{R}(\mathbf{x}_k) + D(\mathbf{R}(\mathbf{x}_k)),[\mathbf{u}] + D(\mathbf{R}(\mathbf{x}_k)),[\boldsymbol{\phi}] + D(\mathbf{R}(\mathbf{x}_k)),[\boldsymbol{\lambda}], \tag{425}$$

where symbol "$D(\ )$" means directional derivatives in the specified direction "[ ]".
Let's now calculate gradually the directional derivatives (425) of equations (422), (423) and (424).

Eq.(422):

$$D(\mathbf{R}(\mathbf{x}_k)),[\mathbf{u}] = \int_V \left(\frac{\partial \tau_{(ij)}}{\partial u^b_n}\frac{\partial N^a}{\partial X_M}F^{-1}_{Mj} + \tau_{(ij)}\frac{\partial N^a}{\partial X_M}\frac{\partial F^{-1}_{Mj}}{\partial u^b_n}\right).\Delta u^b_n dV, \tag{426}$$

where

$$\frac{\partial \tau_{(ij)}}{\partial u^b_n} = \frac{\partial \tau_{(ij)}}{\partial F_{kL}}\frac{\partial F_{kL}}{\partial u^b_n} = \frac{\partial \tau_{(ij)}}{\partial F_{kL}}\frac{\partial N^b}{\partial X_L}\delta_{nk} \tag{427}$$

$$F_{oP} = \delta_{oP} + \frac{\partial u_o}{\partial X_p} = \delta_{oP} + \frac{\partial N^b}{\partial X_P} u_o^b \tag{428}$$

and similary as in (415) we have

$$\frac{\partial F_{Mj}^{-1}}{\partial u_n^b} = -F_{Mo}^{-1} \frac{\partial N^b}{\partial X_P} F_{Pj}^{-1} \delta_{on}. \tag{429}$$

After substituting (427), (428) and (429) into (426) we obtain the final form of directional derivative

$$D(\mathbf{R}(\mathbf{x}_k)), [\mathbf{u}] = \int_V \left(\frac{\partial \tau_{(ij)}}{\partial F_{kL}} \frac{\partial N^a}{\partial X_M} \frac{\partial N^b}{\partial X_L} F_{Mj}^{-1} . \Delta u_k^b - \tau_{(ij)} \frac{\partial N^a}{\partial X_M} \frac{\partial N^b}{\partial X_L} F_{Mk}^{-1} F_{Lj}^{-1} . \Delta u_k^b \right) dV. \tag{430}$$

Next,

$$D(\mathbf{R}(\mathbf{x}_k)), [\boldsymbol{\phi}] = \int_V \frac{\partial \tau_{(ij)}}{\partial \phi_{pQ}} \frac{\partial N^a}{\partial X_M} F_{Mj}^{-1} . \Delta \phi_{pQ}^b dV \tag{431}$$

where

$$\frac{\partial \tau_{(ij)}}{\partial \phi_{pQ}} = \frac{\partial \tau_{(ij)}}{\partial G_{kL}} \frac{\partial G_{kL}}{\partial \phi_{pQ}} = \frac{\partial \tau_{(ij)}}{\partial G_{kL}} A_R \frac{\partial M^b}{\partial X_L} \delta_{kp} \delta_{QR} \tag{432}$$

$$G_{kL} = A_R \frac{\partial \phi_{kR}}{\partial X_L} = A_R \frac{\partial M^b}{\partial X_L} \phi_{kR}^b. \tag{433}$$

Therefore, the final form of directional derivative (430) is

$$D(\mathbf{R}(\mathbf{x}_k)), [\boldsymbol{\phi}] = \int_V \frac{\partial \tau_{(ij)}}{\partial G_{kL}} \frac{\partial N^a}{\partial X_M} \frac{\partial M^b}{\partial X_L} F_{Mj}^{-1} A_R . \Delta \phi_{kR}^b dV. \tag{434}$$

And directional derivative of (422) in the direction $\boldsymbol{\lambda}$ is

$$D(\mathbf{R}(\mathbf{x}_k)), [\boldsymbol{\lambda}] = \int_V \frac{\partial N^a}{\partial X_J} O^b . \Delta \lambda_{iJ}^b dV. \tag{435}$$

Let's continue with **eq.(423)**. Since we can write

$$\frac{\partial \overline{\mu}_{ji}}{\partial u_q^b} = \frac{\partial \overline{\mu}_{ji}}{\partial F_{rS}} \frac{\partial F_{rS}}{\partial u_q^b} \tag{436}$$

and with help of equations (428) and (429) the directional derivative in the direction $\boldsymbol{u}$ yields after some manipulations

$$D(\mathbf{R}(\mathbf{x}_k)),[\boldsymbol{u}] = \int_V \left\{ \frac{\partial M^a}{\partial X_N}\frac{\partial N^b}{\partial X_D}\left[\frac{\partial \overline{\mu}_{ji}}{\partial F_{cD}} F^{-1}_{Mk}F^{-1}_{Nj} - \overline{\mu}_{ji}(F^{-1}_{Mc}F^{-1}_{Dk}F^{-1}_{Nj} + \right.\right.$$
$$+ F^{-1}_{Mk}F^{-1}_{Nc}F^{-1}_{Dj})\Big] + M^a\frac{\partial N^b}{\partial X_D}\frac{\partial \phi_{oP}}{\partial X_N}\left[-\frac{\partial \overline{\mu}_{ji}}{\partial F_{cD}}F^{-1}_{Pk}F^{-1}_{Mo}F^{-1}_{Nj} + \right.$$
$$\left.\left. + \overline{\mu}_{ji}(F^{-1}_{Pc}F^{-1}_{Dk}F^{-1}_{Mo}F^{-1}_{Nj} + F^{-1}_{Pk}F^{-1}_{Mc}F^{-1}_{Do}F^{-1}_{Nj} + F^{-1}_{Pk}F^{-1}_{Mo}F^{-1}_{Nc}F^{-1}_{Dj})\right]\right\}.\Delta u^b_c dV. \tag{437}$$

Next, we can write

$$\frac{\partial \overline{\mu}_{ji}}{\partial \phi_{cD}} = \frac{\partial \overline{\mu}_{ji}}{\partial G_{sT}}\frac{\partial G_{sT}}{\partial \phi_{cD}} \tag{438}$$

and with help of eq. (433) the directional derivative in direction $\boldsymbol{\phi}$ yields

$$D(\mathbf{R}(\mathbf{x}_k)),[\boldsymbol{\phi}] = \int_V \frac{1}{2}\epsilon_{ikl}F^{-1}_{Nj}\left[\frac{\partial \overline{\mu}_{ji}}{\partial G_{sT}}\frac{\partial M^b}{\partial X_T}A_D\left(\frac{\partial M^a}{\partial X_N}F^{-1}_{Mk} - M^a F^{-1}_{Pk}\frac{\partial \phi_{oP}}{\partial X_N}F^{-1}_{Mo}\right) - \right.$$
$$\left. - \overline{\mu}_{ji}M^a\frac{\partial M^b}{\partial X_N}F^{-1}_{Dk}F^{-1}_{Ms}\right].\Delta\phi^b_{sD}dV \tag{439}$$

and directional derivative in direction $\boldsymbol{\lambda}$ is

$$D(\mathbf{R}(\mathbf{x}_k)),[\boldsymbol{\lambda}] = -\int_V M^a O^b.\Delta\lambda^b_{lM}dV. \tag{440}$$

It follows the last three directional derivatives of **eq. (424)**

$$D(\mathbf{R}(\mathbf{x}_k)),[\boldsymbol{u}] = \int_V O^a\frac{\partial N^b}{\partial X_J}.\Delta u^b_i dV, \tag{441}$$

$$D(\mathbf{R}(\mathbf{x}_k)),[\boldsymbol{\phi}] = -\int_V O^a M^b.\Delta\phi^b_{iJ}dV, \tag{442}$$

and

$$D(\mathbf{R}(\mathbf{x}_k)),[\boldsymbol{\lambda}] = 0. \tag{443}$$

After application of the Newton-Raphson procedure to the previous directional derivatives we get a system of three linear equations

$$K^{uu}_{aibk}.\Delta u^b_k + K^{u\phi}_{aibkR}.\Delta\phi^b_{kR} + K^{u\lambda}_{aJb}.\Delta\lambda^b_{iJ} = -R^a_i \tag{444}$$

$$K^{\phi u}_{alMbc}.\Delta u^b_c + K^{\phi\phi}_{alMbsD}.\Delta\phi^b_{sD} + K^{\phi\lambda}_{ab}.\Delta\lambda^b_{lM} = -R^a_{lM} \tag{445}$$

$$K^{\lambda u}_{aJb}.\Delta u^b_i + K^{\lambda\phi}_{ab}.\Delta\phi^b_{iJ} + K^{\lambda\lambda}_{ab}.\Delta\lambda^b_{iJ} = -R^a_{iJ} \tag{446}$$

where residuum R^a_i is given by the left side of eq. (422), R^a_{lM} by the left side of eq. (423), and R^a_{iJ} by the left side of eq. (424). The stiffness matrixes that result from directional derivatives are

$$K^{uu}_{aibk} = \int_V \frac{\partial N^a}{\partial X_M}\frac{\partial N^b}{\partial X_L}\left(\frac{\partial \tau_{(ij)}}{\partial F_{kL}}F^{-1}_{Mj} - \tau_{(ij)}F^{-1}_{Mk}F^{-1}_{Lj}\right)dV, \tag{447}$$

$$K^{u\phi}_{aibkR} = \int_V \frac{\partial \tau_{(ij)}}{\partial G_{kL}}\frac{\partial N^a}{\partial X_M}\frac{\partial M^b}{\partial X_L}F^{-1}_{Mj}A_R dV, \tag{448}$$

$$K^{u\lambda}_{aJb} = \int_V \frac{\partial N^a}{\partial X_J}O^b dV, \tag{449}$$

$$\begin{aligned} K^{\phi u}_{alMbc} = \int_V \Bigg\{ & \frac{\partial M^a}{\partial X_N}\frac{\partial N^b}{\partial X_D}\left[\frac{\partial \overline{\mu}_{ji}}{\partial F_{cD}}F^{-1}_{Mk}F^{-1}_{Nj} - \overline{\mu}_{ji}(F^{-1}_{Mc}F^{-1}_{Dk}F^{-1}_{Nj} + \right. \\ & \left. + F^{-1}_{Mk}F^{-1}_{Nc}F^{-1}_{Dj})\right] + M^a\frac{\partial N^b}{\partial X_D}\frac{\partial \phi_{oP}}{\partial X_N}\left[-\frac{\partial \overline{\mu}_{ji}}{\partial F_{cD}}F^{-1}_{Pk}F^{-1}_{Mo}F^{-1}_{Nj} + \right. \\ & \left. + \overline{\mu}_{ji}(F^{-1}_{Pc}F^{-1}_{Dk}F^{-1}_{Mo}F^{-1}_{Nj} + F^{-1}_{Pk}F^{-1}_{Mc}F^{-1}_{Do}F^{-1}_{Nj} + F^{-1}_{Pk}F^{-1}_{Mo}F^{-1}_{Nc}F^{-1}_{Dj})\right]\Bigg\}dV, \end{aligned} \tag{450}$$

$$\begin{aligned} K^{\phi\phi}_{alMbsD} = \int_V \frac{1}{2}\epsilon_{ikl}F^{-1}_{Nj}\Bigg[& \frac{\partial \overline{\mu}_{ji}}{\partial G_{sT}}\frac{\partial M^b}{\partial X_T}A_D\left(\frac{\partial M^a}{\partial X_N}F^{-1}_{Mk} - M^a F^{-1}_{Pk}\frac{\partial \phi_{oP}}{\partial X_N}F^{-1}_{Mo}\right) - \\ & - \overline{\mu}_{ji}M^a\frac{\partial M^b}{\partial X_N}F^{-1}_{Dk}F^{-1}_{Ms}\Bigg]dV, \end{aligned} \tag{451}$$

$$K^{\phi\lambda}_{ab} = -\int_V M^a O^b dV, \tag{452}$$

$$K^{\lambda u}_{aJb} = \int_V O^a\frac{\partial N^b}{\partial X_J}dV, \tag{453}$$

$$K^{\lambda\phi}_{ab} = -\int_V O^a M^b.\Delta\phi^b_{iJ}dV, \tag{454}$$

and

$$K_{ab}^{\lambda\lambda} = 0. \tag{455}$$

10.3 Hermite C1 elements

10.3.1 Construction of shape functions

Consider a third order polynom in the form

$$f(\xi) = a + b\xi + c\xi^2 + d\xi^3, \tag{456}$$

and its derivative

$$\frac{\partial f(\xi)}{\partial \xi} = b + 2c\xi + 3d\xi^2. \tag{457}$$

Next, consider a one-dimensional element with two nodes. We need to construct **four different shape functions** satisfying the following requirements:

- the value of the **first** shape function φ_1 equals to one at the first node and is zero at the other node. The first derivative of the first shape function φ_1 equals to zero at both nodes,
- the value of the **second** shape function φ_2 equals to one at the second node and is zero at the other node. The first derivative of the second shape function φ_2 equals to zero at both nodes,
- the value of the **third** shape function Φ_1 equals to zero at both nodes. The first derivative of the third shape function Φ_1 equals to one at the first node and is zero at the other node,
- the value of the **fourth** shape function Φ_2 equals to zero at both nodes. The first derivative of the fourth shape function Φ_2 equals to one at the second node and is zero at the other node.

Let's construct the **first shape function** which equals to one at node 1 at the coordinate $\xi = -1$, equals to zero at node 2 at the coordinate $\xi = 1$, and its derivatives are zero at both nodes. For this purpose, substitute appropriate coordinates to the equations (456),

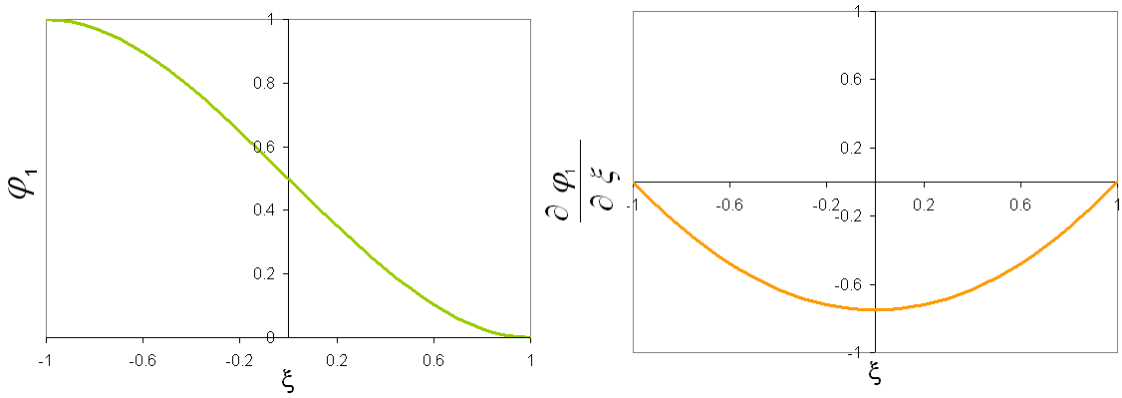

Figure 15: Shape function at node 1.

(457) and set the left hand side of these eqautions to the required values at the appropriate nodes

$$1 = a - b + c - d \tag{458}$$

$$0 = a + b + c + d \tag{459}$$

$$0 = b - 2c + 3d \tag{460}$$

$$0 = b + 2c + 3d. \tag{461}$$

The above system of four equations was solved for four unknows a, b, c, d with the following result

$$a = \frac{1}{2}, b = -\frac{3}{4}, c = 0, d = \frac{1}{4} \tag{462}$$

and the shape function that is depicted in fig. (15) can be written in the form

$$\varphi_1 = \frac{1}{4}(1 - \xi)^2(2 + \xi). \tag{463}$$

Repeat the same process mentioned above and construct the **third shape function**, i.e. find the third shape function that equals to zero at both nodes (i.e. at coordinates $\xi = \pm 1$) and the first derivative of the third shape function equals to one at the first node and is

zero at the other node. So we have

$$0 = a - b + c - d \tag{464}$$

$$0 = a + b + c + d \tag{465}$$

$$1 = b - 2c + 3d \tag{466}$$

$$0 = b + 2c + 3d. \tag{467}$$

Then the unknowns are

$$a = \frac{1}{4}, b = -\frac{1}{4}, c = -\frac{1}{4}, d = \frac{1}{4} \tag{468}$$

and the third shape function is (see also fig. (16))

$$\Phi_1 = \frac{1}{4}(1-\xi)^2(1+\xi). \tag{469}$$

The same procedure was repeated and the second and fourth shape functions were found (see also fig. (16))

$$\varphi_2 = \frac{1}{4}(1+\xi)^2(2-\xi), \tag{470}$$

$$\Phi_2 = \frac{1}{4}(1+\xi)^2(\xi-1). \tag{471}$$

An extension to a three dimensional 8 nodes element can be written in the form

$$\begin{aligned}
N_1 &= \varphi_1(\xi_1)\varphi_1(\xi_2)\varphi_1(\xi_3) & N_5 &= \varphi_1(\xi_1)\varphi_1(\xi_2)\varphi_2(\xi_3) \\
N_2 &= \varphi_2(\xi_1)\varphi_1(\xi_2)\varphi_1(\xi_3) & N_6 &= \varphi_2(\xi_1)\varphi_1(\xi_2)\varphi_2(\xi_3) \\
N_3 &= \varphi_2(\xi_1)\varphi_2(\xi_2)\varphi_1(\xi_3) & N_7 &= \varphi_2(\xi_1)\varphi_2(\xi_2)\varphi_2(\xi_3) \\
N_4 &= \varphi_1(\xi_1)\varphi_2(\xi_2)\varphi_1(\xi_3) & N_8 &= \varphi_1(\xi_1)\varphi_2(\xi_2)\varphi_2(\xi_3)
\end{aligned} \tag{472}$$

$$\begin{aligned}
O_1 &= \Phi_1(\xi_1)\varphi_1(\xi_2)\varphi_1(\xi_3) & O_5 &= \Phi_1(\xi_1)\varphi_1(\xi_2)\varphi_2(\xi_3) \\
O_2 &= \Phi_2(\xi_1)\varphi_1(\xi_2)\varphi_1(\xi_3) & O_6 &= \Phi_2(\xi_1)\varphi_1(\xi_2)\varphi_2(\xi_3) \\
O_3 &= \Phi_2(\xi_1)\varphi_2(\xi_2)\varphi_1(\xi_3) & O_7 &= \Phi_2(\xi_1)\varphi_2(\xi_2)\varphi_2(\xi_3) \\
O_4 &= \Phi_1(\xi_1)\varphi_2(\xi_2)\varphi_1(\xi_3) & O_8 &= \Phi_1(\xi_1)\varphi_2(\xi_2)\varphi_2(\xi_3)
\end{aligned} \tag{473}$$

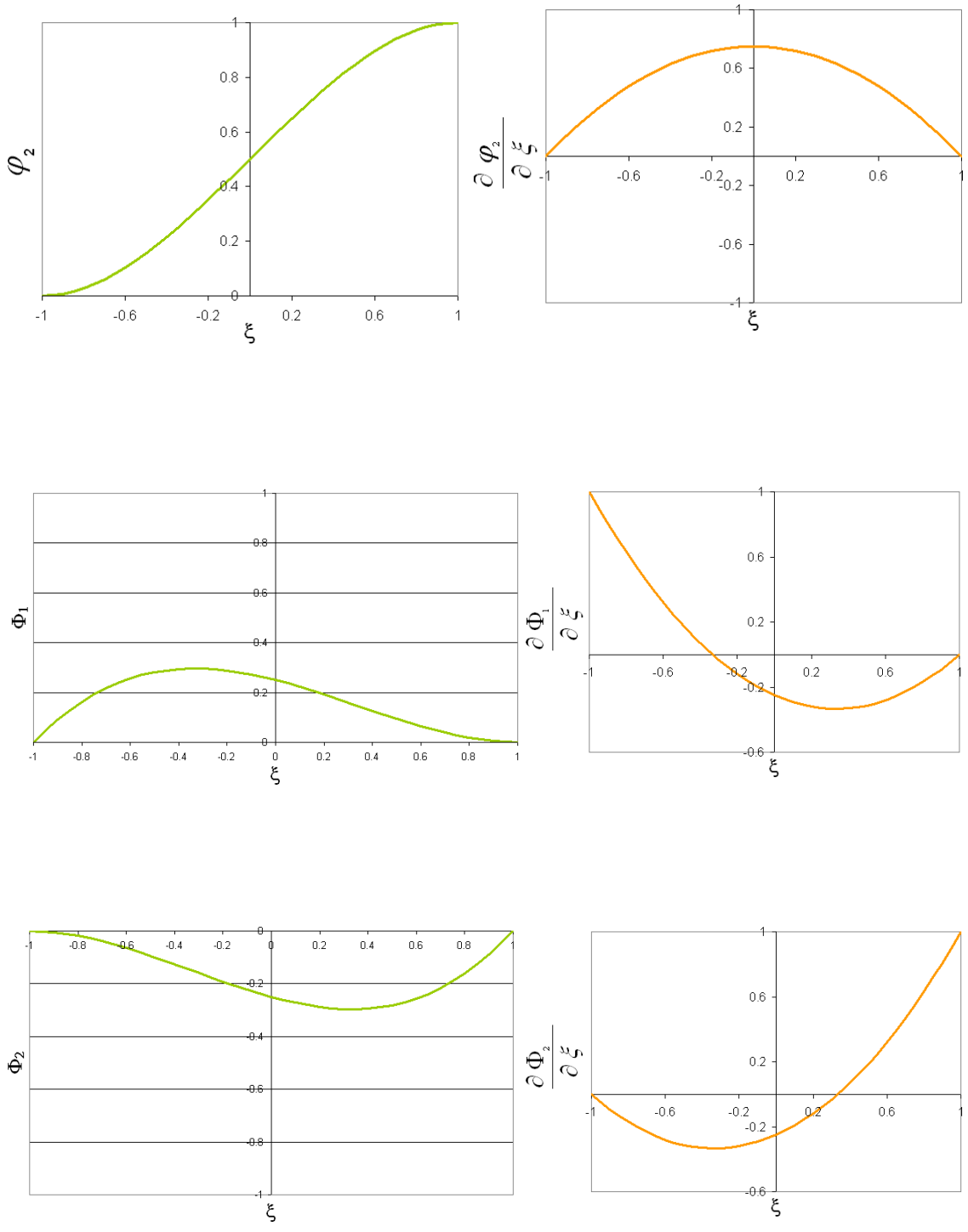

Figure 16: Shape functions.

$$
\begin{aligned}
P_1 &= \varphi_1(\xi_1)\Phi_1(\xi_2)\varphi_1(\xi_3) & P_5 &= \varphi_1(\xi_1)\Phi_1(\xi_2)\varphi_2(\xi_3)\\
P_2 &= \varphi_2(\xi_1)\Phi_1(\xi_2)\varphi_1(\xi_3) & P_6 &= \varphi_2(\xi_1)\Phi_1(\xi_2)\varphi_2(\xi_3)\\
P_3 &= \varphi_2(\xi_1)\Phi_2(\xi_2)\varphi_1(\xi_3) & P_7 &= \varphi_2(\xi_1)\Phi_2(\xi_2)\varphi_2(\xi_3)\\
P_4 &= \varphi_1(\xi_1)\Phi_2(\xi_2)\varphi_1(\xi_3) & P_8 &= \varphi_1(\xi_1)\Phi_2(\xi_2)\varphi_2(\xi_3)
\end{aligned} \tag{474}
$$

$$
\begin{aligned}
Q_1 &= \varphi_1(\xi_1)\varphi_1(\xi_2)\Phi_1(\xi_3) & Q_5 &= \varphi_1(\xi_1)\varphi_1(\xi_2)\Phi_2(\xi_3)\\
Q_2 &= \varphi_2(\xi_1)\varphi_1(\xi_2)\Phi_1(\xi_3) & Q_6 &= \varphi_2(\xi_1)\varphi_1(\xi_2)\Phi_2(\xi_3)\\
Q_3 &= \varphi_2(\xi_1)\varphi_2(\xi_2)\Phi_1(\xi_3) & Q_7 &= \varphi_2(\xi_1)\varphi_2(\xi_2)\Phi_2(\xi_3)\\
Q_4 &= \varphi_1(\xi_1)\varphi_2(\xi_2)\Phi_1(\xi_3) & Q_8 &= \varphi_1(\xi_1)\varphi_2(\xi_2)\Phi_2(\xi_3)
\end{aligned} \tag{475}
$$

Substitution of shape functions (463), (470), (469) and (471) to the expressions (472), (473), (474) and (475) results in the final forms of the shape functions. These final forms can be found in the appendix (A.5).

The approximation of the displacement field is then

$$u_i = N^a u_i^a + O^a \alpha_i^a + P^a \beta_i^a + Q^a \gamma_i^a, \tag{476}$$

where a corresponds to the node number (a=1..8) and $u_i^a, \alpha_i^a, \beta_i^a, \gamma_i^a$ are the unknown displacements and slopes in the i-th node, respectively. Next, approximation of deformation gradient $\mathbf{F}$ and tensor $\mathbf{G}$ can be written

$$F_{iJ} = \delta_{iJ} + \frac{\partial u_i}{\partial X_J} = \delta_{iJ} + \frac{\partial N^a}{\partial X_J} u_i^a + \frac{\partial O^a}{\partial X_J} \alpha_i^a + \frac{\partial P^a}{\partial X_J} \beta_i^a + \frac{\partial Q^a}{\partial X_J} \gamma_i^a, \tag{477}$$

$$G_{iJ} = \frac{\partial (F_{iR} A_R)}{\partial X_J} = A_R \frac{\partial^2 u_i}{\partial X_J \partial X_R} = \tag{478}$$

$$= A_R \left(\frac{\partial^2 N^a}{\partial X_J \partial X_R} u_i^a + \frac{\partial^2 O^a}{\partial X_J \partial X_R} \alpha_i^a + \frac{\partial^2 P^a}{\partial X_J \partial X_R} \beta_i^a + \frac{\partial^2 Q^a}{\partial X_J \partial X_R} \gamma_i^a \right).$$

Since N^a (or any other shape function) depends on the natural coordinates $N^a = N^a(\xi_1, \xi_2, \xi_3)$, we need to determine how the first and second parcial derivatives (479) in previous equations can be calculated

$$\frac{\partial N^a}{\partial X_J}, \frac{\partial O^a}{\partial X_J}, \frac{\partial P^a}{\partial X_J}, \frac{\partial Q^a}{\partial X_J}, \frac{\partial^2 N^a}{\partial X_J \partial X_R}, \frac{\partial^2 O^a}{\partial X_J \partial X_R}, \frac{\partial^2 P^a}{\partial X_J \partial X_R}, \frac{\partial^2 Q^a}{\partial X_J \partial X_R}. \tag{479}$$

In order to obtain them, we can write

$$\frac{\partial N^a}{\partial X_J} = \frac{\partial N^a}{\partial \xi_i}\frac{\partial \xi_i}{\partial X_J}, \tag{480}$$

$$\frac{\partial^2 N^a}{\partial X_J \partial X_R} = \frac{\partial}{\partial X_J}\left(\frac{\partial N^a}{\partial \xi_i}\frac{\partial \xi_i}{\partial X_R}\right) = \frac{\partial \xi_j}{\partial X_J}\frac{\partial}{\partial \xi_j}\left(\frac{\partial N^a}{\partial \xi_i}\frac{\partial \xi_i}{\partial X_R}\right) = \tag{481}$$

$$= \frac{\partial^2 N^a}{\partial \xi_j \partial \xi_i}\frac{\partial \xi_i}{\partial X_J}\frac{\partial \xi_j}{\partial X_R} + \frac{\partial N^a}{\partial \xi_i}\frac{\partial^2 \xi_i}{\partial X_J \partial X_R}.$$

An approximation of the undeformed coordinates was considered as follows

$$X_i = M^a X_i^a, \tag{482}$$

where M^a are the shape functions which are given in the appendix (A.5).

10.3.2 Finite element discretization

The principle of virtual work (401) is a basis for finite element discretization, therefore, let's start with this equation and rewrite it into a more suitable form

$$\int_V \left(\tau_{(ij)}\frac{\partial \delta v_i}{\partial X_M}F^{-1}_{Mj} + \overline{\mu}_{ji}\frac{\partial \delta \omega_i}{\partial X_M}F^{-1}_{Mj}\right)dV = 0. \tag{483}$$

We can write for virtual spin field

$$\delta\omega_i = \frac{1}{2}\epsilon_{ikl}\frac{\partial \delta v_l}{\partial x_k} = \frac{1}{2}\epsilon_{ikl}\frac{\partial \delta v_l}{\partial X_N}F^{-1}_{Nk} \tag{484}$$

and for its deriatives

$$\frac{\partial \delta \omega_i}{\partial X_M} = \frac{1}{2}\epsilon_{ikl}\frac{\partial}{\partial X_M}\left(\frac{\partial \delta v_l}{\partial X_N}F^{-1}_{Nk}\right) = \frac{1}{2}\epsilon_{ikl}\left(\frac{\partial^2 \delta v_l}{\partial X_M \partial X_N}F^{-1}_{Nk} + \frac{\partial \delta v_l}{\partial X_N}\frac{\partial F^{-1}_{Nk}}{\partial X_M}\right). \tag{485}$$

The last equation contains derivatives of inverse of the deformation gradient with respect to the undeformed coordinates. These derivatives can be expressed by the following consideration and procedure

$$F_{oN}F^{-1}_{Nk} = \delta_{ok} \tag{486}$$

and derivatives of the last equation with respect to the undeformed coordinates are

$$\frac{\partial F_{oN}}{\partial X_M}F^{-1}_{Nk} + \frac{\partial F^{-1}_{Nk}}{\partial X_M}F_{oN} = 0. \tag{487}$$

After some manipulations the final form of the respective derivatives will be obtained

$$\frac{\partial F^{-1}_{Nk}}{\partial X_M} = -F^{-1}_{No}\frac{\partial F_{oP}}{\partial X_M}F^{-1}_{Pk} = -F^{-1}_{No}\frac{\partial^2 u_o}{\partial X_M \partial X_P}F^{-1}_{Pk}. \tag{488}$$

Now, substitution of the last equation into eq. (485) gives the final form of derivatives of the virtual spin field

$$\frac{\partial \delta\omega_i}{\partial X_M} = \frac{1}{2}\epsilon_{ikl}\left(\frac{\partial^2 \delta v_l}{\partial X_M \partial X_N}F^{-1}_{Nk} - \frac{\partial \delta v_l}{\partial X_N}\frac{\partial^2 u_o}{\partial X_M \partial X_P}F^{-1}_{No}F^{-1}_{Pk}\right). \tag{489}$$

If we substitute the last equation (489) into the principle of virtual work (483), we can obtain the final form of the principle of virtual work that will be used later in the discretization process

$$\int_V \left[\tau_{(ij)}\frac{\partial \delta v_i}{\partial X_M}F^{-1}_{Mj} + \frac{1}{2}\overline{\mu}_{ji}\epsilon_{ikl}F^{-1}_{Mj}\left(F^{-1}_{Nk}\frac{\partial^2 \delta v_l}{\partial X_M \partial X_N} - \frac{\partial \delta v_l}{\partial X_N}\frac{\partial F_{oP}}{\partial X_M}F^{-1}_{No}F^{-1}_{Pk}\right)\right]dV = 0. \tag{490}$$

Now, let's recall the approximation of displacements field (476)

$$u_i = N^a u_i^a + O^a \alpha_i^a + P^a \beta_i^a + Q^a \gamma_i^a, \tag{491}$$

and similarly to this formula let's introduce an approximation of the velocity field in the form

$$\delta v_i = N^a \delta v_i^a + O^a \delta\alpha_i^a + P^a \delta\beta_i^a + Q^a \delta\gamma_i^a. \tag{492}$$

Equation (492) can be substituted now into the principle of virtual work (490)

$$\begin{aligned}
&\int_V \Bigg\{\tau_{(ij)}F^{-1}_{Mj}\left(\frac{\partial N^a}{\partial X_M}\delta v_i^a + \frac{\partial O^a}{\partial X_M}\delta\alpha_i^a + \frac{\partial P^a}{\partial X_M}\delta\beta_i^a + \frac{\partial Q^a}{\partial X_M}\delta\gamma_i^a\right) + \\
&+ \frac{1}{2}\overline{\mu}_{jl}\epsilon_{lki}F^{-1}_{Mj}\Bigg[F^{-1}_{Nk}\left(\frac{\partial^2 N^a}{\partial X_M \partial X_N}\delta v_i^a + \frac{\partial^2 O^a}{\partial X_M \partial X_N}\delta\alpha_i^a + \frac{\partial^2 P^a}{\partial X_M \partial X_N}\delta\beta_i^a + \frac{\partial^2 Q^a}{\partial X_M \partial X_N}\delta\gamma_i^a\right) \\
&- F^{-1}_{No}F^{-1}_{Pk}\frac{\partial F_{oP}}{\partial X_M}\left(\frac{\partial N^a}{\partial X_N}\delta v_i^a + \frac{\partial O^a}{\partial X_N}\delta\alpha_i^a + \frac{\partial P^a}{\partial X_N}\delta\beta_i^a + \frac{\partial Q^a}{\partial X_N}\delta\gamma_i^a\right)\Bigg]\Bigg\}dV = 0
\end{aligned} \tag{493}$$

and it can be rewritten into the form

$$\left\{\int_V \left[\tau_{(ij)}F^{-1}_{Mj}\frac{\partial N^a}{\partial X_M}+\frac{1}{2}\overline{\mu}_{jl}\epsilon_{lki}F^{-1}_{Mj}\left(F^{-1}_{Nk}\frac{\partial^2 N^a}{\partial X_M\partial X_N}-F^{-1}_{No}F^{-1}_{Pk}\frac{\partial F_{oP}}{\partial X_M}\frac{\partial N^a}{\partial X_N}\right)\right]dV\right\}\delta v_i^a+$$
$$+\left\{\int_V \left[\tau_{(ij)}F^{-1}_{Mj}\frac{\partial O^a}{\partial X_M}+\frac{1}{2}\overline{\mu}_{jl}\epsilon_{lki}F^{-1}_{Mj}\left(F^{-1}_{Nk}\frac{\partial^2 O^a}{\partial X_M\partial X_N}-F^{-1}_{No}F^{-1}_{Pk}\frac{\partial F_{oP}}{\partial X_M}\frac{\partial O^a}{\partial X_N}\right)\right]dV\right\}\delta \alpha_i^a+$$
$$+\left\{\int_V \left[\tau_{(ij)}F^{-1}_{Mj}\frac{\partial P^a}{\partial X_M}+\frac{1}{2}\overline{\mu}_{jl}\epsilon_{lki}F^{-1}_{Mj}\left(F^{-1}_{Nk}\frac{\partial^2 P^a}{\partial X_M\partial X_N}-F^{-1}_{No}F^{-1}_{Pk}\frac{\partial F_{oP}}{\partial X_M}\frac{\partial P^a}{\partial X_N}\right)\right]dV\right\}\delta \beta_i^a+$$
$$+\left\{\int_V \left[\tau_{(ij)}F^{-1}_{Mj}\frac{\partial Q^a}{\partial X_M}+\frac{1}{2}\overline{\mu}_{jl}\epsilon_{lki}F^{-1}_{Mj}\left(F^{-1}_{Nk}\frac{\partial^2 Q^a}{\partial X_M\partial X_N}-F^{-1}_{No}F^{-1}_{Pk}\frac{\partial F_{oP}}{\partial X_M}\frac{\partial Q^a}{\partial X_N}\right)\right]dV\right\}\delta \gamma_i^a=0. \tag{494}$$

Since $\delta v_i, \delta\alpha_i, \delta\beta_i, \delta\gamma_i$ are independent and arbitrary, previous equations (494) will be zero if

$$\int_V \left[\tau_{(ij)}F^{-1}_{Mj}\frac{\partial N^a}{\partial X_M}+\frac{1}{2}\overline{\mu}_{jl}\epsilon_{lki}F^{-1}_{Mj}\left(F^{-1}_{Nk}\frac{\partial^2 N^a}{\partial X_M\partial X_N}-F^{-1}_{No}F^{-1}_{Pk}\frac{\partial F_{oP}}{\partial X_M}\frac{\partial N^a}{\partial X_N}\right)\right]dV=0 \tag{495}$$

$$\int_V \left[\tau_{(ij)}F^{-1}_{Mj}\frac{\partial O^a}{\partial X_M}+\frac{1}{2}\overline{\mu}_{jl}\epsilon_{lki}F^{-1}_{Mj}\left(F^{-1}_{Nk}\frac{\partial^2 O^a}{\partial X_M\partial X_N}-F^{-1}_{No}F^{-1}_{Pk}\frac{\partial F_{oP}}{\partial X_M}\frac{\partial O^a}{\partial X_N}\right)\right]dV=0 \tag{496}$$

$$\int_V \left[\tau_{(ij)}F^{-1}_{Mj}\frac{\partial P^a}{\partial X_M}+\frac{1}{2}\overline{\mu}_{jl}\epsilon_{lki}F^{-1}_{Mj}\left(F^{-1}_{Nk}\frac{\partial^2 P^a}{\partial X_M\partial X_N}-F^{-1}_{No}F^{-1}_{Pk}\frac{\partial F_{oP}}{\partial X_M}\frac{\partial P^a}{\partial X_N}\right)\right]dV=0 \tag{497}$$

$$\int_V \left[\tau_{(ij)}F^{-1}_{Mj}\frac{\partial Q^a}{\partial X_M}+\frac{1}{2}\overline{\mu}_{jl}\epsilon_{lki}F^{-1}_{Mj}\left(F^{-1}_{Nk}\frac{\partial^2 Q^a}{\partial X_M\partial X_N}-F^{-1}_{No}F^{-1}_{Pk}\frac{\partial F_{oP}}{\partial X_M}\frac{\partial Q^a}{\partial X_N}\right)\right]dV=0. \tag{498}$$

The system of four nonlinear equations (495), (496), (497) and (498) was obtained when discretization was applied and this system will be solved by Newton-Raphson iterative procedure in the following section.

10.3.3 Newton-Raphson iterative procedure

The nonlinear system of equations above will be solved similarly to chapter 10.2.4 using Newton-Raphson method. Hence, let's calculate the directional derivatives of eq. (495) in

direction $[\mathbf{u}]$

$$
\begin{aligned}
D(\mathbf{R}(\mathbf{x}_k)),[\mathbf{u}] = \int_V \Bigg\{ & \frac{\partial \tau_{(ij)}}{\partial u_n^b} F_{Mj}^{-1} \frac{\partial N^a}{\partial X_M} + \tau_{(ij)} \frac{\partial F_{Mj}^{-1}}{\partial u_n^b} \frac{\partial N^a}{\partial X_M} + \\
& + \frac{1}{2} \overline{\mu}_{jl} \epsilon_{lki} \frac{\partial F_{Mj}^{-1}}{\partial u_n^b} \left(F_{Nk}^{-1} \frac{\partial^2 N^a}{\partial X_M \partial X_N} - F_{No}^{-1} F_{Pk}^{-1} \frac{\partial N^a}{\partial X_N} \frac{\partial F_{oP}}{\partial X_M} \right) + \\
& + \frac{1}{2} \frac{\partial \overline{\mu}_{jl}}{\partial u_n^b} \epsilon_{lki} F_{Mj}^{-1} \left(F_{Nk}^{-1} \frac{\partial^2 N^a}{\partial X_M \partial X_N} - F_{No}^{-1} F_{Pk}^{-1} \frac{\partial N^a}{\partial X_N} \frac{\partial F_{oP}}{\partial X_M} \right) + \\
& + \frac{1}{2} \overline{\mu}_{jl} \epsilon_{lki} F_{Mj}^{-1} \Bigg[\frac{\partial F_{Nk}^{-1}}{\partial u_n^b} \frac{\partial^2 N^a}{\partial X_M \partial X_N} - \frac{\partial F_{No}^{-1}}{\partial u_n^b} F_{Pk}^{-1} \frac{\partial N^a}{\partial X_N} \frac{\partial F_{oP}}{\partial X_M} - \\
& - F_{No}^{-1} \frac{\partial F_{Pk}^{-1}}{\partial u_n^b} \frac{\partial N^a}{\partial X_N} \frac{\partial F_{oP}}{\partial X_M} - F_{No}^{-1} F_{Pk}^{-1} \frac{\partial N^a}{\partial X_N} \frac{\partial}{\partial u_n^b} \left(\frac{\partial F_{oP}}{\partial X_M} \right) \Bigg] \Bigg\} dV . \Delta u_n^b
\end{aligned}
\tag{499}
$$

Since the deformation gradient is given by

$$
F_{kL} = \delta_{kL} + \frac{\partial u_k}{\partial X_L} = \delta_{kL} + \frac{\partial N^b}{\partial X_L} u_k^b + \frac{\partial O^b}{\partial X_L} \alpha_k^b + \frac{\partial P^b}{\partial X_L} \beta_k^b + \frac{\partial Q^b}{\partial X_L} \gamma_k^b, \tag{500}
$$

we can write

$$
\frac{\partial F_{kL}}{\partial u_n^b} = \frac{\partial N^b}{\partial X_L} \delta_{kn} \tag{501}
$$

$$
\frac{\partial \tau_{(ij)}}{\partial u_n^b} = \frac{\partial \tau_{(ij)}}{\partial F_{kL}} \frac{\partial F_{kL}}{\partial u_n^b} = \frac{\partial \tau_{(ij)}}{\partial F_{kL}} \frac{\partial N^b}{\partial X_L} \delta_{kn}
$$

$$
\frac{\partial \overline{\mu}_{jl}}{\partial u_n^b} = \frac{\partial \overline{\mu}_{jl}}{\partial F_{rS}} \frac{\partial F_{rS}}{\partial u_n^b} = \frac{\partial \tau_{(ij)}}{\partial F_{rS}} \frac{\partial N^b}{\partial X_S} \delta_{rn}
$$

and

$$
\frac{\partial F_{Mj}^{-1}}{\partial u_n^b} = -F_{Mk}^{-1} \frac{\partial N^b}{\partial X_Q} F_{Qj}^{-1} \delta_{nk}. \tag{502}
$$

Substituting (501) and (502) back into (499), the final form of the directional derivatives $D(\mathbf{R}(\mathbf{x}_k)),[\mathbf{u}]$ can be obtained

$$
\begin{aligned}
D(\mathbf{R}(\mathbf{x}_k)),[\mathbf{u}] = \int_V \Bigg[& \frac{\partial N^a}{\partial X_M} \frac{\partial N^b}{\partial X_L} \left(\frac{\partial \tau_{(ij)}}{\partial F_{kL}} F_{Mj}^{-1} - \tau_{(ij)} F_{Mk}^{-1} F_{Lj}^{-1} \right) + \\
& + \frac{1}{2} \epsilon_{lri} \frac{\partial N^b}{\partial X_S} \left(\frac{\partial \overline{\mu}_{jl}}{\partial F_{kS}} F_{Mj}^{-1} - \overline{\mu}_{jl} F_{Mk}^{-1} F_{Sj}^{-1} \right) \left(F_{Nr}^{-1} \frac{\partial^2 N^a}{\partial X_M \partial X_N} - \right. \\
& \left. - F_{No}^{-1} F_{Pr}^{-1} \frac{\partial N^a}{\partial X_N} \frac{\partial F_{oP}}{\partial X_M} \right) + \frac{1}{2} \overline{\mu}_{jl} \epsilon_{lri} F_{Mj}^{-1} \left(-F_{Nk}^{-1} \frac{\partial N^b}{\partial X_S} F_{Sr}^{-1} \frac{\partial^2 N^a}{\partial X_M \partial X_N} + \right. \\
& + F_{Nk}^{-1} \frac{\partial N^b}{\partial X_S} F_{So}^{-1} F_{Pr}^{-1} \frac{\partial N^a}{\partial X_N} \frac{\partial F_{oP}}{\partial X_M} + F_{No}^{-1} F_{Pk}^{-1} \frac{\partial N^b}{\partial X_S} F_{Sr}^{-1} \frac{\partial N^a}{\partial X_N} \frac{\partial F_{oP}}{\partial X_M} - \\
& \left. - F_{Nk}^{-1} F_{Pr}^{-1} \frac{\partial N^a}{\partial X_N} \frac{\partial^2 N^b}{\partial X_M \partial X_P} \right) \Bigg] dV . \Delta u_k
\end{aligned}
\tag{503}
$$

Hence, the stifness matrix resulting from the previous directional derivatives is

$$
\begin{aligned}
K^{uu}_{aibk} = \int_V \Bigg[& \frac{\partial N^a}{\partial X_M}\frac{\partial N^b}{\partial X_L}\left(\frac{\partial \tau_{(ij)}}{\partial F_{kL}}F^{-1}_{Mj} - \tau_{(ij)}F^{-1}_{Mk}F^{-1}_{Lj}\right) + \\
& + \frac{1}{2}\epsilon_{lri}\frac{\partial N^b}{\partial X_S}\left(\frac{\partial \overline{\mu}_{jl}}{\partial F_{kS}}F^{-1}_{Mj} - \overline{\mu}_{jl}F^{-1}_{Mk}F^{-1}_{Sj}\right)\left(F^{-1}_{Nr}\frac{\partial^2 N^a}{\partial X_M \partial X_N} - \right. \\
& \left. - F^{-1}_{No}F^{-1}_{Pr}\frac{\partial N^a}{\partial X_N}\frac{\partial F_{oP}}{\partial X_M}\right) + \frac{1}{2}\overline{\mu}_{jl}\epsilon_{lri}F^{-1}_{Mj}\left(-F^{-1}_{Nk}\frac{\partial N^b}{\partial X_S}F^{-1}_{Sr}\frac{\partial^2 N^a}{\partial X_M \partial X_N} + \right. \\
& + \frac{\partial N^a}{\partial X_N}\frac{\partial N^b}{\partial X_S}\frac{\partial F_{oP}}{\partial X_M}\left(F^{-1}_{Nk}F^{-1}_{So}F^{-1}_{Pr} + F^{-1}_{No}F^{-1}_{Pk}F^{-1}_{Sr}\right) - \\
& \left. - F^{-1}_{Nk}F^{-1}_{Pr}\frac{\partial N^a}{\partial X_N}\frac{\partial^2 N^b}{\partial X_M \partial X_P}\right)\Bigg] dV,
\end{aligned}
\tag{504}
$$

When the above mentioned process is repeated in order to calculate the rest of the directional derivatives of eqs. (495), (496), (497) and (498) in directions $[\mathbf{u}], [\boldsymbol{\alpha}], [\boldsymbol{\beta}]$ and $[\boldsymbol{\gamma}]$, the following stiffness matrixes can be obtained:

$$
\begin{aligned}
K^{u\alpha}_{aibk} = \int_V \Bigg[& \frac{\partial N^a}{\partial X_M}\frac{\partial O^b}{\partial X_L}\left(\frac{\partial \tau_{(ij)}}{\partial F_{kL}}F^{-1}_{Mj} - \tau_{(ij)}F^{-1}_{Mk}F^{-1}_{Lj}\right) + \\
& + \frac{1}{2}\epsilon_{lri}\frac{\partial O^b}{\partial X_S}\left(\frac{\partial \overline{\mu}_{jl}}{\partial F_{kS}}F^{-1}_{Mj} - \overline{\mu}_{jl}F^{-1}_{Mk}F^{-1}_{Sj}\right)\left(F^{-1}_{Nr}\frac{\partial^2 N^a}{\partial X_M \partial X_N} - \right. \\
& \left. - F^{-1}_{No}F^{-1}_{Pr}\frac{\partial N^a}{\partial X_N}\frac{\partial F_{oP}}{\partial X_M}\right) + \frac{1}{2}\overline{\mu}_{jl}\epsilon_{lri}F^{-1}_{Mj}\left(-F^{-1}_{Nk}\frac{\partial O^b}{\partial X_S}F^{-1}_{Sr}\frac{\partial^2 N^a}{\partial X_M \partial X_N} + \right. \\
& + \frac{\partial N^a}{\partial X_N}\frac{\partial O^b}{\partial X_S}\frac{\partial F_{oP}}{\partial X_M}\left(F^{-1}_{Nk}F^{-1}_{So}F^{-1}_{Pr} + F^{-1}_{No}F^{-1}_{Pk}F^{-1}_{Sr}\right) - \\
& \left. - F^{-1}_{Nk}F^{-1}_{Pr}\frac{\partial N^a}{\partial X_N}\frac{\partial^2 O^b}{\partial X_M \partial X_P}\right)\Bigg] dV,
\end{aligned}
\tag{505}
$$

$$
\begin{aligned}
K^{u\beta}_{aibk} = \int_V \Bigg[& \frac{\partial N^a}{\partial X_M}\frac{\partial P^b}{\partial X_L}\left(\frac{\partial \tau_{(ij)}}{\partial F_{kL}}F^{-1}_{Mj} - \tau_{(ij)}F^{-1}_{Mk}F^{-1}_{Lj}\right) + \\
& + \frac{1}{2}\epsilon_{lri}\frac{\partial P^b}{\partial X_S}\left(\frac{\partial \overline{\mu}_{jl}}{\partial F_{kS}}F^{-1}_{Mj} - \overline{\mu}_{jl}F^{-1}_{Mk}F^{-1}_{Sj}\right)\left(F^{-1}_{Nr}\frac{\partial^2 N^a}{\partial X_M \partial X_N} - \right. \\
& \left. - F^{-1}_{No}F^{-1}_{Pr}\frac{\partial N^a}{\partial X_N}\frac{\partial F_{oP}}{\partial X_M}\right) + \frac{1}{2}\overline{\mu}_{jl}\epsilon_{lri}F^{-1}_{Mj}\left(-F^{-1}_{Nk}\frac{\partial P^b}{\partial X_S}F^{-1}_{Sr}\frac{\partial^2 N^a}{\partial X_M \partial X_N} + \right. \\
& + \frac{\partial N^a}{\partial X_N}\frac{\partial P^b}{\partial X_S}\frac{\partial F_{oP}}{\partial X_M}\left(F^{-1}_{Nk}F^{-1}_{So}F^{-1}_{Pr} + F^{-1}_{No}F^{-1}_{Pk}F^{-1}_{Sr}\right) - \\
& \left. - F^{-1}_{Nk}F^{-1}_{Pr}\frac{\partial N^a}{\partial X_N}\frac{\partial^2 P^b}{\partial X_M \partial X_P}\right)\Bigg] dV,
\end{aligned}
\tag{506}
$$

$$K^{u\gamma}_{aibk} = \int\limits_V \Bigg[\frac{\partial N^a}{\partial X_M} \frac{\partial Q^b}{\partial X_L} \left(\frac{\partial \tau_{(ij)}}{\partial F_{kL}} F^{-1}_{Mj} - \tau_{(ij)} F^{-1}_{Mk} F^{-1}_{Lj} \right) +$$
$$+ \frac{1}{2} \epsilon_{lri} \frac{\partial Q^b}{\partial X_S} \left(\frac{\partial \overline{\mu}_{jl}}{\partial F_{kS}} F^{-1}_{Mj} - \overline{\mu}_{jl} F^{-1}_{Mk} F^{-1}_{Sj} \right) \left(F^{-1}_{Nr} \frac{\partial^2 N^a}{\partial X_M \partial X_N} - \right.$$
$$\left. - F^{-1}_{No} F^{-1}_{Pr} \frac{\partial N^a}{\partial X_N} \frac{\partial F_{oP}}{\partial X_M} \right) + \frac{1}{2} \overline{\mu}_{jl} \epsilon_{lri} F^{-1}_{Mj} \left(-F^{-1}_{Nk} \frac{\partial Q^b}{\partial X_S} F^{-1}_{Sr} \frac{\partial^2 N^a}{\partial X_M \partial X_N} + \right. \tag{507}$$
$$+ \frac{\partial N^a}{\partial X_N} \frac{\partial Q^b}{\partial X_S} \frac{\partial F_{oP}}{\partial X_M} \left(F^{-1}_{Nk} F^{-1}_{So} F^{-1}_{Pr} + F^{-1}_{No} F^{-1}_{Pk} F^{-1}_{Sr} \right) -$$
$$\left. - F^{-1}_{Nk} F^{-1}_{Pr} \frac{\partial N^a}{\partial X_N} \frac{\partial^2 Q^b}{\partial X_M \partial X_P} \right) \Bigg] dV,$$

$$K^{\alpha u}_{aibk} = \int\limits_V \Bigg[\frac{\partial O^a}{\partial X_M} \frac{\partial N^b}{\partial X_L} \left(\frac{\partial \tau_{(ij)}}{\partial F_{kL}} F^{-1}_{Mj} - \tau_{(ij)} F^{-1}_{Mk} F^{-1}_{Lj} \right) +$$
$$+ \frac{1}{2} \epsilon_{lri} \frac{\partial N^b}{\partial X_S} \left(\frac{\partial \overline{\mu}_{jl}}{\partial F_{kS}} F^{-1}_{Mj} - \overline{\mu}_{jl} F^{-1}_{Mk} F^{-1}_{Sj} \right) \left(F^{-1}_{Nr} \frac{\partial^2 O^a}{\partial X_M \partial X_N} - \right.$$
$$\left. - F^{-1}_{No} F^{-1}_{Pr} \frac{\partial O^a}{\partial X_N} \frac{\partial F_{oP}}{\partial X_M} \right) + \frac{1}{2} \overline{\mu}_{jl} \epsilon_{lri} F^{-1}_{Mj} \left(-F^{-1}_{Nk} \frac{\partial N^b}{\partial X_S} F^{-1}_{Sr} \frac{\partial^2 O^a}{\partial X_M \partial X_N} + \right. \tag{508}$$
$$+ \frac{\partial O^a}{\partial X_N} \frac{\partial N^b}{\partial X_S} \frac{\partial F_{oP}}{\partial X_M} \left(F^{-1}_{Nk} F^{-1}_{So} F^{-1}_{Pr} + F^{-1}_{No} F^{-1}_{Pk} F^{-1}_{Sr} \right) -$$
$$\left. - F^{-1}_{Nk} F^{-1}_{Pr} \frac{\partial O^a}{\partial X_N} \frac{\partial^2 N^b}{\partial X_M \partial X_P} \right) \Bigg] dV,$$

$$K^{\alpha\alpha}_{aibk} = \int\limits_V \Bigg[\frac{\partial O^a}{\partial X_M} \frac{\partial O^b}{\partial X_L} \left(\frac{\partial \tau_{(ij)}}{\partial F_{kL}} F^{-1}_{Mj} - \tau_{(ij)} F^{-1}_{Mk} F^{-1}_{Lj} \right) +$$
$$+ \frac{1}{2} \epsilon_{lri} \frac{\partial O^b}{\partial X_S} \left(\frac{\partial \overline{\mu}_{jl}}{\partial F_{kS}} F^{-1}_{Mj} - \overline{\mu}_{jl} F^{-1}_{Mk} F^{-1}_{Sj} \right) \left(F^{-1}_{Nr} \frac{\partial^2 O^a}{\partial X_M \partial X_N} - \right.$$
$$\left. - F^{-1}_{No} F^{-1}_{Pr} \frac{\partial O^a}{\partial X_N} \frac{\partial F_{oP}}{\partial X_M} \right) + \frac{1}{2} \overline{\mu}_{jl} \epsilon_{lri} F^{-1}_{Mj} \left(-F^{-1}_{Nk} \frac{\partial O^b}{\partial X_S} F^{-1}_{Sr} \frac{\partial^2 O^a}{\partial X_M \partial X_N} + \right. \tag{509}$$
$$+ \frac{\partial O^a}{\partial X_N} \frac{\partial O^b}{\partial X_S} \frac{\partial F_{oP}}{\partial X_M} \left(F^{-1}_{Nk} F^{-1}_{So} F^{-1}_{Pr} + F^{-1}_{No} F^{-1}_{Pk} F^{-1}_{Sr} \right) -$$
$$\left. - F^{-1}_{Nk} F^{-1}_{Pr} \frac{\partial O^a}{\partial X_N} \frac{\partial^2 O^b}{\partial X_M \partial X_P} \right) \Bigg] dV,$$

$$K^{\alpha\beta}_{aibk} = \int\limits_V \Bigg[\frac{\partial O^a}{\partial X_M} \frac{\partial P^b}{\partial X_L} \left(\frac{\partial \tau_{(ij)}}{\partial F_{kL}} F^{-1}_{Mj} - \tau_{(ij)} F^{-1}_{Mk} F^{-1}_{Lj} \right) +$$
$$+ \frac{1}{2} \epsilon_{lri} \frac{\partial P^b}{\partial X_S} \left(\frac{\partial \overline{\mu}_{jl}}{\partial F_{kS}} F^{-1}_{Mj} - \overline{\mu}_{jl} F^{-1}_{Mk} F^{-1}_{Sj} \right) \left(F^{-1}_{Nr} \frac{\partial^2 O^a}{\partial X_M \partial X_N} - \right.$$
$$\left. - F^{-1}_{No} F^{-1}_{Pr} \frac{\partial O^a}{\partial X_N} \frac{\partial F_{oP}}{\partial X_M} \right) + \frac{1}{2} \overline{\mu}_{jl} \epsilon_{lri} F^{-1}_{Mj} \left(-F^{-1}_{Nk} \frac{\partial P^b}{\partial X_S} F^{-1}_{Sr} \frac{\partial^2 O^a}{\partial X_M \partial X_N} + \right. \tag{510}$$
$$+ \frac{\partial O^a}{\partial X_N} \frac{\partial P^b}{\partial X_S} \frac{\partial F_{oP}}{\partial X_M} \left(F^{-1}_{Nk} F^{-1}_{So} F^{-1}_{Pr} + F^{-1}_{No} F^{-1}_{Pk} F^{-1}_{Sr} \right) -$$
$$\left. - F^{-1}_{Nk} F^{-1}_{Pr} \frac{\partial O^a}{\partial X_N} \frac{\partial^2 P^b}{\partial X_M \partial X_P} \right) \Bigg] dV,$$

$$K^{\alpha\gamma}_{aibk} = \int\limits_V \Bigg[\frac{\partial O^a}{\partial X_M} \frac{\partial Q^b}{\partial X_L} \left(\frac{\partial \tau_{(ij)}}{\partial F_{kL}} F^{-1}_{Mj} - \tau_{(ij)} F^{-1}_{Mk} F^{-1}_{Lj} \right) +$$
$$+ \frac{1}{2} \epsilon_{lri} \frac{\partial Q^b}{\partial X_S} \left(\frac{\partial \overline{\mu}_{jl}}{\partial F_{kS}} F^{-1}_{Mj} - \overline{\mu}_{jl} F^{-1}_{Mk} F^{-1}_{Sj} \right) \left(F^{-1}_{Nr} \frac{\partial^2 O^a}{\partial X_M \partial X_N} - \right.$$
$$\left. - F^{-1}_{No} F^{-1}_{Pr} \frac{\partial O^a}{\partial X_N} \frac{\partial F_{oP}}{\partial X_M} \right) + \frac{1}{2} \overline{\mu}_{jl} \epsilon_{lri} F^{-1}_{Mj} \left(-F^{-1}_{Nk} \frac{\partial Q^b}{\partial X_S} F^{-1}_{Sr} \frac{\partial^2 O^a}{\partial X_M \partial X_N} + \right. \tag{511}$$
$$+ \frac{\partial O^a}{\partial X_N} \frac{\partial Q^b}{\partial X_S} \frac{\partial F_{oP}}{\partial X_M} \left(F^{-1}_{Nk} F^{-1}_{So} F^{-1}_{Pr} + F^{-1}_{No} F^{-1}_{Pk} F^{-1}_{Sr} \right) -$$
$$\left. - F^{-1}_{Nk} F^{-1}_{Pr} \frac{\partial O^a}{\partial X_N} \frac{\partial^2 Q^b}{\partial X_M \partial X_P} \right) \Bigg] dV,$$

$$K^{\beta u}_{aibk} = \int\limits_V \Bigg[\frac{\partial P^a}{\partial X_M} \frac{\partial N^b}{\partial X_L} \left(\frac{\partial \tau_{(ij)}}{\partial F_{kL}} F^{-1}_{Mj} - \tau_{(ij)} F^{-1}_{Mk} F^{-1}_{Lj} \right) +$$
$$+ \frac{1}{2} \epsilon_{lri} \frac{\partial N^b}{\partial X_S} \left(\frac{\partial \overline{\mu}_{jl}}{\partial F_{kS}} F^{-1}_{Mj} - \overline{\mu}_{jl} F^{-1}_{Mk} F^{-1}_{Sj} \right) \left(F^{-1}_{Nr} \frac{\partial^2 P^a}{\partial X_M \partial X_N} - \right.$$
$$\left. - F^{-1}_{No} F^{-1}_{Pr} \frac{\partial P^a}{\partial X_N} \frac{\partial F_{oP}}{\partial X_M} \right) + \frac{1}{2} \overline{\mu}_{jl} \epsilon_{lri} F^{-1}_{Mj} \left(-F^{-1}_{Nk} \frac{\partial N^b}{\partial X_S} F^{-1}_{Sr} \frac{\partial^2 P^a}{\partial X_M \partial X_N} + \right. \tag{512}$$
$$+ \frac{\partial P^a}{\partial X_N} \frac{\partial N^b}{\partial X_S} \frac{\partial F_{oP}}{\partial X_M} \left(F^{-1}_{Nk} F^{-1}_{So} F^{-1}_{Pr} + F^{-1}_{No} F^{-1}_{Pk} F^{-1}_{Sr} \right) -$$
$$\left. - F^{-1}_{Nk} F^{-1}_{Pr} \frac{\partial P^a}{\partial X_N} \frac{\partial^2 N^b}{\partial X_M \partial X_P} \right) \Bigg] dV,$$

$$
\begin{aligned}
K^{\beta\alpha}_{aibk} = \int\limits_V \Bigg[& \frac{\partial P^a}{\partial X_M}\frac{\partial O^b}{\partial X_L}\left(\frac{\partial \tau_{(ij)}}{\partial F_{kL}}F^{-1}_{Mj} - \tau_{(ij)}F^{-1}_{Mk}F^{-1}_{Lj}\right) + \\
& + \frac{1}{2}\epsilon_{lri}\frac{\partial O^b}{\partial X_S}\left(\frac{\partial \overline{\mu}_{jl}}{\partial F_{kS}}F^{-1}_{Mj} - \overline{\mu}_{jl}F^{-1}_{Mk}F^{-1}_{Sj}\right)\left(F^{-1}_{Nr}\frac{\partial^2 P^a}{\partial X_M \partial X_N} - \right. \\
& \left. - F^{-1}_{No}F^{-1}_{Pr}\frac{\partial P^a}{\partial X_N}\frac{\partial F_{oP}}{\partial X_M}\right) + \frac{1}{2}\overline{\mu}_{jl}\epsilon_{lri}F^{-1}_{Mj}\left(-F^{-1}_{Nk}\frac{\partial O^b}{\partial X_S}F^{-1}_{Sr}\frac{\partial^2 P^a}{\partial X_M \partial X_N} + \right. \\
& + \frac{\partial P^a}{\partial X_N}\frac{\partial O^b}{\partial X_S}\frac{\partial F_{oP}}{\partial X_M}\left(F^{-1}_{Nk}F^{-1}_{So}F^{-1}_{Pr} + F^{-1}_{No}F^{-1}_{Pk}F^{-1}_{Sr}\right) - \\
& \left. - F^{-1}_{Nk}F^{-1}_{Pr}\frac{\partial P^a}{\partial X_N}\frac{\partial^2 O^b}{\partial X_M \partial X_P}\right)\Bigg] dV,
\end{aligned}
\tag{513}
$$

$$
\begin{aligned}
K^{\beta\beta}_{aibk} = \int\limits_V \Bigg[& \frac{\partial P^a}{\partial X_M}\frac{\partial P^b}{\partial X_L}\left(\frac{\partial \tau_{(ij)}}{\partial F_{kL}}F^{-1}_{Mj} - \tau_{(ij)}F^{-1}_{Mk}F^{-1}_{Lj}\right) + \\
& + \frac{1}{2}\epsilon_{lri}\frac{\partial P^b}{\partial X_S}\left(\frac{\partial \overline{\mu}_{jl}}{\partial F_{kS}}F^{-1}_{Mj} - \overline{\mu}_{jl}F^{-1}_{Mk}F^{-1}_{Sj}\right)\left(F^{-1}_{Nr}\frac{\partial^2 P^a}{\partial X_M \partial X_N} - \right. \\
& \left. - F^{-1}_{No}F^{-1}_{Pr}\frac{\partial P^a}{\partial X_N}\frac{\partial F_{oP}}{\partial X_M}\right) + \frac{1}{2}\overline{\mu}_{jl}\epsilon_{lri}F^{-1}_{Mj}\left(-F^{-1}_{Nk}\frac{\partial P^b}{\partial X_S}F^{-1}_{Sr}\frac{\partial^2 P^a}{\partial X_M \partial X_N} + \right. \\
& + \frac{\partial P^a}{\partial X_N}\frac{\partial P^b}{\partial X_S}\frac{\partial F_{oP}}{\partial X_M}\left(F^{-1}_{Nk}F^{-1}_{So}F^{-1}_{Pr} + F^{-1}_{No}F^{-1}_{Pk}F^{-1}_{Sr}\right) - \\
& \left. - F^{-1}_{Nk}F^{-1}_{Pr}\frac{\partial P^a}{\partial X_N}\frac{\partial^2 P^b}{\partial X_M \partial X_P}\right)\Bigg] dV,
\end{aligned}
\tag{514}
$$

$$
\begin{aligned}
K^{\beta\gamma}_{aibk} = \int\limits_V \Bigg[& \frac{\partial P^a}{\partial X_M}\frac{\partial Q^b}{\partial X_L}\left(\frac{\partial \tau_{(ij)}}{\partial F_{kL}}F^{-1}_{Mj} - \tau_{(ij)}F^{-1}_{Mk}F^{-1}_{Lj}\right) + \\
& + \frac{1}{2}\epsilon_{lri}\frac{\partial Q^b}{\partial X_S}\left(\frac{\partial \overline{\mu}_{jl}}{\partial F_{kS}}F^{-1}_{Mj} - \overline{\mu}_{jl}F^{-1}_{Mk}F^{-1}_{Sj}\right)\left(F^{-1}_{Nr}\frac{\partial^2 P^a}{\partial X_M \partial X_N} - \right. \\
& \left. - F^{-1}_{No}F^{-1}_{Pr}\frac{\partial P^a}{\partial X_N}\frac{\partial F_{oP}}{\partial X_M}\right) + \frac{1}{2}\overline{\mu}_{jl}\epsilon_{lri}F^{-1}_{Mj}\left(-F^{-1}_{Nk}\frac{\partial Q^b}{\partial X_S}F^{-1}_{Sr}\frac{\partial^2 P^a}{\partial X_M \partial X_N} + \right. \\
& + \frac{\partial P^a}{\partial X_N}\frac{\partial Q^b}{\partial X_S}\frac{\partial F_{oP}}{\partial X_M}\left(F^{-1}_{Nk}F^{-1}_{So}F^{-1}_{Pr} + F^{-1}_{No}F^{-1}_{Pk}F^{-1}_{Sr}\right) - \\
& \left. - F^{-1}_{Nk}F^{-1}_{Pr}\frac{\partial P^a}{\partial X_N}\frac{\partial^2 Q^b}{\partial X_M \partial X_P}\right)\Bigg] dV,
\end{aligned}
\tag{515}
$$

$$K^{\gamma u}_{aibk} = \int\limits_V \Bigg[\frac{\partial Q^a}{\partial X_M} \frac{\partial N^b}{\partial X_L} \left(\frac{\partial \tau_{(ij)}}{\partial F_{kL}} F^{-1}_{Mj} - \tau_{(ij)} F^{-1}_{Mk} F^{-1}_{Lj} \right) + \\ + \frac{1}{2} \epsilon_{lri} \frac{\partial N^b}{\partial X_S} \left(\frac{\partial \overline{\mu}_{jl}}{\partial F_{kS}} F^{-1}_{Mj} - \overline{\mu}_{jl} F^{-1}_{Mk} F^{-1}_{Sj} \right) \left(F^{-1}_{Nr} \frac{\partial^2 Q^a}{\partial X_M \partial X_N} - \right. \\ \left. - F^{-1}_{No} F^{-1}_{Pr} \frac{\partial Q^a}{\partial X_N} \frac{\partial F_{oP}}{\partial X_M} \right) + \frac{1}{2} \overline{\mu}_{jl} \epsilon_{lri} F^{-1}_{Mj} \left(-F^{-1}_{Nk} \frac{\partial N^b}{\partial X_S} F^{-1}_{Sr} \frac{\partial^2 Q^a}{\partial X_M \partial X_N} + \right. \\ + \frac{\partial Q^a}{\partial X_N} \frac{\partial N^b}{\partial X_S} \frac{\partial F_{oP}}{\partial X_M} \left(F^{-1}_{Nk} F^{-1}_{So} F^{-1}_{Pr} + F^{-1}_{No} F^{-1}_{Pk} F^{-1}_{Sr} \right) - \\ \left. - F^{-1}_{Nk} F^{-1}_{Pr} \frac{\partial Q^a}{\partial X_N} \frac{\partial^2 N^b}{\partial X_M \partial X_P} \right) \Bigg] dV, \tag{516}$$

$$K^{\gamma \alpha}_{aibk} = \int\limits_V \Bigg[\frac{\partial Q^a}{\partial X_M} \frac{\partial O^b}{\partial X_L} \left(\frac{\partial \tau_{(ij)}}{\partial F_{kL}} F^{-1}_{Mj} - \tau_{(ij)} F^{-1}_{Mk} F^{-1}_{Lj} \right) + \\ + \frac{1}{2} \epsilon_{lri} \frac{\partial O^b}{\partial X_S} \left(\frac{\partial \overline{\mu}_{jl}}{\partial F_{kS}} F^{-1}_{Mj} - \overline{\mu}_{jl} F^{-1}_{Mk} F^{-1}_{Sj} \right) \left(F^{-1}_{Nr} \frac{\partial^2 Q^a}{\partial X_M \partial X_N} - \right. \\ \left. - F^{-1}_{No} F^{-1}_{Pr} \frac{\partial Q^a}{\partial X_N} \frac{\partial F_{oP}}{\partial X_M} \right) + \frac{1}{2} \overline{\mu}_{jl} \epsilon_{lri} F^{-1}_{Mj} \left(-F^{-1}_{Nk} \frac{\partial O^b}{\partial X_S} F^{-1}_{Sr} \frac{\partial^2 Q^a}{\partial X_M \partial X_N} + \right. \\ + \frac{\partial Q^a}{\partial X_N} \frac{\partial O^b}{\partial X_S} \frac{\partial F_{oP}}{\partial X_M} \left(F^{-1}_{Nk} F^{-1}_{So} F^{-1}_{Pr} + F^{-1}_{No} F^{-1}_{Pk} F^{-1}_{Sr} \right) - \\ \left. - F^{-1}_{Nk} F^{-1}_{Pr} \frac{\partial Q^a}{\partial X_N} \frac{\partial^2 O^b}{\partial X_M \partial X_P} \right) \Bigg] dV, \tag{517}$$

$$K^{\gamma \beta}_{aibk} = \int\limits_V \Bigg[\frac{\partial Q^a}{\partial X_M} \frac{\partial P^b}{\partial X_L} \left(\frac{\partial \tau_{(ij)}}{\partial F_{kL}} F^{-1}_{Mj} - \tau_{(ij)} F^{-1}_{Mk} F^{-1}_{Lj} \right) + \\ + \frac{1}{2} \epsilon_{lri} \frac{\partial P^b}{\partial X_S} \left(\frac{\partial \overline{\mu}_{jl}}{\partial F_{kS}} F^{-1}_{Mj} - \overline{\mu}_{jl} F^{-1}_{Mk} F^{-1}_{Sj} \right) \left(F^{-1}_{Nr} \frac{\partial^2 Q^a}{\partial X_M \partial X_N} - \right. \\ \left. - F^{-1}_{No} F^{-1}_{Pr} \frac{\partial Q^a}{\partial X_N} \frac{\partial F_{oP}}{\partial X_M} \right) + \frac{1}{2} \overline{\mu}_{jl} \epsilon_{lri} F^{-1}_{Mj} \left(-F^{-1}_{Nk} \frac{\partial P^b}{\partial X_S} F^{-1}_{Sr} \frac{\partial^2 Q^a}{\partial X_M \partial X_N} + \right. \\ + \frac{\partial Q^a}{\partial X_N} \frac{\partial P^b}{\partial X_S} \frac{\partial F_{oP}}{\partial X_M} \left(F^{-1}_{Nk} F^{-1}_{So} F^{-1}_{Pr} + F^{-1}_{No} F^{-1}_{Pk} F^{-1}_{Sr} \right) - \\ \left. - F^{-1}_{Nk} F^{-1}_{Pr} \frac{\partial Q^a}{\partial X_N} \frac{\partial^2 P^b}{\partial X_M \partial X_P} \right) \Bigg] dV, \tag{518}$$

$$
\begin{aligned}
K^{\gamma\gamma}_{aibk} = \int_V \Bigg[& \frac{\partial Q^a}{\partial X_M}\frac{\partial Q^b}{\partial X_L}\left(\frac{\partial \tau_{(ij)}}{\partial F_{kL}}F^{-1}_{Mj} - \tau_{(ij)}F^{-1}_{Mk}F^{-1}_{Lj}\right) + \\
& + \frac{1}{2}\epsilon_{lri}\frac{\partial Q^b}{\partial X_S}\left(\frac{\partial \overline{\mu}_{jl}}{\partial F_{kS}}F^{-1}_{Mj} - \overline{\mu}_{jl}F^{-1}_{Mk}F^{-1}_{Sj}\right)\left(F^{-1}_{Nr}\frac{\partial^2 Q^a}{\partial X_M \partial X_N} - \right. \\
& \left. - F^{-1}_{No}F^{-1}_{Pr}\frac{\partial Q^a}{\partial X_N}\frac{\partial F_{oP}}{\partial X_M}\right) + \frac{1}{2}\overline{\mu}_{jl}\epsilon_{lri}F^{-1}_{Mj}\left(-F^{-1}_{Nk}\frac{\partial Q^b}{\partial X_S}F^{-1}_{Sr}\frac{\partial^2 Q^a}{\partial X_M \partial X_N} + \right. \\
& + \frac{\partial Q^a}{\partial X_N}\frac{\partial Q^b}{\partial X_S}\frac{\partial F_{oP}}{\partial X_M}\left(F^{-1}_{Nk}F^{-1}_{So}F^{-1}_{Pr} + F^{-1}_{No}F^{-1}_{Pk}F^{-1}_{Sr}\right) - \\
& \left. - F^{-1}_{Nk}F^{-1}_{Pr}\frac{\partial Q^a}{\partial X_N}\frac{\partial^2 Q^b}{\partial X_M \partial X_P}\right)\Bigg] dV,
\end{aligned}
\tag{519}
$$

The Newton-Raphson proces applied above results in the following system of four linear equations

$$K^{uu}_{aibk}.\Delta u^b_k + K^{u\alpha}_{aibk}.\Delta \alpha^b_k + K^{u\beta}_{aibk}.\Delta \beta^b_k + K^{u\gamma}_{aibk}.\Delta \gamma^b_k = R^a_i \tag{520}$$

$$K^{\alpha u}_{aibk}.\Delta u^b_k + K^{\alpha\alpha}_{aibk}.\Delta \alpha^b_k + K^{\alpha\beta}_{aibk}.\Delta \beta^b_k + K^{\alpha\gamma}_{aibk}.\Delta \gamma^b_k = S^a_i \tag{521}$$

$$K^{\beta u}_{aibk}.\Delta u^b_k + K^{\beta\alpha}_{aibk}.\Delta \alpha^b_k + K^{\beta\beta}_{aibk}.\Delta \beta^b_k + K^{\beta\gamma}_{aibk}.\Delta \gamma^b_k = T^a_i \tag{522}$$

$$K^{\gamma u}_{aibk}.\Delta u^b_k + K^{\gamma\alpha}_{aibk}.\Delta \alpha^b_k + K^{\gamma\beta}_{aibk}.\Delta \beta^b_k + K^{\gamma\gamma}_{aibk}.\Delta \gamma^b_k = U^a_i, \tag{523}$$

where residua R^a_i, S^a_i, T^a_i and U^a_i are given by the left hand side of equations (495), (496), (497) and (498), respectively.

10.3.4 Numerical integration

In order to evaluate the integrals introduced in the previous section in the stifnesses **K**, a numerical integration, so called **Gauss integration**, was used.

Let's consider a 1D element with n integration points. Then Gauss integration gives an exact result for a *2n - 1* order polynom. The mentioned integrals contain polynoms of the fifth order maximally corresponding to one variable, therefore, three integration points ($n = 3$) have to be used at least in order to obtain accurate values of the integrals and to achive convergence of the solution. That means n^3 integration points in 3D, i.e. 27

integration points in total per each 3D element. Then the Gauss integration scheme to be used for such element can be written as follows

$$\int_{-1}^{+1}\int_{-1}^{+1}\int_{-1}^{+1} f(\xi_1,\xi_2,\xi_3)d\xi_1 d\xi_2 d\xi_3 = \sum_{I=1}^{3}\sum_{J=1}^{3}\sum_{K=1}^{3} w_I w_J w_K f(\xi_1^I,\xi_2^J,\xi_3^K) \tag{524}$$

where f is the function to be integrated, w_I, w_J, w_K are weighting factors and $\xi_1^I, \xi_2^J, \xi_3^K$ are locations of integration points. When considering

$$j = 1..3, \quad k = 1..3, \quad l = 1..3 \quad and \quad i = 3^2(l-1) + 3(k-1) + j,$$

the weighting factors and locations of the integration points can be generated by the following scheme

$$w_i = \nu_j \nu_k \nu_l, \quad \xi_1^i = \eta_j, \quad \xi_2^i = \eta_k, \quad \xi_3^i = \eta_l, \tag{525}$$

where

$$\eta_1 = -0.7745966692, \quad \eta_2 = 0, \quad \eta_3 = 0.7745966692 \tag{526}$$

and

$$\nu_1 = 0.5555555555 \quad \nu_2 = 0.8888888888 \quad \nu_3 = 0.5555555555. \tag{527}$$

The first three weighting factors and coordinates of integration points are presented in table 1, as an example.

point	w	ξ_1	ξ_2	ξ_3
1	0.1714677640	-0.7745966692	-0.7745966692	-0.7745966692
2	0.2743842241	0	-0.7745966692	-0.7745966692
3	0.1714677640	0.7745966692	-0.7745966692	-0.7745966692
...				

Table 1: Weighting factors and coordinates of the first three integration points

10.4 Results of simulations using Hermite C1 elements

The finite element implementation introduced in chapter 10.3 was applied to write a new finite element solver in MATLAB software as a so called "m" file. The MATLAB m-file reads the input text file, runs the solver and generates an output text file with results. The

input file contains information about nodes, elements, and prescribed boundary conditions and can be created in a text editor or using an other finite element software. The output text file contains results such as displacements, strains and stresses in the nodes, and this output file can be opened in the free finite element software Calculix in order to show the results in a graphical representation.

In order to verify the theory presented in this thesis with the new constitutive equations comprehending the bending stiffness on the basis of Cosserat continuum, a simple three-point bending test was simulated using the new finite element solver created specifically for this purpose (m-file). A very simple unimaterial finite element model was created with two planes of symetry and a very rough mesh - fig. 17 (this model is called ***unimaterial Cosserat model*** hereafter). The model contained 8 finite elements in total with each element having 8 nodes and 27 integration points. The applied boundary conditions are presented in fig. 18.

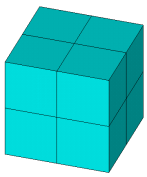

Figure 17: Meshed simplified model.

The strain energy density function presented in (297) was used in the simulations with the following material parameters: $k_1 = 1$ MPa, $k_2 = 1400$ MPa, $d = 0.0001$, while different values of k_6 were considered. Remember that parameters k_1, d correspond to the hyperelastic matrix and parameters k_2, k_6 correspond to the fibres, where k_2 represents their tension (compression) stiffness and k_6 their bending stiffness. Hence, the values of $k_6 = 0, k_6 = 100$ and $k_6 = 1000$ were considered in order to see if the new model is able to consider different bending stiffnesses of the fibres.
The three-point bending test was also simulated in Ansys software using unimaterial finite element model based on "classical" Cauchy contiuum (this model is called ***unimaterial Cauchy model***) with the aim to compare the results with the unimaterial Cosserat model.

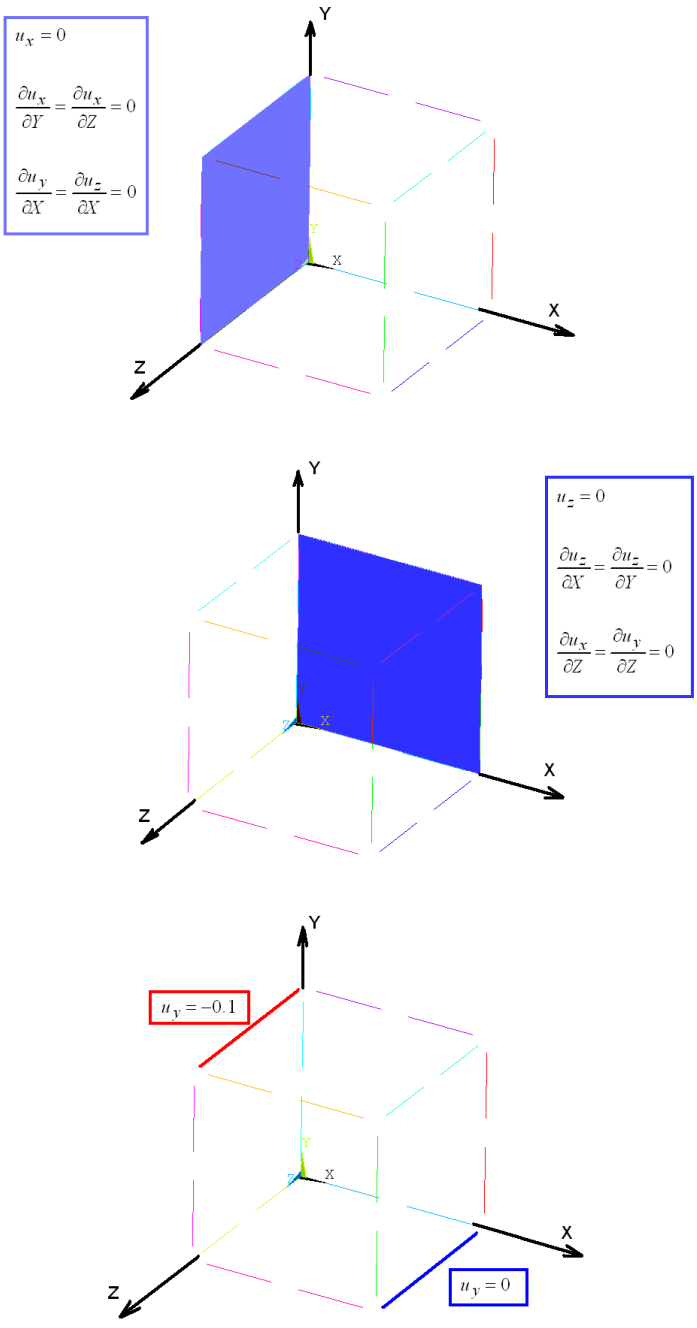

Figure 18: Prescribed boundary conditions.

The unimaterial Cauchy model contained 8 elements in total and either 8 or 20 nodes and either 8 or 27 integration points per each element. The used strain energy density function had the following form

$$W = k_1(\overline{I}_1 - 3) + k_2(\overline{I}_4 - 1)^2 + \frac{1}{d}(J-1)^2. \tag{528}$$

If we compare the strain energy density function (528) used in the unimaterial Cauchy model with eq. (297) used in the unimaterial Cosserat model, we can see that both models use almost the same strain energy density function except for the term containing parametr k_6. As it was mentioned in previous chapters, the unimaterial Cauchy model is not able to include the bending stiffness of fibres, therefore this model does not contain material parameter k_6 that corresponds to bending of fibres and Cosserat theory.

Results of simulations using both Cosserat and Cauchy unimaterial models are depicted in fig. 19. In this figure the abbreviation "Cauchy" means that Cauchy unimaterial model was used and the numbers 185 or 186 mean hexahedron elements (according to Ansys software) with 8 or 20 nodes respectively. The abbreviation "FULL" or "Reduced" means that either full integration with 27 integration points or reduced integration with 8 integration points was used. Next, "Cosserat" means that results were obtained using the unimaterial Cosserat model with different values of material parameter k_6.

When we compare first the results obtained by Cauchy model , we can see that the 20 nodes element with the higher number of integration points (186 FULL - 27 int. points) gives stiffer response than the same element with the lower number of integration points (186 Reduced - 8 int. points) and the 8 nodes element with 8 int. points (Cauchy 185) gives the stiffest response among the Cauchy models. So we can draw conclusion - an increasing number of integration points makes the resulting behaviour stiffer and the 8 nodes element gives stiffer results than the 20 nodes one.

Let's pay attention to the Cosserat models now. As we know, the unimaterial Cosserat model uses 8 nodes elements with 27 integration points. The strain energy density function (297) used in Cosserat model is reduced into the strain energy density function (528) of the Cauchy model when using $k_6 = 0$. Hence, both models (Cosserat $k_6 = 0$ and Cauchy 185) should give the same results. However, we can see from fig. 19 that Cosserat model with $k_6 = 0$ gives results a little bit stiffer than Cauchy 185 model. This can be explained

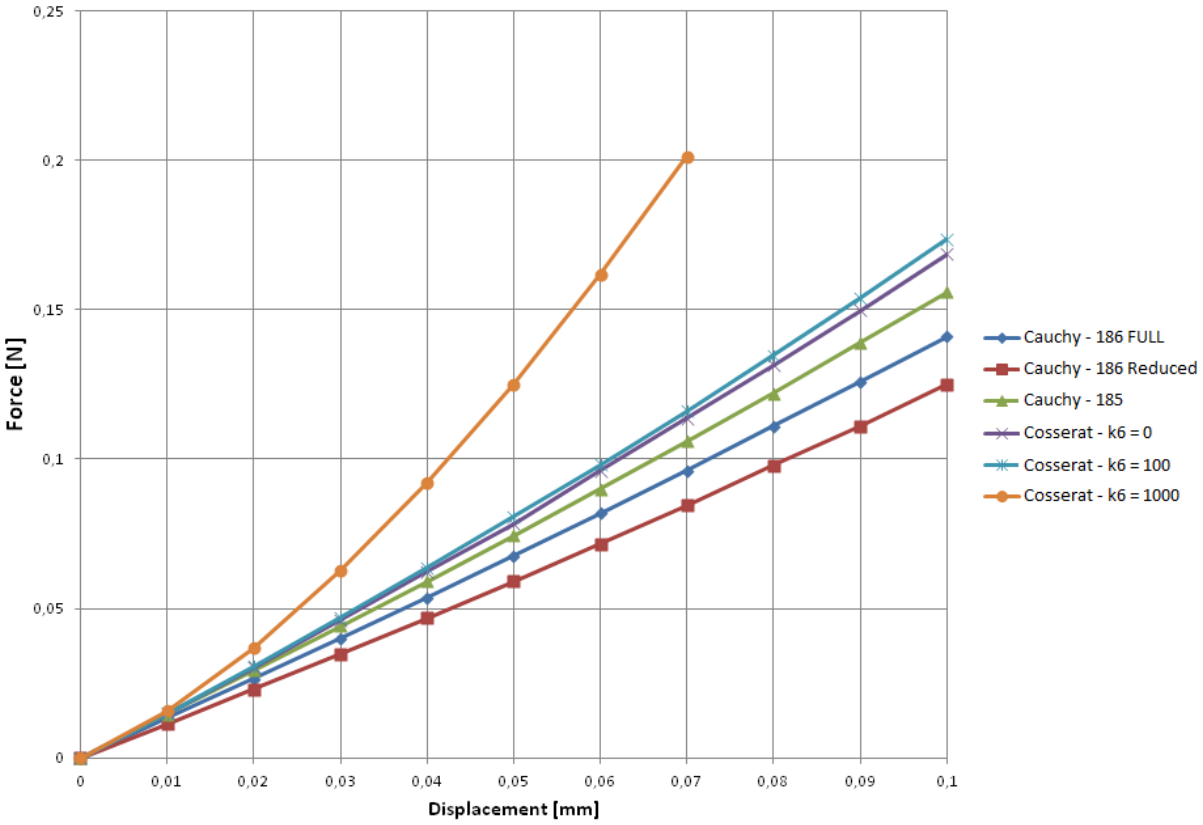

Figure 19: Simulations - bending test.

on the basis of the number of integration points, as mentioned above - a higher number of integration points gives stiffer resulting behaviour (Cosserat $k_6 = 0$ has 27 int. points while Cauchy 185 has 8 int. points only).

Finally, we can see from the same figure that the increasing parameter k_6 increases stiffness of the resulting curves, i.e. in contrast to the Cauchy models, the ***unimaterial Cosserat model is able to take the bending stiffness of the fibres into account***.

11 Conclusion

This thesis deals with computational simulations of composite material made of elastomer matrix and steel fibres. Two different approaches were considered in the simulations – bimaterial and unimaterial computational models. The bimaterial model reflects the structure of the composite material in detail, i.e. it works with matrix and each individual fibre. On the other side, fibres are not created in the unimaterial model and their reinforcement effect is included in the strain energy density function. Since fibres are not modelled, the unimaterial computational model has a significantly lower number of elements, and consequently the computational time decreases significantly.

Computational simulations of uniaxial tension and bending tests of composite material were performed using both (bi- and unimaterial) computational models. The results showed that both models give the same results in simulations of uniaxial tension tests, but they disagree significantly in simulations of bending tests. It was found out that the disagreement is caused by the assumption of infinitesimaly thin fibres in the unimaterial model causing a zero bending stiffness of the fibres. Hence, the unimaterial computational model is not able to take the bending stiffness of fibres into account and consequently it can work with tension (or compression) load only.

Real experiments (tension and bending tests) of composite material were carried out with the aim to compare the results of simulations with experimental results. However, the experiments have shown that mechanical properties of the elastomeric matrix are highly dependent on the pre-cycling of specimens (so called Mullins effect). The specimen that was pre-cycled to a certain value of elongation (or strain) showed different mechanical properties from another specimen pre-cycled to another elongation value. Since there is a nonhomogeneous strain state in the composite specimen (due to fibres), each part of the specimen is loaded by another value of elongation (strain) and due to mentioned Mullins effect the stress-strain curve is changed. To compare such experiments with simulations it would be necessary to use such material models in simulations that are able to account for pre-cycling of the elastomeric matrix and can work with different amplitude of elongation (or strain).

In order to verify the hypothesis that in case of tension tests the disagreement between

experiments and simulations was caused by Mullins effect, new experiments with another elastomer matrix were carried out. A new elastomer matrix was chosen showing a very low Mullins effect. Then experiments and simulations of uniaxial tension tests were in mutual agreement for both (bi- and unimaterial) computational models.

The next goal was to extend the unimaterial model by bending stiffness of the fibres. In 2007 Spencer and Soldatos published new constitutive equations based on Cosserat continuum that are able to work with bending stiffness of the fibres under large strain conditions. Cosserat continuum is more general than Cauchy continuum, it considers both displacements and rotations as independent variables and works with force and couple stresses. However, the equations introduced by Spencer and Soldatos are very complicated and very difficult for practical application. Hence, a system of simplified constitutive equations was formulated in the thesis on the basis of the equations introduced by Spencer and Soldatos. After determination of the simplified constitutive equations (valid under restrictions for bending load of the fibres being parallel and straight in the undeformed state), a new form of strain energy density function was introduced. This form can be decoupled into three main parts – the first part corresponds to the hyperelastic elastomer matrix, the second one to tension (or compression) of the fibres and the third part relates to bending of the fibres.

In order to verify whether the new unimaterial model with bending stiffness is able to work with bending stiffness of fibres correctly, a new finite element (FE) solver had to be written. It was not possible to use any commercial or available FE solver, since the new solver was based on Cosserat continuum and included a new strain energy density function with new constitutive equations comprehending additional variables. Hence, after determination of finite element formulation, the new FE solver was written in Matlab software. Since the Cosserat theory leads to the second derivatives of displacements, it was necessary to use also the so called C^1 elements in order to ensure the convergence of the solution. In C^1 elements both displacements field and derivatives of displacements are continuous over the elements and at their boundaries. Hence, a new 8 nodes C^1 element with Hermite polynoms as shape functions was proposed in the thesis.

A simplified three-point bending test was simulated using the new FE solver in order to verify that the new unimaterial model based on Cosserat continuum is able to comprehend

the bending stiffness of fibres. It was shown that the bending stiffness of fibres can be driven by changing the appropriate material parameter and the new solver gives results comparable with standard hyperelastic models for a negligible influence of the bending stiffness of fibres. In this way, the capability of the new model was verified.

This work showed that standard unimaterial models available in commercial software are able to provide the same results as the bimaterial ones and being in agreement with real experiments in the case of tension (or compression) tests only. Next, it was shown that, the standard unimaterial models are not able to include any stiffness of the fibres when they are bended. Therefore, the extension of the unimaterial model was introduced in this work, and this extension allows us to incorporate the bending stiffness of fibres into the unimaterial model. Then the proposed unimaterial model can be used correctly under both tension (compression) and bending loads.

12 List of the most frequented symbols

All symbols are described immediatly after their introduction in the appropriate chapter, therefore, the following list of used symbols shows only the most frequented symbols that are used in this work.

$\mathbf{A}$, A_I	unit vector of undeformed fibres
b	no name vector defined by eq. (226)
$\mathbf{B}$, B_{ij}	left Cauchy - Green deformation tensor
$\mathbf{C}$, C_{IJ}	right Cauchy - Green deformation tensor
$\mathbf{E}$, E_{IJ}	Lagrangian strain tensor
E_c	Young's modulus of composite material
E_f	Young's modulus of fibres
E_m	Young's modulus of matrix
$\mathbf{F}$, F_{iJ}	deformation gradient
$\mathbf{G}$, G_{iJ}	no name tensor defined in (230)
J	volume ratio
K(t)	kinetic energy
$K^{\alpha\beta}_{abcd}$	stiffness matrix
$\mathbf{l}$	couple-stress vector (Cauchy)
$\mathbf{m}$	total moment of momentum
m_{ji}	Cauchy couple-stress tensor
$\overline{m}_{ji}$	deviatoric part of Cauchy couple-stress tensor
$\overline{m}_{ii}$	spherical part of Cauchy couple-stress tensor
$\mathbf{M}$, M_{Ji}	first Piola-Kirchoff couple-stress tensor
n_j, N_j	outward normal of deformed and undeformed body respectively
N^a	shape functions
O^a	shape functions
p	hydrostatic pressure (Lagrange multiplier)

$\mathbf{p}$	total momentum
$P_{ext}(t)$	external mechanical power
$P_{int}(t)$	internal mechanical power (stress power)
P^a	shape functions
$\mathbf{P}$, P_{Ij}	first Piola-Kirchoff force-stress tensor
Q^a	shape functions
$\mathbf{S}$, S_{IJ}	second Piola-Kirchoff force-stress tensor
t	time
$\mathbf{t}$	force-stress vector (Cauchy)
$\mathbf{u}$, u_i	displacement vector
u_i^a	unknown displacements at node a
$\mathbf{U}$	right (mateial) stretch tensor
v	deformed volume
v_f	volume fraction of fibres
v_m	volume fraction of matrix
$\mathbf{v}$	left (spatial) stretch tensor or velocity vector
V	undeformed volume
W	strain energy density function
W_d	deviatoric part of strain energy density function
W_v	volumetric part of strain energy density function
$\mathbf{x}$, x_i	position vector in deformed system; deformed coordinates
$\mathbf{X}$, X_i	position vector in reference (undeformed) system; undeformed coordinates

α_i^a	unknown slopes at node a
β_i^a	unknown slopes at node a
γ_i^a	unknown slopes at node a
δ_{ij}	Kronecker's delta
ε_{ij}	engineering strain
ε_{log}	Hencky(logarithmic) strain tensor
ϵ_{ijk}	Levi-Civita symbol
ϕ_k	components of microrotation vector
φ_k	components of macrorotation vector
ν_k	components of microgyration vector
ν_{kl}	gyration tensor
λ_i	principal stretch ratios
λ_{iJ}	Lagrange multipliers
Λ_{RS}	no name tensor defined in (251)
μ_{ji}	Kirchoff couple-stress tensor
$\overline{\mu}_{ji}, \overline{\mu}_{ii}$	deviatoric and spherical part of Kirchoff couple-stress tensor respectively
Π	total potential energy functional
ρ	density
σ_{ij}	Cauchy force-stress tensor
$\sigma_{(ij)}$	symmetric part of Cauchy force-stress tensor
$\sigma_{[ji])}$	antisymmetric part of Cauchy force-stress tensor
τ_{ij}	Kirchoff force-stress tensor
ω_i, ω_{ij}	spin vector and spin tensor respectively

A Appendixes

A.1 Invariants of general constitutive model (Cosserat continuum)

The strain energy density function depends on tensors $\boldsymbol{C}, \boldsymbol{\Lambda}$ and unit vector $\mathbf{A}$ as was mentioned in chapter 6. The strain energy density function can be expressed as a function of 33 independent invariants. These invariants are introduced into this appendix (or can be found in the appendix A in [32] or in table 1 in [36]).

Symbols $\boldsymbol{\Lambda_s}$ and $\boldsymbol{\Lambda_a}$ are symmetric and antisymmetric part respectively of the tensor $\boldsymbol{\Lambda}$, then

$$\boldsymbol{\Lambda} = \boldsymbol{\Lambda}_s + \boldsymbol{\Lambda}_a, \quad \boldsymbol{\Lambda}^T = \boldsymbol{\Lambda}_s - \boldsymbol{\Lambda}_a, \quad 2\boldsymbol{\Lambda}_s = \boldsymbol{\Lambda} + \boldsymbol{\Lambda}^T, \quad 2\boldsymbol{\Lambda}_a = \boldsymbol{\Lambda} - \boldsymbol{\Lambda}^T \tag{529}$$

The 33 independent invariants:

$$I_1 = tr\mathbf{C}, \quad I_2 = \tfrac{1}{2}[(tr\mathbf{C})^2 - tr\mathbf{C}^2], \quad I_3 = det\mathbf{C}, \quad I_4 = \mathbf{ACA}, \quad I_5 = \mathbf{AC}^2\mathbf{A},$$

$$I_6 = tr\boldsymbol{\Lambda}_s = tr\boldsymbol{\Lambda}, \quad I_7 = tr\boldsymbol{\Lambda}_s^2, \quad I_8 = tr\boldsymbol{\Lambda}_a^2, \quad I_9 = tr\boldsymbol{\Lambda}_s^3,$$

$$I_{10} = tr\mathbf{C}\boldsymbol{\Lambda}_s = tr\mathbf{C}\boldsymbol{\Lambda}, \quad I_{11} = tr\mathbf{C}^2\boldsymbol{\Lambda}_s = tr\mathbf{C}^2\boldsymbol{\Lambda}, \quad I_{12} = tr\mathbf{C}\boldsymbol{\Lambda}_s^2,$$

$$I_{13} = tr\mathbf{C}^2\boldsymbol{\Lambda}_s^2, \quad I_{14} = tr\mathbf{C}\boldsymbol{\Lambda}_a^2, \quad I_{15} = tr\mathbf{C}^2\boldsymbol{\Lambda}_a^2, \quad I_{16} = tr\mathbf{C}^2\boldsymbol{\Lambda}_a^2\mathbf{C}\boldsymbol{\Lambda}_a,$$

$$I_{17} = tr\boldsymbol{\Lambda}_s\boldsymbol{\Lambda}_a^2, \quad I_{18} = tr\boldsymbol{\Lambda}_s^2\boldsymbol{\Lambda}_a^2, \quad I_{19} = tr\boldsymbol{\Lambda}_s^2\boldsymbol{\Lambda}_a^2\boldsymbol{\Lambda}_s\boldsymbol{\Lambda}_a, \quad I_{20} = \mathbf{A}\boldsymbol{\Lambda}_s\mathbf{A} = \mathbf{A}\boldsymbol{\Lambda}\mathbf{A},$$

$$I_{21} = \mathbf{A}\boldsymbol{\Lambda}_s^2\mathbf{A}, \quad I_{22} = \mathbf{A}\boldsymbol{\Lambda}_a^2\mathbf{A}, \quad I_{23} = \mathbf{AC}\boldsymbol{\Lambda}_s\mathbf{A}, \quad I_{24} = \mathbf{AC}\boldsymbol{\Lambda}_a\mathbf{A},$$

$$I_{25} = \mathbf{AC}^2\boldsymbol{\Lambda}_a\mathbf{A}, \quad I_{26} = \mathbf{A}\boldsymbol{\Lambda}_a\mathbf{C}\boldsymbol{\Lambda}_a^2\mathbf{A}, \quad I_{27} = \mathbf{A}\boldsymbol{\Lambda}_s\boldsymbol{\Lambda}_a\mathbf{A}, \quad I_{28} = \mathbf{A}\boldsymbol{\Lambda}_s^2\boldsymbol{\Lambda}_a\mathbf{A},$$

$$I_{29} = \mathbf{A}\boldsymbol{\Lambda}_a\boldsymbol{\Lambda}_s\boldsymbol{\Lambda}_a^2\mathbf{A}, \quad I_{30} = tr\mathbf{C}\boldsymbol{\Lambda}_s\boldsymbol{\Lambda}_a, \quad I_{31} = tr\mathbf{C}^2\boldsymbol{\Lambda}_s\boldsymbol{\Lambda}_a, \quad I_{32} = tr\mathbf{C}\boldsymbol{\Lambda}_s^2\boldsymbol{\Lambda}_a,$$

$$I_{33} = tr\mathbf{C}\boldsymbol{\Lambda}_a^2\boldsymbol{\Lambda}_s\boldsymbol{\Lambda}_a. \tag{530}$$

A.2 Invariants of simplified constitutive model (Cosserat continuum)

It was considered in chapter 6.2 that strain energy density function depends on the tensor $\boldsymbol{C}$, vectors $\mathbf{K}$, $\mathbf{A}$ and scalar κ^2. The strain energy density function can be then expressed as a function of 11 independent invariants. These invariants are introduced into this appendix.

$$I_1 = tr\mathbf{C}, \quad I_2 = \tfrac{1}{2}[(tr\mathbf{C})^2 - tr\mathbf{C}^2], \quad I_3 = det\mathbf{C}, \quad I_4 = \mathbf{ACA}, \quad I_5 = \mathbf{AC}^2\mathbf{A},$$

$$I_6 = \mathbf{K}.\mathbf{K} = \mathbf{A}\boldsymbol{\Lambda}^T\boldsymbol{\Lambda}\mathbf{A}, \quad I_7 = \mathbf{KCK} = \mathbf{A}\boldsymbol{\Lambda}^T\mathbf{C}\boldsymbol{\Lambda}\mathbf{A}, \quad I_8 = \mathbf{KC}^2\mathbf{K} = \mathbf{A}\boldsymbol{\Lambda}^T\mathbf{C}^2\boldsymbol{\Lambda}\mathbf{A},$$

$$I_9 = \mathbf{A}.\mathbf{K} = \mathbf{A}\boldsymbol{\Lambda}\mathbf{A}, \quad I_{10} = \mathbf{ACK} = \mathbf{AC}\boldsymbol{\Lambda}\mathbf{A}, \quad I_{11} = \mathbf{AC}^2\mathbf{K} = \mathbf{AC}^2\boldsymbol{\Lambda}\mathbf{A}. \tag{531}$$

Next:

$$\frac{\partial I_1}{\partial \boldsymbol{C}} = \mathbf{I}, \quad \frac{\partial I_2}{\partial \boldsymbol{C}} = I_1\mathbf{I} - \mathbf{C}, \quad \frac{\partial I_3}{\partial \boldsymbol{C}} = I_2\mathbf{I} - I_1\mathbf{C} + \mathbf{C}^2,$$

$$\frac{\partial I_4}{\partial \boldsymbol{C}} = \mathbf{A} \otimes \mathbf{A}, \quad \frac{\partial I_5}{\partial \boldsymbol{C}} = \mathbf{A} \otimes (\mathbf{CA}) + (\mathbf{CA}) \otimes \mathbf{A},$$

$$\frac{\partial I_6}{\partial \boldsymbol{C}} = \mathbf{0}, \quad \frac{\partial I_7}{\partial \boldsymbol{C}} = (\boldsymbol{\Lambda}\mathbf{A}) \otimes (\boldsymbol{\Lambda}\mathbf{A}), \quad \frac{\partial I_8}{\partial \boldsymbol{C}} = (\boldsymbol{\Lambda}\mathbf{A}) \otimes (\mathbf{C}\boldsymbol{\Lambda}\mathbf{A}),$$

$$\frac{\partial I_9}{\partial \boldsymbol{C}} = \mathbf{0}, \quad \frac{\partial I_{10}}{\partial \boldsymbol{C}} = \mathbf{A} \otimes (\boldsymbol{\Lambda}\mathbf{A}), \quad \frac{\partial I_{11}}{\partial \boldsymbol{C}} = \mathbf{A} \otimes (\mathbf{C}\boldsymbol{\Lambda}\mathbf{A}),$$

$$\frac{\partial I_1}{\partial \boldsymbol{\Lambda}} = \mathbf{0}, \quad \frac{\partial I_2}{\partial \boldsymbol{\Lambda}} = \mathbf{0}, \quad \frac{\partial I_3}{\partial \boldsymbol{\Lambda}} = \mathbf{0}, \quad \frac{\partial I_4}{\partial \boldsymbol{\Lambda}} = \mathbf{0}, \quad \frac{\partial I_5}{\partial \boldsymbol{\Lambda}} = \mathbf{0},$$

$$\frac{\partial I_6}{\partial \boldsymbol{\Lambda}} = 2\boldsymbol{\Lambda}\mathbf{A} \otimes \mathbf{A}, \quad \frac{\partial I_7}{\partial \boldsymbol{\Lambda}} = 2(\mathbf{C}\boldsymbol{\Lambda}\mathbf{A}) \otimes \mathbf{A}, \quad \frac{\partial I_8}{\partial \boldsymbol{\Lambda}} = 2(\mathbf{C}^2\boldsymbol{\Lambda}\mathbf{A}) \otimes \mathbf{A},$$

$$\frac{\partial I_9}{\partial \boldsymbol{\Lambda}} = \mathbf{A} \otimes \mathbf{A}, \quad \frac{\partial I_{10}}{\partial \boldsymbol{\Lambda}} = (\mathbf{CA}) \otimes \mathbf{A}, \quad \frac{\partial I_{11}}{\partial \boldsymbol{\Lambda}} = (\mathbf{C}^2\mathbf{A}) \otimes \mathbf{A}. \tag{532}$$

A.3 Results of simulations and experiments

The results of simulations and experiments of tension and bending tests are presented in this appendix

Uniaxial tension tests

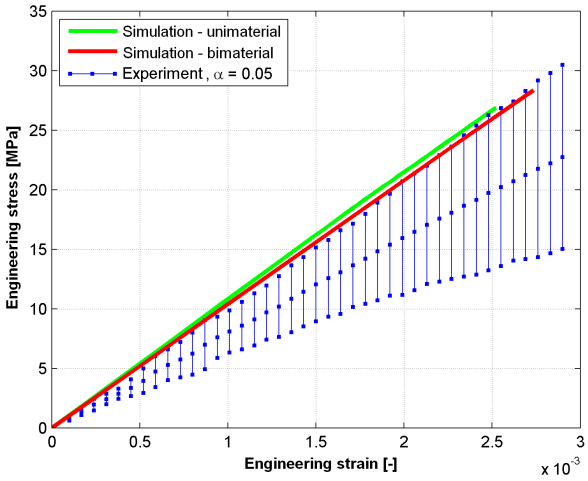

Figure 20: Tension test - fibres 0°.

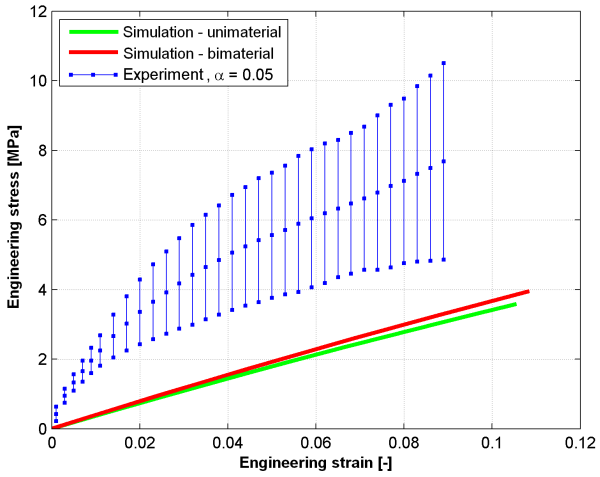

Figure 21: Tension test - fibres 15°.

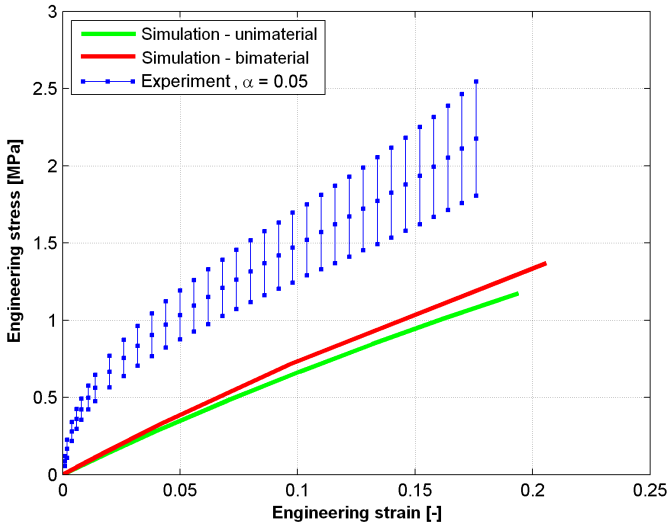

Figure 22: Tension test - fibres 45°.

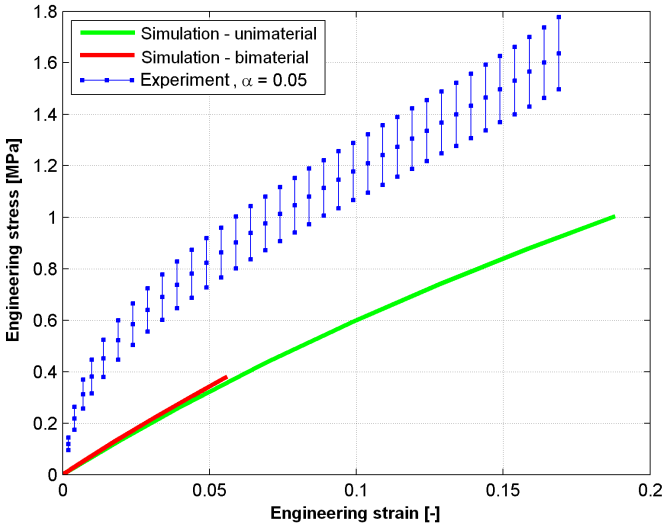

Figure 23: Tension test - fibres 60°.

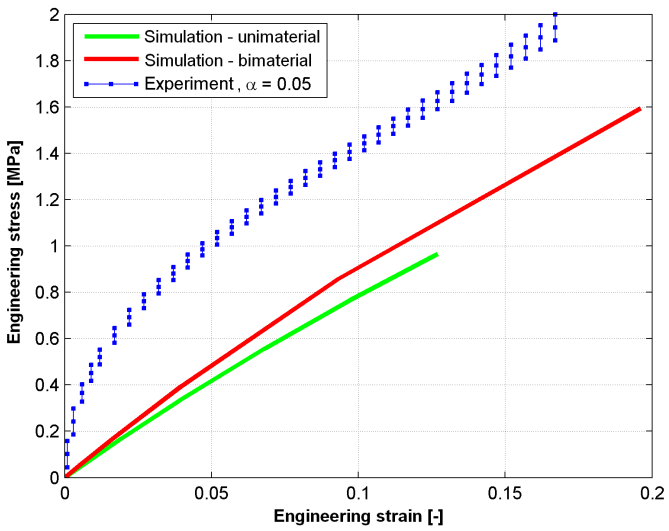

Figure 24: Tension test - fibres 90°.

Bending tests

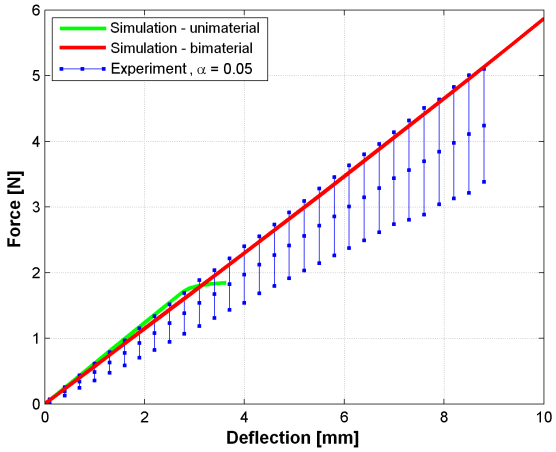

Figure 25: Bending test - fibres 0°.

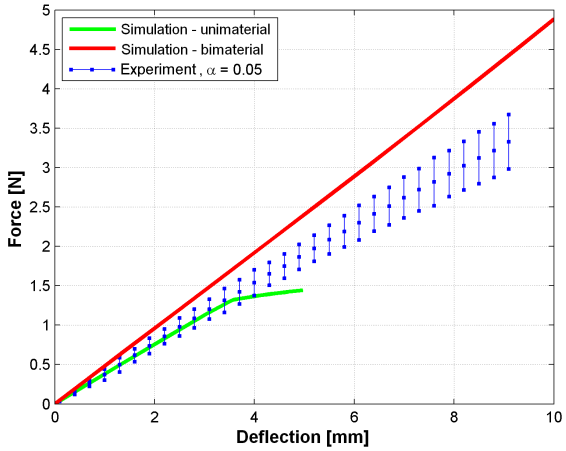

Figure 26: Bending test - fibres 15°.

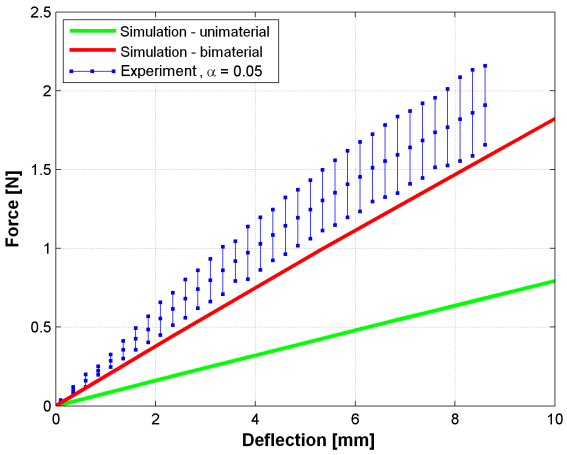

Figure 27: Bending test - fibres 45°.

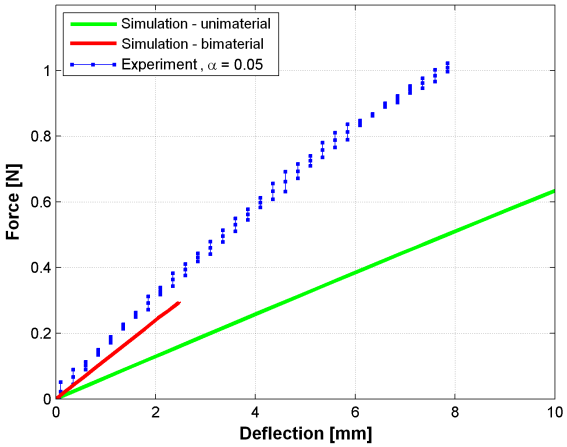

Figure 28: Bending test - fibres 60°.

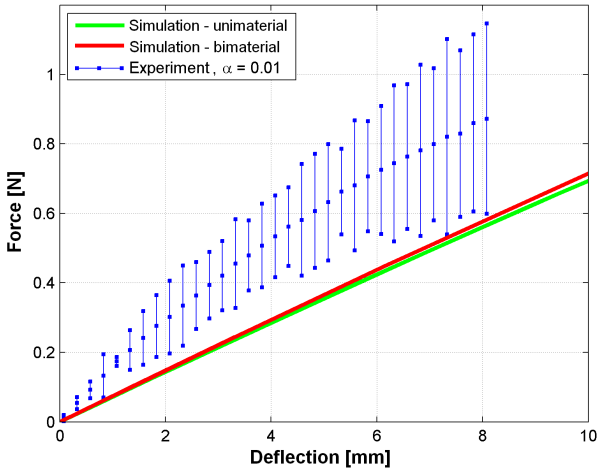

Figure 29: Bending test - fibres 90°.

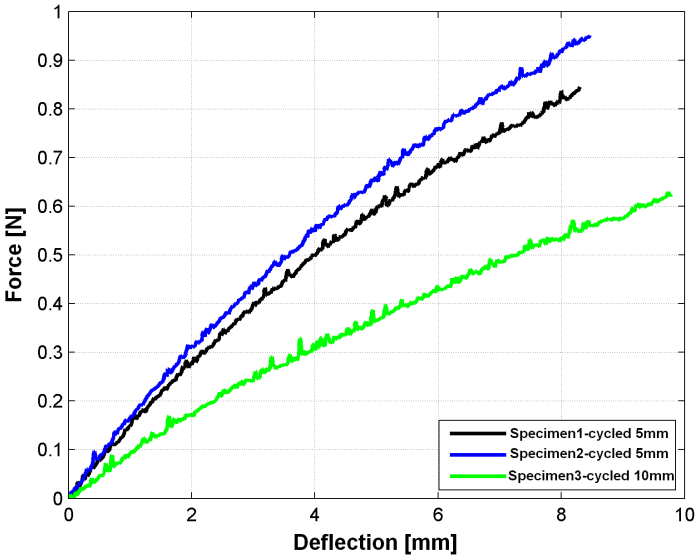

Figure 30: Bending test - fibres 90°. Influence of cycling.

A.4 Proof of the equation (302)

In this appendix we give a proof of the relation (302)

$$\frac{\partial^2 u_k}{\partial X_J \partial X_L}\frac{\partial X_L}{\partial x_k} = \frac{\partial^2 x_k}{\partial X_J \partial X_L}\frac{\partial X_L}{\partial x_k} = 0. \tag{533}$$

This proof can be also found in [30] and is valid in case of incompressibility.

By a well-known property of determinants and using the incompressibility relation

$$\frac{\partial(x_1, x_2, x_3)}{\partial(X_1, X_2, X_3)} = 1 \tag{534}$$

we have

$$\epsilon_{ijk}\frac{\partial x_i}{\partial X_R}\frac{\partial x_j}{\partial X_S}\frac{\partial x_k}{\partial X_T} = \epsilon_{RST}\frac{\partial(x_1, x_2.x_3)}{\partial(X_1, X_2, X_3)} = \epsilon_{RST}. \tag{535}$$

We differentiate this with respect to X_P, which gives

$$\epsilon_{ijk}\left(\frac{\partial^2 x_i}{\partial X_P \partial X_R}\frac{\partial x_j}{\partial X_S}\frac{\partial x_k}{\partial X_T} + \frac{\partial^2 x_j}{\partial X_P \partial X_S}\frac{\partial x_i}{\partial X_R}\frac{\partial x_k}{\partial X_T} + \frac{\partial^2 x_k}{\partial X_P \partial X_T}\frac{\partial x_i}{\partial X_R}\frac{\partial x_j}{\partial X_S}\right) = 0, \tag{536}$$

and multiply by

$$\frac{\partial X_R}{\partial x_1}\frac{\partial X_S}{\partial x_2}\frac{\partial X_T}{\partial x_3}$$

to obtain

$$\epsilon_{ijk}\left(\frac{\partial^2 x_i}{\partial X_P \partial X_R}\frac{\partial X_R}{\partial x_1}\delta_{j2}\delta_{k3} + \frac{\partial^2 x_j}{\partial X_P \partial X_S}\frac{\partial X_S}{\partial x_2}\delta_{i1}\delta_{k3} + \frac{\partial^2 x_k}{\partial X_P \partial X_T}\frac{\partial X_T}{\partial x_3}\delta_{i1}\delta_{j2}\right) = 0. \tag{537}$$

Then, for example

$$\epsilon_{ijk}\frac{\partial^2 x_i}{\partial X_P \partial X_R}\frac{\partial X_R}{\partial x_1}\delta_{j2}\delta_{k3} = \frac{\partial^2 x_1}{\partial X_P \partial X_R}\frac{\partial X_R}{\partial x_1}, \tag{538}$$

and adding the three terms of this kind in (537), we have

$$\frac{\partial^2 x_i}{\partial X_P \partial X_R}\frac{\partial X_R}{\partial x_i} = 0. \tag{539}$$

A.5 Shape functions

Hermite C1 shape functions

$$
\begin{aligned}
N_1 &= \frac{1}{64}(1-\xi_1)^2(2+\xi_1)(1-\xi_2)^2(2+\xi_2)(1-\xi_3)^2(2+\xi_3)\\
N_2 &= \frac{1}{64}(1+\xi_1)^2(2-\xi_1)(1-\xi_2)^2(2+\xi_2)(1-\xi_3)^2(2+\xi_3)\\
N_3 &= \frac{1}{64}(1+\xi_1)^2(2-\xi_1)(1+\xi_2)^2(2-\xi_2)(1-\xi_3)^2(2+\xi_3)\\
N_4 &= \frac{1}{64}(1-\xi_1)^2(2+\xi_1)(1+\xi_2)^2(2-\xi_2)(1-\xi_3)^2(2+\xi_3)\\
N_5 &= \frac{1}{64}(1-\xi_1)^2(2+\xi_1)(1-\xi_2)^2(2+\xi_2)(1+\xi_3)^2(2-\xi_3)\\
N_6 &= \frac{1}{64}(1+\xi_1)^2(2-\xi_1)(1-\xi_2)^2(2+\xi_2)(1+\xi_3)^2(2-\xi_3)\\
N_7 &= \frac{1}{64}(1+\xi_1)^2(2-\xi_1)(1+\xi_2)^2(2-\xi_2)(1+\xi_3)^2(2-\xi_3)\\
N_8 &= \frac{1}{64}(1-\xi_1)^2(2+\xi_1)(1+\xi_2)^2(2-\xi_2)(1+\xi_3)^2(2-\xi_3)
\end{aligned}
$$

$$
\begin{aligned}
O_1 &= \frac{1}{64}(1-\xi_1)^2(1+\xi_1)(1-\xi_2)^2(2+\xi_2)(1-\xi_3)^2(2+\xi_3)\\
O_2 &= \frac{1}{64}(1+\xi_1)^2(\xi_1-1)(1-\xi_2)^2(2+\xi_2)(1-\xi_3)^2(2+\xi_3)\\
O_3 &= \frac{1}{64}(1+\xi_1)^2(\xi_1-1)(1+\xi_2)^2(2-\xi_2)(1-\xi_3)^2(2+\xi_3)\\
O_4 &= \frac{1}{64}(1-\xi_1)^2(1+\xi_1)(1+\xi_2)^2(2-\xi_2)(1-\xi_3)^2(2+\xi_3)\\
O_5 &= \frac{1}{64}(1-\xi_1)^2(1+\xi_1)(1-\xi_2)^2(2+\xi_2)(1+\xi_3)^2(2-\xi_3)\\
O_6 &= \frac{1}{64}(1+\xi_1)^2(\xi_1-1)(1-\xi_2)^2(2+\xi_2)(1+\xi_3)^2(2-\xi_3)\\
O_7 &= \frac{1}{64}(1+\xi_1)^2(\xi_1-1)(1+\xi_2)^2(2-\xi_2)(1+\xi_3)^2(2-\xi_3)\\
O_8 &= \frac{1}{64}(1-\xi_1)^2(1+\xi_1)(1+\xi_2)^2(2-\xi_2)(1+\xi_3)^2(2-\xi_3)
\end{aligned}
$$

$$P_1 = \frac{1}{64}(1-\xi_1)^2(2+\xi_1)(1-\xi_2)^2(1+\xi_2)(1-\xi_3)^2(2+\xi_3)$$
$$P_2 = \frac{1}{64}(1+\xi_1)^2(2-\xi_1)(1-\xi_2)^2(1+\xi_2)(1-\xi_3)^2(2+\xi_3)$$
$$P_3 = \frac{1}{64}(1+\xi_1)^2(2-\xi_1)(1+\xi_2)^2(\xi_2-1)(1-\xi_3)^2(2+\xi_3)$$
$$P_4 = \frac{1}{64}(1-\xi_1)^2(2+\xi_1)(1+\xi_2)^2(\xi_2-1)(1-\xi_3)^2(2+\xi_3)$$
$$P_5 = \frac{1}{64}(1-\xi_1)^2(2+\xi_1)(1-\xi_2)^2(1+\xi_2)(1+\xi_3)^2(2-\xi_3)$$
$$P_6 = \frac{1}{64}(1+\xi_1)^2(2-\xi_1)(1-\xi_2)^2(1+\xi_2)(1+\xi_3)^2(2-\xi_3)$$
$$P_7 = \frac{1}{64}(1+\xi_1)^2(2-\xi_1)(1+\xi_2)^2(\xi_2-1)(1+\xi_3)^2(2-\xi_3)$$
$$P_8 = \frac{1}{64}(1-\xi_1)^2(2+\xi_1)(1+\xi_2)^2(\xi_2-1)(1+\xi_3)^2(2-\xi_3)$$

$$Q_1 = \frac{1}{64}(1-\xi_1)^2(2+\xi_1)(1-\xi_2)^2(2+\xi_2)(1-\xi_3)^2(1+\xi_3)$$
$$Q_2 = \frac{1}{64}(1+\xi_1)^2(2-\xi_1)(1-\xi_2)^2(2+\xi_2)(1-\xi_3)^2(1+\xi_3)$$
$$Q_3 = \frac{1}{64}(1+\xi_1)^2(2-\xi_1)(1+\xi_2)^2(2-\xi_2)(1-\xi_3)^2(1+\xi_3)$$
$$Q_4 = \frac{1}{64}(1-\xi_1)^2(2+\xi_1)(1+\xi_2)^2(2-\xi_2)(1-\xi_3)^2(1+\xi_3)$$
$$Q_5 = \frac{1}{64}(1-\xi_1)^2(2+\xi_1)(1-\xi_2)^2(2+\xi_2)(1+\xi_3)^2(\xi_3-1)$$
$$Q_6 = \frac{1}{64}(1+\xi_1)^2(2-\xi_1)(1-\xi_2)^2(2+\xi_2)(1+\xi_3)^2(\xi_3-1)$$
$$Q_7 = \frac{1}{64}(1+\xi_1)^2(2-\xi_1)(1+\xi_2)^2(2-\xi_2)(1+\xi_3)^2(\xi_3-1)$$
$$Q_8 = \frac{1}{64}(1-\xi_1)^2(2+\xi_1)(1+\xi_2)^2(2-\xi_2)(1+\xi_3)^2(\xi_3-1)$$

Lagrange C0 shape functions

$$
\begin{aligned}
M_1 &= \frac{1}{8}(1-\xi_1)(1-\xi_2)(1-\xi_3) \\
M_2 &= \frac{1}{8}(1+\xi_1)(1-\xi_2)(1-\xi_3) \\
M_3 &= \frac{1}{8}(1+\xi_1)(1+\xi_2)(1-\xi_3) \\
M_4 &= \frac{1}{8}(1-\xi_1)(1+\xi_2)(1-\xi_3) \\
M_5 &= \frac{1}{8}(1-\xi_1)(1-\xi_2)(1+\xi_3) \\
M_6 &= \frac{1}{8}(1+\xi_1)(1-\xi_2)(1+\xi_3) \\
M_7 &= \frac{1}{8}(1+\xi_1)(1+\xi_2)(1+\xi_3) \\
M_8 &= \frac{1}{8}(1-\xi_1)(1+\xi_2)(1+\xi_3)
\end{aligned}
$$

A.6 Displacement field of axially loaded bar

This appendix deals with derivation of the deformation field in an axially loaded bar. The field is used in chapter 9.1.1.

Let's consider a uniform prismatic bar made of a homogenous and isotropic linear elastic material with its mantle free of surface tractions. One end of the bar is loaded by a uniformly distributed surface traction σ, acting along the axis of the bar, the centroid of the other end is rigidly clamped to prevent rigid motion of the bar, and the clamped end is loaded to keep the bar in equilibrium.

The stress field is

$$\sigma_{11} = \sigma, \ \sigma_{22} = \sigma_{33} = \sigma_{12} = \sigma_{23} = \sigma_{31} = 0. \tag{540}$$

From Hooke's law we obtain

$$\varepsilon_{11} = \frac{\sigma}{E}, \ \varepsilon_{22} = -\frac{\mu\sigma}{E}, \ \varepsilon_{33} = -\frac{\mu\sigma}{E}, \ \varepsilon_{12} = \varepsilon_{23} = \varepsilon_{31} = 0. \tag{541}$$

Hence,

$$\frac{\partial u_1}{\partial X_1} = \frac{\sigma}{E}, \ \frac{\partial u_2}{\partial X_2} = -\frac{\mu\sigma}{E}, \ \frac{\partial u_3}{\partial X_3} = -\frac{\mu\sigma}{E}, \tag{542}$$

$$\frac{\partial u_1}{\partial X_2} + \frac{\partial u_2}{\partial X_1} = 0, \ \frac{\partial u_2}{\partial X_3} + \frac{\partial u_3}{\partial X_2} = 0, \ \frac{\partial u_3}{\partial X_1} + \frac{\partial u_1}{\partial X_3} = 0. \tag{543}$$

Integration of equations (542) results in

$$u_1 = \frac{\sigma}{E} X_1 + f_1(X_2, X_3),$$

$$u_2 = -\frac{\mu\sigma}{E} X_2 + f_2(X_1, X_3),$$

$$u_3 = -\frac{\mu\sigma}{E} X_3 + f_3(X_1, X_2). \tag{544}$$

Substitution from (544) into (543) yields

$$\frac{\partial f_1}{\partial X_2} + \frac{\partial f_2}{\partial X_1} = 0, \ \frac{\partial f_2}{\partial X_3} + \frac{\partial f_3}{\partial X_2} = 0, \ \frac{\partial f_3}{\partial X_1} + \frac{\partial f_1}{\partial X_3} = 0. \tag{545}$$

Recalling that f_1 is a function of X_2 and X_3, f_2 is a function of X_1 and X_3, f_3 is a function of X_1 and X_2, we conclude from (545) that

$$\frac{\partial^2 f_1}{\partial X_2^2} = \frac{\partial^2 f_1}{\partial X_3^2} = \frac{\partial^2 f_2}{\partial X_1^2} = \frac{\partial^2 f_2}{\partial X_3^2} = \frac{\partial^2 f_3}{\partial X_1^2} = \frac{\partial^2 f_3}{\partial X_2^2} = 0. \tag{546}$$

Hence,

$$f_1 = c_{11} + c_{12}X_2 + c_{13}X_3 + c_1X_2X_3,$$

$$f_2 = c_{22} + c_{21}X_1 + c_{23}X_3 + c_2X_1X_3,$$

$$f_3 = c_{33} + c_{31}X_1 + c_{32}X_2 + c_3X_1X_2, \tag{547}$$

where $c_{11}, c_{12}, ..c_{32}, c_1, ..c_3$ are constants. We now substitute (547) into (545) to obtain

$$c_{12} + c_{21} + (c_1 + c_2)X_3 = 0,$$

$$c_{23} + c_{32} + (c_2 + c_3)X_1 = 0,$$

$$c_{31} + c_{13} + (c_3 + c_1)X_2 = 0. \tag{548}$$

Since these equations must hold for all points inside the bar, it holds

$$c_{12} = -c_{21},\ \ c_{23} = -c_{32},\ \ c_{31} = -c_{13}$$

$$c_1 + c_2 = c_2 + c_3 = c_3 + c_1 = 0. \tag{549}$$

The second set of equations (549) gives

$$c_1 = c_2 = c_3 = 0. \tag{550}$$

By substitution of (550) and (549) into (547) and then into (544), we obtain

$$u_1 = \frac{\sigma}{E}X_1 + c_{12}X_2 + c_{13}X_3 + c_{11},$$

$$u_2 = -\frac{\mu\sigma}{E}X_2 - c_{12}X_1 + c_{23}X_3 + c_{22},$$

$$u_3 = -\frac{\mu\sigma}{E}X_3 - c_{13}X_1 - c_{23}X_2 + c_{33}. \tag{551}$$

Since $u_1 = u_2 = u_3 = 0$ at the centroid $X_1 = X_2 = X_3 = 0$ of the bar, (551) yields

$$c_{11} = c_{22} = c_{33} = 0. \tag{552}$$

In order to eliminate rigid rotations of the bar

$$\left(\frac{\partial u_1}{\partial X_2} - \frac{\partial u_2}{\partial X_1}\right) = 0, \ \left(\frac{\partial u_2}{\partial X_3} - \frac{\partial u_3}{\partial X_2}\right) = 0, \ \left(\frac{\partial u_3}{\partial X_1} - \frac{\partial u_1}{\partial X_3}\right) = 0 \tag{553}$$

at (0,0,0). That is, a small region around the centroid of the cross-section at $X_3 = 0$ is rigidly clamped. Equations (551) and (553) give

$$c_{12} = c_{13} = c_{23} = 0. \tag{554}$$

Thus, the displacement field in the bar is given by

$$u_1 = \frac{\sigma}{E} X_1, \ u_2 = -\frac{\mu\sigma}{E} X_2, \ u_3 = -\frac{\mu\sigma}{E} X_3. \tag{555}$$

A.7 Displacement field of bended beam

This appendix contains derivation of deformation field in the bended beam. Let's consider deformation of a straight prismatic bar, made of a homogenous linear elastic isotropic material, due to a pair of couples of magnitude M applied onto the ends of the beam. Let's assume that plane sections of the beam normal to its undeformed centreline remain planar and normal to the deformed centreline. X_1 axis is coincident with the centreline and X_2 axis is in the opposite direction as is the direction of deflection of the beam. Let's assume that the stresses in the beam are given by

$$\sigma_{11} = \frac{M}{J} X_2, \;\; \sigma_{22} = \sigma_{33} = \sigma_{12} = \sigma_{23} = \sigma_{31} = 0, \tag{556}$$

where J is the moment of inertia of the cross-section with respect to X_3 axis. Using Hooke's law we obtain

$$\varepsilon_{11} = \frac{M}{EJ} X_2, \;\; \varepsilon_{22} = -\frac{\mu M}{EJ} X_2, \;\; \varepsilon_{33} = -\frac{\mu M}{EJ} X_2,$$

$$\varepsilon_{12} = \varepsilon_{23} = \varepsilon_{31} = 0. \tag{557}$$

Hence,

$$\frac{\partial u_1}{\partial X_1} = \frac{M}{EJ} X_2, \;\; \frac{\partial u_2}{\partial X_2} = -\frac{\mu M}{EJ} X_2, \;\; \frac{\partial u_3}{\partial X_3} = -\frac{\mu M}{EJ} X_2, \tag{558}$$

$$\frac{\partial u_1}{\partial X_2} + \frac{\partial u_2}{\partial X_1} = 0, \;\; \frac{\partial u_2}{\partial X_3} + \frac{\partial u_3}{\partial X_2} = 0, \;\; \frac{\partial u_3}{\partial X_1} + \frac{\partial u_1}{\partial X_3} = 0. \tag{559}$$

By integration of the first equation of the (558) we find

$$u_1 = \frac{M}{EJ} X_1 X_2 + f(X_2, X_3). \tag{560}$$

From (559) it follows that

$$\frac{\partial u_1}{\partial X_2} = -\frac{\partial u_2}{\partial X_1}, \quad \frac{\partial u_1}{\partial X_3} = -\frac{\partial u_3}{\partial X_1}. \tag{561}$$

Substitution of (560) into (561) results in

$$\frac{\partial u_2}{\partial X_1} = -\frac{M}{EJ} X_1 - \frac{\partial f}{\partial X_2}, \quad \frac{\partial u_3}{\partial X_1} = -\frac{\partial f}{\partial X_3}. \tag{562}$$

Hence,

$$u_2 = -\frac{M}{2EJ} X_1^2 - \frac{\partial f}{\partial X_2} X_1 + h(X_2, X_3),$$

$$u_3 = -\frac{\partial f}{\partial X_3} X_1 + g(X_2, X_3) \tag{563}$$

where g and h are unknown functions of X_2 and X_3. Now we substitute (563) into last two equations in (558) to obtain

$$-\frac{\partial^2 f}{\partial X_2^2} X_1 + \frac{\partial h}{\partial X_2} = -\frac{\mu M}{EJ} X_2, \qquad -\frac{\partial^2 f}{\partial X_3^2} X_1 + \frac{\partial g}{\partial X_3} = -\frac{\mu M}{EJ} X_2. \tag{564}$$

These equations hold for all values of X_1, therefore

$$-\frac{\partial^2 f}{\partial X_2^2} = 0, \qquad \frac{\partial h}{\partial X_2} = -\frac{\mu M}{EJ} X_2,$$

$$-\frac{\partial^2 f}{\partial X_3^2} = 0, \qquad \frac{\partial g}{\partial X_3} = -\frac{\mu M}{EJ} X_2. \tag{565}$$

An integration of these equations gives

$$f = \beta X_2 + \gamma X_3 + c + X_2 X_3 d,$$

$$g = -\frac{\mu M}{EJ} X_2 X_3 + g_0(X_2)$$

$$h = -\frac{\mu M}{2EJ} X_2^2 + h_0(X_3). \tag{566}$$

Substituting (566) into (560) and (563) and then into (559), we have

$$-2X_1 d + \frac{dh_0}{dX_3} + \frac{dg_0}{dX_2} - \frac{\mu M}{EJ} X_3 = 0. \tag{567}$$

This equation holds at every point in the bar if and only if

$$d = 0, \qquad h_0 = -\frac{\mu M}{2EJ} X_3^2 + \alpha X_3 + a, \qquad g_0 = -\alpha X_2 + b. \tag{568}$$

Then

$$u_1 = \frac{M}{EJ} X_1 X_2 + \beta X_2 + \gamma X_3 + c$$

$$u_2 = -\frac{M}{2EJ} X_1^2 - \beta X_1 - \frac{\mu M}{2EJ} X_2^2 + \frac{\mu M}{2EJ} X_3^2 + \alpha X_3 + a$$

$$u_3 = -\gamma X_1 - \frac{\mu M}{EJ} X_2 X_3 - \alpha X_2 + b. \tag{569}$$

Constants a, b, c, α, β and γ represent the rigid body motion of the bar. In order to determine these constants, we fix the beam at the origin by fixing an element of the X_1 axis, and an element of the X_1X_2 plane at the origin. Thus

$$u_1 = u_2 = u_3 = \frac{\partial u_2}{\partial X_1} = \frac{\partial u_3}{\partial X_1} = \frac{\partial u_2}{\partial X_3} = 0 \tag{570}$$

at (0,0,0). From conditions (570) it follows that

$$a = b = c = \beta = \gamma = \alpha = 0. \tag{571}$$

Therefore, the displacement field of the bended beam is

$$u_1 = \frac{M}{EJ} X_1 X_2,$$

$$u_2 = \frac{\mu M}{2EJ}(X_3^2 - X_2^2) - \frac{M}{2EJ} X_1^2,$$

$$u_3 = -\frac{\mu M}{EJ} X_2 X_3. \tag{572}$$

References

[1] J.E. Adkins, R.S. Rivlin, Large elastic deformations of isotropic materials X. Reinforcement by inextensible cords, Philos. Trans. R. Soc. London A 248, (1955), 201–223.

[2] ANSYS, Inc.. Hyperelasticity. In Release 11.0 Documentation for ANSYS. Canonsburg: ANSYS, Inc., 2007.

[3] Bonet J., Wood R.D., Nonlinear Continuum Mechanics for Finite Element Analysis, Cambridge University Press, 1997, [ISBN 052157272X]

[4] F. Cacho, P.J. Elbischger, J.F. Rodríguez, M. Doblaré, G.A. Holzapfel, A constitutive model for fibrous tissues considering collagen fiber crimp, International Journal of Non-Linear Mechanics, Volume 42, Issue 2, March 2007, 391-402.

[5] E. Cosserat, F. Cosserat, Théorie des corps déformables, Hermann et fils, Paris, (1909).

[6] A.C. Eringen, Nonlinear Theory of Continuous Media, McGraw-Hill, New York, (1962).

[7] A.C. Eringen, E.S. Suhubi, Nonlinear theory of micropolar elastic solids, Int. J. Eng. Sci. 2, (1964), 189-203.

[8] A.C. Eringen, E.S. Suhubi, Int. J. Eng. Sci. 2, (1964), 389-404.

[9] A.C. Eringen, Mechanics of Micromorphic Materials, in "Proceedings of the 11 th International Congress of Applied Mechanics, Munich", (1964), 131-138, Springer, Berlin.

[10] A.C. Eringen, Theory of micropolar elasticity, in: H. Leibowitz, ed., Fracture, An Advanced Treatise (Academic Press, New York, 1968), 621-729.

[11] Fedorova S., Lasota T., Burša J., Skácel P., Experimental verification of a constitutive model of fibre composite with hyperelastic matrix

[12] S. Forest, Homogenization methods and the mechanics of generalized continua, Geometry, Continua and Microstructure, ed. by G. Maugin, Travaux en Cours No. 60, Hermann, Paris, France, pp. 35-48, 1999.

[13] S. Forest, F. Pradel and K. Sab, Asymptotic Analysis of Heterogeneous Cosserat Media, International Journal of Solids and Structures, vol. 38, pp. 4585-4608, 2001.

[14] S. Forest, Homogenization methods and the mechanics of generalized continua - Part2, Theoretical and Applied Mechanics, vol. 28-29, pp. 117-148, 2002.

[15] A.E. Green, J.E. Adkins, Large Elastic Deformations, second ed., Oxford University Press, London, (1970).

[16] Hoang Sy Tuan, Marvalova, B., Constitutive material model of fiber-reinforced composites in Comsol Multiphysics, Technical computing 2007, Prague, 2007.

[17] Nam T.H., Marvalova B., Deformation analysis of inflated cylindrical membrane of composite with rubber matrix reinforced by cords, in XXI International Congress of theoretical and applied mechanics ICTAM 2004.

[18] Holzapfel G. A. (2000) Nonlinear solid mechanics. A Ccontinuum Approach for Engineering, John Wiley & Son, Chichester.

[19] Holzapfel G.A., T.C. Gasser, M. Stadler, A structural model for the viscoelastic behavior of arterial walls: Continuum formulation and finite element analysis, European Journal of Mechanics - A/Solids, Volume 21, Issue 3, 2002, 441-463.

[20] Holzapfel G.A., Gasser T.C., Ogden R.W., A new constitutive framework for arterial wall mechanics and a comparative study of material models, Journal of Elasticity, vol. 61, 2000, 1-47.

[21] Hori, M., Nemat-Nasser, S., 1999, On two micromechanics theories for determining micro - macro relations in heterogeneous solids, Mech.Mater., 31, pp.667 – 682.

[22] Lasota T., Comparison of various levels of computational models of composites with hyperelastic matrix, FSI Junior conference, Brno University of Technology, 2008.

[23] Lasota T., Burša J., Simulation of mechanical tests of composite material using anisotropic hyperelastic constitutive models. Engineering Mechanics, 2011, roč. 18, č. 1, s. 23-32. ISSN: 1802- 1484.

[24] R.D. Mindlin, H.F. Tiersten, Effects of couple stress in linear elasticity, Arch. Rational Mech. Analysis 11, (1962), 415-448.

[25] Mullins L. (1947) Effect of stretching on the properties of rubber. Journal of rubber research 16, 275-289.

[26] W. Nowacki, Couple stresses in theory of thermoelasticity, Proc. of the IUTAM symposia, Vienna, (1966).

[27] Ogden R. W., Roxburgh D.G. (1999) A pseudo-elastic model for the Mullins effect in filled rubber. Proceedings of Royal Society London A 455, pp. 2861 - 2877.

[28] R.S. Rivlin, Constitutive equations for a fibre-reinforced lamina, in: D.F. Parker, A.H. England (Eds.), IUTAM Symposium on Anisotropy, Inhomogenity and Nonlinearity in Solid Mechanics, Kluwer Academic Publishers, Dordrecht, 1995, pp. 379-384.

[29] O. van der Sluis, P.H.J. Vosbeek, P.J.G. Schreurs, H.E.H.Meijer. Homogenization of heterogeneous polymers. International Journal of Solids and Structures, 1999.

[30] A.J.M. Spencer, Deformations of Fibre-reinforced Materials, Oxford University Press, London, (1972).

[31] A.J.M. Spencer (Ed.), Continuum Theory of the Mechanics of Fibre-reinforced Composites, CISM Courses and Lectures, vol. 282, Springer, Wien, (1984).

[32] A.J.M. Spencer, K.P. Soldatos, Finite deformations of fibre-reinforced elastic solid with fibre bending stiffness, Int. J. Nonlinear Mech. 42, (2007), 355-368.

[33] R.A. Toupin, Elastic materials with couple stresses, Arch. Rational Mech. Analysis 11, (1962), 385-414.

[34] C. Truesdell, R.A. Toupin, The classical field theories, Encyclopedia of Physics, Vol. 3, No 1, Springer Verlag, Berlin, (1960).

[35] W. Voigt, Theoretische Studien über die Wissenschaften zu Elastizitätsverhältnisse der Krystalle, Abhandl, Ges., Göttingen, (1887), 34.

[36] Q.S. Zheng, Theory of representations for tensor functions, Appl. Mech. Rev. 47, (1994), 554.

[37] R. W. Ogden. Nonlinear Elastic Deformations. Dover Publications, Inc.. 1984.

[38] M.A. Crisfield. Non-linear Finite Element Analysis of Solids and Structures. Vol. 2, Advanced Topics. John Wiley & Sons. 1997.

[39] J.C. Simo and T.J.R. Hughes. Computational Inelasticity. Springer-Verlag. 1997.